EMEP Status Report 2/2010

June 2010

Heavy Metals:
Transboundary Pollution of the Environment

METEOROLOGICAL SYNTHESIZING CENTRE - EAST

I. Ilyin, O. Rozovskaya, V. Sokovykh, O. Travnikov, M. Varygina

CHEMICAL CO-ORDINATING CENTRE

W. Aas, H.T. Uggerud

ccc

Norwegian Institute for Air Research (NILU)
P.O.Box 100
N-2027 Kjeller
Norway
Phone: +47 63 89 81 58
Fax: +47 63 89 81 58
E-mail: kjetil.torseth@nilu.no
Internet: www.nilu.no

msc-e

Meteorological Synthesizing Centre - East
Krasina pereulok, 16/1
123056 Moscow
Russia
Tel.: +7 495 981 15 66
Fax: +7 495 981 15 67
E-mail: msce@msceast.org
Internet: www.msceast.org

EXECUTIVE SUMMARY

Meteorological Synthesizing Centre – East (MSC-E) and Chemical Co-ordinating Centre (CCC) continued to work on the evaluation of heavy metal atmospheric pollution levels in the EMEP domain in accordance with the EMEP Work plan for 2010. Operational information on modelled and measured pollution levels of lead, cadmium and mercury was prepared. Contribution of transboundary transport to pollution levels in the EMEP countries was evaluated. New developments were focused on further elaboration of the common global modelling framework, modification of mercury chemistry, and improvement of heavy metal modelling approaches within the EMEP Case Study project. This report summarises the progress in the field of heavy metal modelling and monitoring achieved under EMEP in 2010.

Global modelling framework

Development of the common global modelling framework is one of the priority tasks within EMEP. To facilitate its development MSC-E has elaborated a pilot version of the framework based on the newly developed Global EMEP Multi-media Modelling System (GLEMOS). The elaborated framework was adapted and applied for simulation of two groups of contaminants with diverse properties and characters of the environmental cycling – heavy metals and persistent organic pollutants.

Scheme of mercury chemical transformations in the atmosphere employed in GLEMOS was updated according to the recent scientific results. In particular, chemical reactions of elemental mercury with reactive halogens (Br, BrO) and prompt re-emission of newly deposited mercury were included into the model in order to describe mercury fate during the Atmospheric Mercury Depletion Events (AMDEs) in the Polar Regions. Pilot modelling results demonstrate considerable improvement of the model performance with regard to observational data.

The framework was applied for simulation of mercury dispersion on a global scale. The calculated levels of mercury concentration and deposition were analyzed and evaluated against measurements. Measured air concentrations of Hg^0 were reproduced successfully by the model. The model tends to somewhat overestimate measured wet deposition but in 80% of cases the deviation between model and observations does not exceed a factor of 2. The source attribution estimates show that contribution of intercontinental transport from external anthropogenic and natural sources to mercury deposition in Europe varies from 40% in Central Europe to about 80% in Scandinavia and in the eastern part of the European territory of Russia.

EMEP contribution to TF HTAP

Within the framework of cooperation with the EMEP Task Force on Hemispheric Transport of Air Pollution (TF HTAP) MSC-E contributed to the preparation of the HTAP 2010 Assessment Report. MSC-E coordinated the TF HTAP activities in inter-comparison of global scale chemical transport models for mercury, and led publication of the multi-model experiment results in the Report. The multi-model experiment for mercury was a part of the HTAP modelling study. Its main objective was providing answers to the policy relevant questions concerning the current state-of-knowledge on mercury pollution on a global scale, importance of intercontinental transport for regional pollution, and expected changes of mercury pollution levels in future.

The results of the multi-model experiment show that ambient concentrations of elemental gaseous mercury, species responsible for long-range atmospheric transport, are reliably simulated by contemporary models. For the most model-measurement pairs the deviation between simulated and observed values does not exceed a factor of 1.2. Uncertainty of simulated mercury deposition is higher and largely associated with dry uptake of various Hg forms by the surface because of the absence of systematic observations of dry deposition. The contribution of mercury intercontinental transport is significant, particularly in regions with few local emission sources. The contribution of foreign anthropogenic sources to annual deposition fluxes varies from 10% to 30%, on average anywhere on the globe. Besides, global natural and secondary emissions contribute from 35 to 70% of total deposition in most regions.

EMEP Case Study on heavy metal pollution assessment

In order to improve quality of the assessment of heavy metal pollution levels in the EMEP region a Case Study project was initiated by MSC-E and the Task Force on Measurements and Modelling of EMEP (TFMM). The main method of the EMEP Case Study is the joint analysis of factors affecting quality of the assessment including emissions, measurements, and modelling in individual countries.

Six countries-volunteers (the Czech Republic, Croatia, Italy, the Netherlands, Slovakia, Spain) expressed their wish to take part in this project. Some countries (the Czech Republic, Croatia, the Netherlands) have started to provide MSC-E with necessary country-specific data (emissions, monitoring etc.). Input data (meteorology, land cover, soil concentrations) with fine resolution (10×10 km^2) were prepared by MSC-E for the Czech Republic, the Netherlands and Croatia, and pilot modelling of deposition and concentrations was performed for the Czech Republic this year.

Assessment of heavy metal pollution levels

Assessment of pollution levels in the EMEP region was carried out applying the integrated approach which involved analysis of emission inventories, monitoring data and modelling results. Information on heavy metal emission totals is annually reported by Parties to the Convention. The reported data were collected and processed by the EMEP Centre on Emission Inventories and Projections (CEIP). If countries did not report their national emission data, unofficial expert estimates were applied for modelling purposes. Gridded emission data were prepared by MSC-E and CEIP.

The measurement obligations set by the EMEP monitoring strategy for 2009 - 2019 led to improvements of spatial coverage of the EMEP region. Number of sites submitting measurement information in 2008 increased compared to previous year. However, there is still a lack of measurements in the south-eastern and eastern parts of Europe and in Central Asia. Results of most of national laboratories participated in the intercalibration tests meet the requirements of the current data quality objective. However, some countries submitting measurement data to CCC do not participate in these intercomparisons. Data from these countries are of unknown quality. Therefore they are strongly recommended to take part in the annual laboratory intercomparisons.

Information on HM concentrations, deposition and transboundary transport was prepared for each EMEP country using regional scale MSC-HM model. Spatial distribution of concentrations and deposition of lead, cadmium and mercury was characterized by measurement data and modelling results. The highest regional-scale heavy metal pollution levels were obtained for Poland, north of Italy,

the Benelux, the Balkan region, and the European part of Russia. In the Central Asian region elevated concentrations occurred in the southern parts of Kazakhstan. It was shown that transboundary transport was one of the most important factors controlling pollution levels in the EMEP domain. Its contribution to deposition from anthropogenic sources in Europe and Central Asia exceeded 50% in 38, 35 and 27 countries for lead, cadmium and mercury, respectively.

Changes of modelled pollution levels of lead, cadmium and mercury between 2007 and 2008 were analysed. Deposition of lead and cadmium in Europe and Central Asia as a whole in 2008 was about 14% and 10% lower than that in 2007, respectively. Mercury deposition to the EMEP region remained almost the same. Decrease of lead and cadmium deposition in the southern, central and western parts of Europe was caused by decline of anthropogenic emissions and re-suspension. Increase of precipitation amounts caused the rise of deposition of lead and cadmium in the western part of the United Kingdom and the central part of Kazakhstan and of mercury in the north-western Italy, Russia and most of Scandinavia. Deposition of mercury in Denmark, Cyprus, France, Norway and Germany decreased, whereas in Slovakia and Romania increased because of the corresponding changes of the emissions.

Quality of the air pollution assessment for the EMEP region was characterized by means of integrated approach taking into account uncertainties of the model, emission data and measurements. The uncertainty of countries totals of heavy metal emission typically ranged between 30 – 60%. Based on the results of field campaigns the overall uncertainty of measured wet deposition was around 20% for lead and cadmium, and 40% of mercury. Modelling results agreed with measurement data with satisfactory accuracy, keeping in mind uncertainties of the emission and monitoring data. At most of stations modelled and observed levels of lead and cadmium agreed within ±50%. The discrepancy between the simulated and observed mercury concentrations did not exceed ±15% for air concentrations. For concentrations in precipitation and wet deposition fluxes the bias was within ±30% for most of stations.

Cooperation

In the framework of evaluation of heavy metal pollution levels MSC-E and CCC closely cooperated with TFMM, TFHTAP, TFEIP, international organizations (AMAP, HELCOM, OSPAR, UNEP) and the Working Group on Effects (WGE). In particular, MSC-E together with the ICP-Vegetation of WGE continued joint analysis of the pollution levels of lead, cadmium and mercury on the base of measured concentrations of heavy metals in mosses. MSC-E took part in preparation of the AMAP Assessment 2010 for mercury. Information on lead, cadmium and mercury deposition to the Baltic Sea in 2007 was delivered to HELCOM/MONAS. The Centres were actively involved in cooperation with national experts, especially from the EECCA countries. To support EECCA countries country-oriented reports were prepared in Russian language.

MSC-E took part in the project in support of the revision of the Heavy Metal Protocol initiated by the Dutch Ministry of Hosing, Spatial Planning and the Environment (VROM). Information on deposition and concentrations of the priority metals was prepared on the base of four scenarios (one for 2010 and three for 2020) of heavy metal emissions developed by TNO. It was shown that the reduction of deposition between 2010 and scenarios for 2020 was 15 – 24% for lead and 15 – 27% for cadmium. For mercury the changes varied between 4% growth and 5% reduction. Relatively low changes of mercury deposition were explained by the significant influence of intercontinental transport. The changes for individual countries were highly variable because of the influence of transboundary transport.

Acknowledgments

The authors of this report are grateful to the representatives of countries involved in the EMEP Case Study for providing valuable comments and contributions to the report: Milan Vana (the Czech Republic), Amela Jericevic (Croatia), Eric van der Swaluw (the Netherlands), Mihaela Mircea (Italy), Marta Mitoshinkova (Slovakia), Marta Garcia Vivanco (Spain) and Alberto González Ortiz(Spain). We would like to thank Harry Harmens (ICP-Vegetation) for the fruitful cooperation in the field of pollution level analysis using data on heavy metal concentrations in mosses. We gratefully acknowledge Umberto Modigliani (ECMWF) for the important consultations concerning the ECMWF meteorological data and Irina Yeserkepova (Kazakhstan) for providing MSC-E with national monitoring data. The Centres would like to thank Irina Strizhkina (MSC-E) for formatting and printing this report.

CONTENTS

INTRODUCTION

A number of heavy metals and their compounds are known as toxics harmfully affecting human health and biota. Besides, some of heavy metals accumulate in soils, waters and tissues of living organisms increasing the risk of the harmful effects in future. Therefore a number of national and international organizations are working on the reduction of the environmental pollution by heavy metals. In particular, in order to take control over the atmospheric emissions of heavy metals 36 Parties to the Convention on Long-Range Transboundary Air Pollution (Convention) ratified the Protocol on Heavy Metals (Protocol). Heavy metals targeted by the Protocol are lead (Pb), cadmium (Cd) and mercury (Hg).

According to the Protocol, the Cooperative Programme for Monitoring and Evaluation of Long-range Transmission of Air Pollutants in Europe (EMEP) provides the Executive Body for the Convention with information on deposition and transboundary transport of heavy metals within the geographical scope of EMEP. Centre of Emission Inventories and Projections (CEIP) prepares emission data based on information reported by the EMEP countries. Measurements of heavy metal concentrations in air and precipitation are carried out at the EMEP monitoring network under the methodological guidance of the Chemical Coordinating Centre (CCC). Along with that the Meteorological Synthesizing Centre – East (MSC-E) performs the model assessment of deposition and air concentrations of heavy metals over the EMEP region as well as the transboundary fluxes between the EMEP countries involving information on emissions and measurements. The aim of this report is to overview the main results of the activities of MSC-E and CCC in 2010 in the field of heavy metal pollution. This work was carried out according to the EMEP Workplan [ECE/EB.AIR/2009/7].

In order to increase the quality of the assessment of pollution levels over the EMEP region the development of modelling approaches proceeds in two directions: expansion of the geographical scope (up to global scale) and refinement of spatial resolution. Since mercury is a global pollutant, the former is needed to evaluate contribution of remote sources of mercury to pollution levels in Europe. Besides, levels of regional-scale pollutants, such as lead and cadmium, in Central Asia, Caucasus and the eastern part of Russia are affected by atmospheric transport from the Asian sources located in China, India, Middle East, etc. Refinement of spatial resolution is aimed at the improvement of the pollution level evaluation both in individual countries and the entire EMEP domain and will be realised in the framework of the Case Study project initiated by MSC-E and the Task Force on Measurements and Modelling (TFMM).

Development of a common global modelling framework was initiated within EMEP in 2007 to consolidate the modelling activities of the two EMEP modelling Centres (MSC-W and MSC-E) on a global scale. In order to facilitate development of the modelling framework MSC-E has elaborated a pilot version of the modular architecture based on the newly developed Global EMEP Multi-media Modelling System (GLEMOS). GLEMOS was adapted and applied for simulation of two groups of contaminants with diverse properties and characters of the environmental cycling – heavy metals and POPs. It was also tested in the multi–model experiment organized by the EMEP Task Force on Hemispheric Transport of Air Pollution (TF HTAP) aimed at evaluation of global dispersion of atmospheric pollutants (including mercury) and the role of intercontinental transport. The results of this study as well as main findings and recommendations to scientific community are to be published in the HTAP 2010 Assessment Report.

The main approach of the EMEP Case Study project is the integrated analysis of factors affecting quality of the assessment including emissions, measurements, and modelling in individual countries. In the framework of the project it is planned to use more detailed input data (emission, land-cover, meteorology etc.) with finer (e.g., 10×10 or 5×5 km^2) spatial resolution and measurement data collected at national monitoring networks together with data from the EMEP stations. Six countries (the Czech

Republic, Croatia, the Netherlands, Italy, Slovakia and Spain) expressed their wish to participate in this activity. The experience which will be gained in this Case Study could be applied to other EMEP countries.

The integrated approach was applied for the assessment of pollution levels in the EMEP region. It is based on the combined usage of monitoring and modelling information. There were 70 stations measuring concentrations of lead, cadmium and mercury in air or in precipitation in 2008. Most of them are located in the western, central and northern parts of Europe. Coverage of South-eastern and Eastern Europe by monitoring stations still needs improvement. It means that the assessment of pollution levels in these regions is based entirely on modelling. Modelling of concentrations, deposition and source-receptor relationships in Europe and Central Asia is made by the MSCE-HM regional-scale model. This report describes the results achieved by MSC-E and CCC in the field of heavy metals in 2010.

Chapter 1 includes an overview of MSC-E contribution to the development of the common EMEP global modelling framework as well as other research activities associated with model assessment of heavy metal pollution levels on a global scale. In particular, the current view on a general concept of the modelling framework and its practical implementation are discussed along with its pilot realization for heavy metals and POPs based on the GLEMOS modelling system. The GLEMOS application to simulations of mercury is given in more detail in joint MSC-E/MSC-W Technical report [*Jonson and Travnikov*, 2010].

Chapter 2 describes MSC-E contribution to preparation of the HTAP 2010 Assessment Report. In particular, the Centre coordinated activities of the modelling community in comparison of global scale chemical transport models for mercury and publication of the multi-model experiment results in the HTAP 2010 Assessment Report. Major results of the study are presented in the chapter along with estimates of the simulation uncertainty and discussion of the key findings and recommendations.

Chapter 3 is focused on the EMEP Case Study on heavy metal pollution assessment. The approach, the main stages and expected outcomes of the Case Study are considered. Besides, current progress and preliminary results of the project are described. In particular, for several countries input information with fine spatial resolution was prepared and preliminary modelling results were obtained. Contributions of the six countries-volunteers to the Case Study are overviewed.

Chapter 4 is devoted to the assessment of pollution levels of HMs in 2008. Heavy metal emission data used in modelling and results of background monitoring in EMEP guided by CCC are overviewed. Quality of monitoring data, in particular, the results of laboratory intercalibrations and estimates of the overall uncertainty of measured values are characterized. Meteorological conditions in 2008 are analysed and sensitivity of pollution levels to meteorological parameters associated with climate change is investigated. Analysis of the pollution levels based on modelled and measured data and source-receptor relationships for individual countries and regional seas is performed. Quality of the pollution levels assessment is evaluated taking into account uncertainties of the model, emission, and measurement data.

Chapter 5 is focused on cooperation of MSC-E and CCC with subsidiary bodies to the Convention, international organizations and programmes as well as with national experts. Special attention is paid to the countries of Eastern Europe, Caucasus and Central Asia (EECCA).

In *Chapter 6* proposals of MSC-E and CCC for future activities in the field of heavy metals are outlined. Main results of the EMEP Centres work for 2008 are summarized in section *Conclusions*. Detailed source-receptor matrices of lead, cadmium and mercury for 2008 are presented in *Annex A*. The contribution of the Italian experts containing comparison of the results of mercury transport models is given in *Annexes B*.

1. EMEP GLOBAL MODELLING FRAMEWORK: MERCURY CASE

This chapter includes an overview of MSC-E contribution to the development of the common EMEP global modelling framework as well as other research activities associated with model assessment of heavy metal pollution levels on a global scale. In particular, the current view on a general concept of the modelling framework and its practical implementation are discussed below along with its pilot realization for heavy metals and POPs based on the GLEMOS modelling system. Its application to simulations of mercury is given in more detail. New model developments include updates of the mercury chemical scheme in accordance with the new findings of the research community. Model assessment of mercury levels on a global scale is presented along with evaluation against measurements and estimates of intercontinental transport. Besides, evaluation of the GLEMOS model in the HTAP multi-model experiment is described in Chapter 2. These and other aspects of the global modelling activities of the EMEP modelling Centres are given in detail in the Joint MSC-E and MSC-W Technical Report [*Jonson and Travnikov,* 2010].

1.1. Towards development of the common EMEP global modelling framework

Development of the common global modelling framework is one of the priority task within EMEP. The motivation and main requirements to the modelling framework as well as progress in its elaboration were described in the technical reports [*Tarrasón and Gusev*, 2008; *Travnikov et al*., 2009]. The requirements to the framework include a flexible choice of the model domain and grid resolution, multi-pollutant and multi-media approach, a modular architecture and computational efficiency of the modelling. The modular architecture is aimed to provide flexibility for simulation of pollutants with very different properties (e. g. ozone and POPs) either simultaneously as it is in the "one atmosphere" approach or separately using less demanding computer resources. It also allows considering different number of environmental media depending on pollutant properties: solely the atmosphere for the air pollutants or other media as well (soil, vegetation, the ocean etc.) for pollutants with complex environmental cycling. The mentioned flexibility is highly relevant for the framework application for both detailed research studies and cumbersome operational simulations of transboundary pollution.

The optimal way of practical implementation of the modelling framework concept under the current EMEP conditions is elaboration of a common library of physical and chemical modules and a database of harmonized input parameters (meteorology, land cover, soil properties etc.) keeping individuality of the modelling systems existing at the moment within EMEP (Fig. 1.1). Indeed, the large experience gained by the EMEP modelling groups has been realized into the well

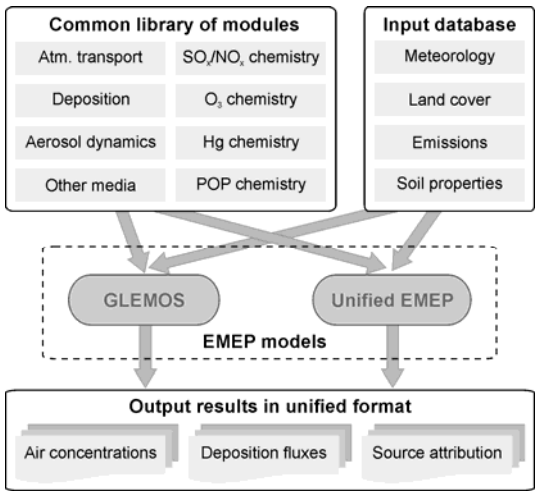

Fig. 1.1. *General concept of the common EMEP global modelling framework*

developed and tested global modelling systems oriented at different pollutants groups (Unified EMEP – SO_x, NO_x, ozone, PM; GLEMOS – heavy metals and POPs). Each group of the pollutants has pronounced specifics which are reflected in the peculiarities of appropriate modelling systems. Therefore, direct fusion of the models or development of a new one combining all required properties would require unacceptable amount of resources and time.

On the other hand, both modelling systems contain modules with similar functionalities (e.g. atmospheric transport, wet and dry deposition etc.) and utilize similar input data. To avoid duplication and harmonize modelling approaches it seems rational to develop a common library of the modules as well as input data base which could be applicable to both modelling systems. For these purpose it is necessary to update the existing modelling systems (if necessary) to support the modular architecture, harmonize the modules interfaces and unify formats of the input datasets as well as auxiliary program solutions for their processing. For meteorological data, in particular, it could involve unification of the meteorological pre-processor. Development of the module library and input database does not necessarily imply existence of a single set of modules and datasets. On the contrary, it allows availability of a number of parallel approaches suitable for different applications (for instance, modules with different parameterization complexity). Along with harmonisation of the modelling approaches, it seems useful to unify formats of the modelling output results as well to ensure consistency of the EMEP model estimates in different fields and provide possibility of the output data exchange.

In order to evaluate the general concept and to facilitate the framework development MSC-E has elaborated a pilot version of the framework with modular architecture based on the newly developed the Global EMEP Multi-media Modelling System (GLEMOS). It was adapted and applied for simulation of two groups of contaminants with diverse properties and characters of the environmental cycling – heavy metals and POPs. Parameterizations of media processes for these pollutants applied in the model are largely based on the previous well developed and extensively tested hemispheric models MSCE-HM [*Travnikov and Ilyin*, 2009] and MCSE-POP [*Gusev et al.*, 2005]. The heavy metal group among others includes mercury that is a substance characterized by long residence time in the atmosphere, chemical speciation and transformations as well as intensive air-surface exchange. The large group of POPs is commonly characterized by long-term accumulation in the environment, phase partitioning and degradation in different media.

Recent MSC-E activities in the field of development of the GLEMOS modelling framework as well as its application for simulations of mercury and POPs on a global scale are described in detail in the Joint MSC-E and MSC-W Technical Report [*Jonson and Travnikov,* 2010]. Some aspects of mercury pollution modelling are briefly discussed below.

1.2. Update of mercury chemical scheme

Mercury is found in the atmosphere in a number of chemical forms with distinctively different properties. The atmospheric fate of mercury from the moment of its release from an emission source up to deposition to the ground commonly includes a set of physical and chemical transformations (dissolution in could water, redox reactions) which largely define the pathways and character of mercury atmospheric dispersion. The chemical scheme of mercury transformations implemented in the modelling system includes oxidation of elemental gaseous mercury (Hg^0) by ozone, chlorine and hydroxyl radical in gaseous phase and aqueous phase of cloud water, aqueous-phase reduction via decomposition of sulphite complexes, formation of chloride complexes, and adsorption by soot particles in cloud water [*Travnikov and Ilyin*, 2009].

However, recent studies have demonstrated that chemical oxidation of Hg^0 by reactive halogens (first of all, Br and BrO) may essentially affect or even determine the mercury cycle in the atmosphere, in particular, in the Polar Regions [*Steffen et al.*, 2008; *Ebinghaus et al*., 2002] and the marine boundary layer [*Laurier et al.,* 2003; *Sprovieri, et al.,* 2010]. There is also some observational evidence of Hg^0 fast oxidation in the upper troposphere – lower stratosphere, probably, also due to reactions with halogens, where these radicals are present in sufficient concentrations [*Murphy et al*., 2006; *Talbot et al.,* 2007]. In the Arctic and Antarctic it was observed that during spring time Hg^0 concentration episodically dropped down to very low concentrations due to rapid transformation to short lived oxidized forms with the following deposition to the surface [*Lindberg et al.*, 2002; *Aria et al.*, 2004; *Skov et al*., 2004]. This phenomenon, termed as the Atmospheric Mercury Depletion Events (AMDE), leads to considerable increase of annual mercury deposition to the Polar Regions.

In order to take into account this important phenomenon for the Arctic pollution we added into the model chemical scheme the reactions of Hg^0 oxidation by Br and BrO. For the first reaction we adapted the temperature dependent reaction rate constant from [*Goodsite et al*., 2004] assuming that the formation of the reaction intermediate HgBr* is the rate limiting step in the formation of divalent Hg(II) [*Sprovieri, et al*., 2010]. For the reaction with BrO we utilized the reaction rate constant from [*Raofie and Ariya*, 2003].

Concentration of bromine compounds in the atmosphere is one of the most uncertain parts of the applied approach. Direct measurements of Br and its species in the lower troposphere are scarce and simulated concentration fields are quite unreliable. Therefore, concentration of BrO were derived from the GOME (Global Ozone Monitoring Experiment) satellite observations [*Nicolas Theys,* 2009, personal communication]. Global distribution of total tropospheric BrO column was obtained by *Theys et al.* [2004] applying a combined retrieval/modelling approach using 3D chemistry-transport model calculations. Besides, following [*Dastoor et al*., 2008] we subtracted the global background BrO concentration from the tropospheric column to derive total BrO content in the atmospheric boundary layer. Mixing ratio of BrO was subsequently obtained assuming its uniform vertical distribution in the boundary layer and the boundary layer height derived from the meteorological data. Keeping in mind that formation and destruction cycles of Br and BrO are linked closely, we assume similar spatial distributions of these two substances and apply a constant Br/BrO ratio equal to 0.1 [*Seigneur and Lohman*, 2008].

Another important process accompanying the enhanced mercury deposition during AMDEs is prompt re-emission of newly deposited mercury. Measurements in snowpack show that high mercury concentrations in the surface snow following the AMDEs are substantially reduced during few days due to photoreduction of deposited mercury and re-emission to the atmosphere [*Kirk et al*., 2006; *Johnson et al*., 2008; *Ferrari et al*., 2008]. Thus, it considerably reduces mercury accumulation in snow and adverse effects of the Arctic vulnerable ecosystems. Observed temporal changes of total mercury concentration in snowpack during the recovering period after AMDEs are given in Fig. 1.2. As seen, within first two days mercury concentration in snowpack decreased by more than 70%.

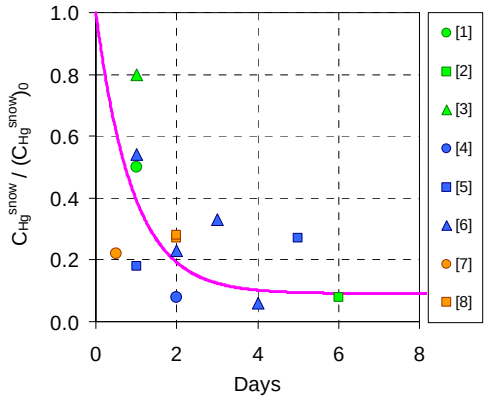

Fig. 1.2. *Reduction of total Hg concentration in snowpack during the recovering period after AMDEs. Markers present measurements: [1] - Lalonde et al., 2002; [2] - Lindberg et al., 2002; [3] - Dommergue et al., 2003; [4] - Poulain et al., 2004; [5] - St. Louis et al., 2005; [6] - Kirk et al., 2006 ; [7] - Constant, et al., 2007; [9] - Johnson et al., 2008 . Solid line depicts the approximation*

To account for this essential process we developed an empirical parameterization of the prompt re-emission based on the observational data. Assuming that re-emission occurs only for newly deposited mercury in the presence of solar radiation we have introduced two competing processes – photoreduction and ageing of newly deposited mercury with characteristic times 1 day and 10 days, respectively. It is assumed that all reduced mercury is immediately recycled back to the atmosphere. The aged fraction of mercury does not undergo reduction and accumulated in snowpack. It should be noted that this accumulated mercury can be mobilized during snow melt with the following run-off to soil water or re-emission. But correct treatment of this process in the model requires separate consideration.

Figure 1.3 shows simulated Hg^0 concentration at Canadian site Alert in comparison with daily observations. Two different model runs are presented in the figure to evaluate effect of the new parameterisation. The first simulation does not include neither AMDEs treatment nor prompt re-emission, whereas the second simulation includes both. As seen the model successfully reproduces the period of AMDEs as well as some of individual events. However, not all of the events are captured and depth of Hg^0 depletion is not sufficient. The reason for that is uncertain spatial distribution of Br/BrO concentration used in the modelling and relatively coarse resolution of the model grid (1º×1º), which complicates reproducing this local phenomenon.

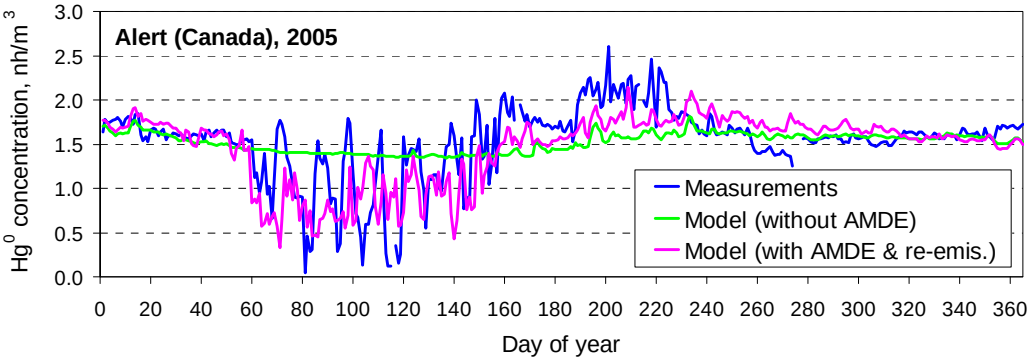

Fig. 1.3. *Daily mean Hg^0 concentration in the surface air at site Alert (Canada)*

1.3. Application of the GLEMOS framework for mercury simulations on a global scale

The GLEMOS modelling framework was applied for simulation of mercury dispersion on a global scale as well as for evaluation of intercontinental transport and source attribution of mercury deposition. A one-year model run was performed for 2005 preceded by three-year model spin-up. The global inventory of mercury anthropogenic emissions for 2005 was used for the simulations [*AMAP/UNEP*, 2008]. According to this dataset the total global mercury emissions from anthropogenic sources in 2005 amounted to 1930 t/y. Besides, we utilized spatially resolved estimates of mercury emissions from natural and secondary sources based on the approach described in [*Travnikov and Ilyin*, 2009] with total annual contribution of around 4320 tonnes. Thus, the overall mercury input to the atmosphere made up about 6250 t/y. Moreover, about 700 tonnes were re-emitted annually to the atmosphere from the snow and ice surfaces according the prompt re-emission parameterization described above. The standard version of the GLEMOS framework with spatial resolution 1º×1º was applied for simulation of spatial distribution of concentration and deposition levels as well as the model evaluation against measurements. The lower resolution version (5º×5º) was applied for evaluation of the source-receptor relationships.

Spatial distribution of mercury concentration and deposition levels

Simulated spatial distributions of mean annual ambient concentration of Hg^0 concentration and total (wet and dry) deposition flux are given in Fig. 1.4. Available long-term measurements of Hg^0 concentration are also presented in Fig. 1.4a for comparison. Observations of total mercury deposition are not available but measurements of wet deposition flux are also involved into the analysis. More detailed evaluation of the modelling results against measurements is given below in this section. As seen from Fig. 1.4a the simulated Hg^0 concentrations demonstrate a pronounced gradient between the Southern and the Northern Hemispheres. It agrees well with available measurements but the observations are very limited, particularly, in the Southern Hemisphere. In general, the model reproduces the measured concentration levels except for a few sites in Europe and North America, where the measurements give somewhat lower values. The global concentration pattern allows revealing a number of regions with increased concentration levels – South-Eastern Asia, Europe and Middle East, the eastern part of North America and the western coast of North and South Americas. These regions are characterized by elevated emissions from anthropogenic and/or natural sources. Over the Atlantic and Pacific oceans Hg^0 concentrations increase gradually from the Equator to the north except for the Arctic region, where the quick Hg^0 oxidation during the AMDEs results in lower levels of annual mean concentrations.

The global deposition pattern also partly reflects spatial distribution of major source regions (Fig. 1.4b). In this case location of anthropogenic sources has a stronger effect on the spatial pattern because of deposition of primarily emitted short-lived mercury forms. Another factor significantly affecting deposition flux is the spatial distribution of precipitation. Wet scavenging considerably contributes to the total mercury deposition. Therefore, mercury deposition is higher in areas with intensive precipitation (e.g. the equatorial Atlantic and Pacific, equatorial Africa, the Indian Ocean), and it is lower in areas with small precipitation amount (northern Africa, Antarctica, Greenland). Besides, high deposition fluxes are also predicted over the high Arctic and the South Ocean next to the Antarctic coast. Elevated deposition in these areas can be explained by intensive mercury oxidation and removal during the AMDEs. However, it should be noted that considerable part of this deposition to the snow and ice surface is promptly re-emitted back to the atmosphere.

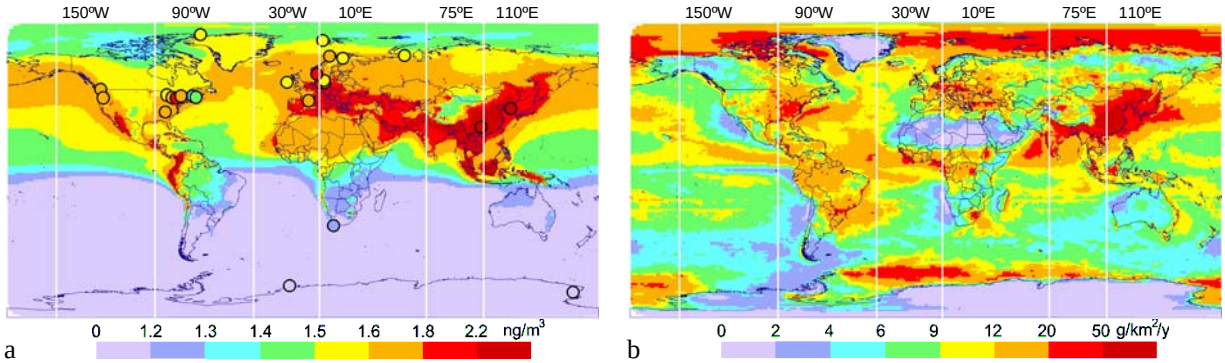

Fig. 1.4. *Spatial distribution of annual mean concentration of Hg^0 in the surface air (a) and total annual mercury deposition flux (b). Circles present long-term observations from the AMAP, EMEP, CAMnet networks and at some other monitoring sites: Look Rock, USA [Valente et al., 2007]; Mount Bachelor Observatory, USA [Jaffe et al., 2005]; Cape Point, South Africa [Baker et al., 2002]; Kang Hwa, Korea [Kim et al., 2002]; Mt. Leigong, China [Fu et al., 2010]; Terra Nova Bay, Antarctica [Sprovieri et al., 2002]; Neumayer Station, Antarctica [Temme et al., 2003]*

Spatial variation of mercury levels is clearly seen in the south-to-north cross-sections of mercury concentrations and deposition fluxes presented in Fig. 1.5. Directions of the considered cross-sections are shown in Fig. 1.4. As seen background concentrations of Hg^0 are very even in remote regions of both Hemispheres. It alters around 1 and 1.6 ng/m^3 in the Southern and Northern Hemispheres, respectively. The inter-hemispheric gradient is relatively strong near the Equator indicating restricted air exchange between the Hemispheres. Elevated concentrations are characteristics of the major source regions where Hg^0 reaches 2-3 ng/m^3. Variation of deposition flux is noticeably larger because it is determined by a number of different factors mentioned above. It alters within 0-30 μg/m^2 per year in the Southern Hemisphere and reaches 80 μg/m^2/y in the Northern Hemisphere. Distribution of the deposition flux over the ocean is more even and varies mostly within 5-20 μg/m^2/y. Enhanced deposition levels (around 30 μg/m^2/y) are typical for the high latitudes areas where the AMDEs take place.

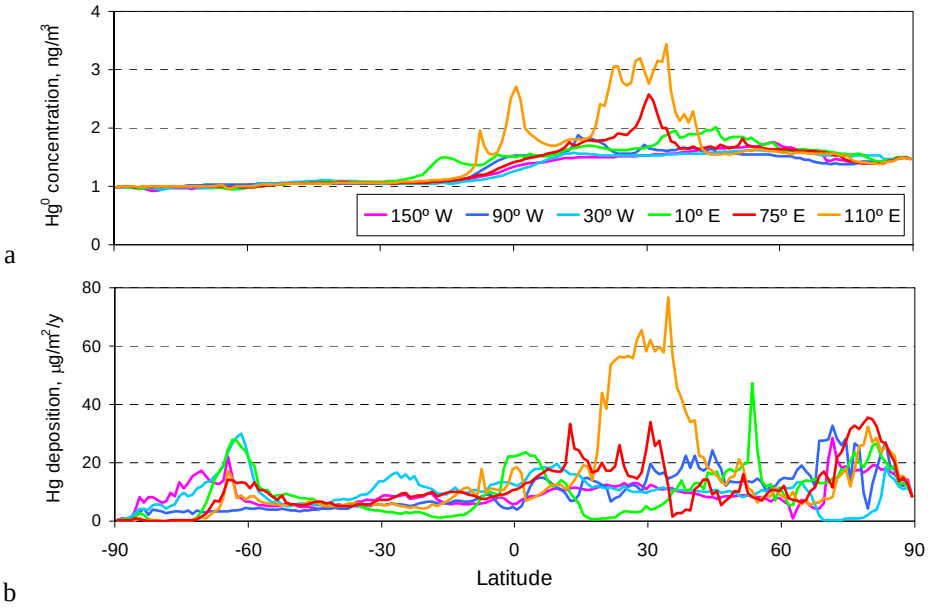

Fig. 1.5. *South-to-north cross-sections of simulated annual mean Hg^0 concentration in the ambient air (a) and total annual mercury deposition (b) corresponding to fixed geographical longitudes. Directions of the cross-sections are depicted in Fig. 1.4*

The simulation results were evaluated against long-term measurements available from different monitoring network (EMEP, AMAP, CAMnet, NADP/MDN) and other observational data available from literature (see the caption to Fig. 1.4). The comparison results are presented in Fig. 1.6. The model successfully reproduces measured Hg^0 air concentration. For the most model-measurement pairs the deviation between simulated and observed values does not exceed a factor of 1.2. The model evaluation for wet deposition fluxes is less successful but still quite promising. The model tends to somewhat overestimate measurements, particularly, for low deposition levels. It could be connected with uncertainties of atmospheric chemistry, overestimation of precipitation rates by the meteorological input, uncertainties in spatial distribution and speciation of anthropogenic emissions. Nevertheless, in more than half of considered model-measurement pairs (55%) the deviation of falls into a factor of 1.5 and in 80% of cases does not exceed a factor of 2.

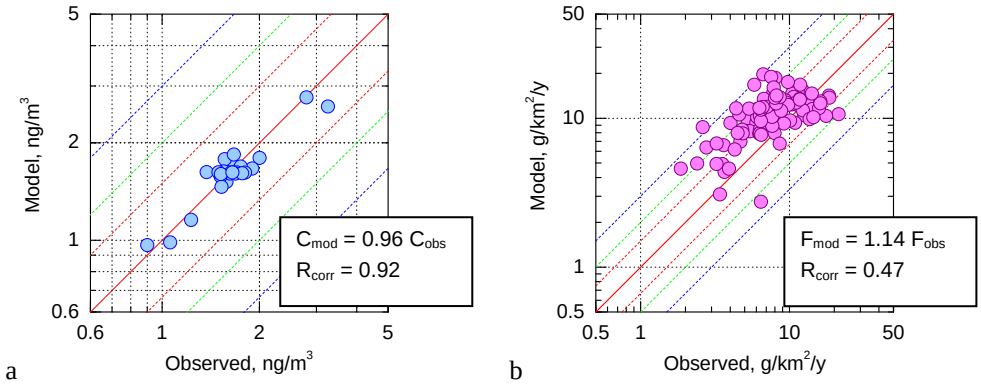

Fig. 1.6. *Comparison of simulated and measured annual mean Hg^0 concentration in surface air (a) and wet deposition flux (b). Red solid line depicts the 1:1 ratio; dashed lines show different deviation levels: red – by factor of 1.5, green – by factor of 2, blue – by factor of 3*

Intercontinental transport and source attribution of mercury deposition

To evaluate the source attribution of mercury deposition and the role of intercontinental transport in mercury pollution a number of perturbation runs have been performed zeroing out emissions in one of the eight source regions - Europe, North and South America, East, South and Central Asia, Africa and Australia with Indonesia. Total emissions from these regions (both anthropogenic and natural/secondary) are presented in Fig. 1.7. As seen, East Asia makes the largest contribution to the global mercury emission (26%). It is comparable with the contribution of mercury evasion from the global ocean (25%). Other major source regions of the Northern Hemisphere – Europe, North America and South Asia – contribute 8%, 6%, and 8%, respectively. Contribution of other source regions makes up 27% of total emission.

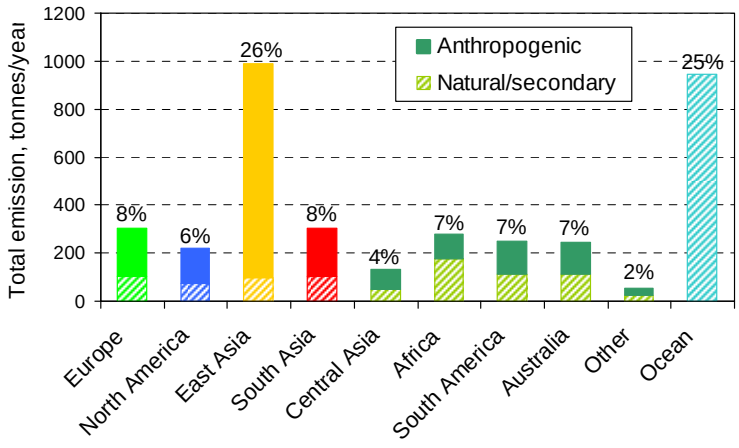

Fig. 1.7. *Total anthropogenic and natural/secondary emission of mercury from different regions of the globe in 2005*

Source attribution of mercury deposition in the Northern and Southern Hemispheres is shown in Fig. 1.8. Contributions of four major source regions (Europe, North America, East Asia, and South Asia) present combination of both anthropogenic and natural/secondary emissions from these regions. Contributions of anthropogenic sources from other regions are aggregated into one group 'Other anthropogenic', whereas natural/secondary sources from other regions are divided into two groups - 'Other land' and 'Ocean', for emissions from land and the ocean, respectively.

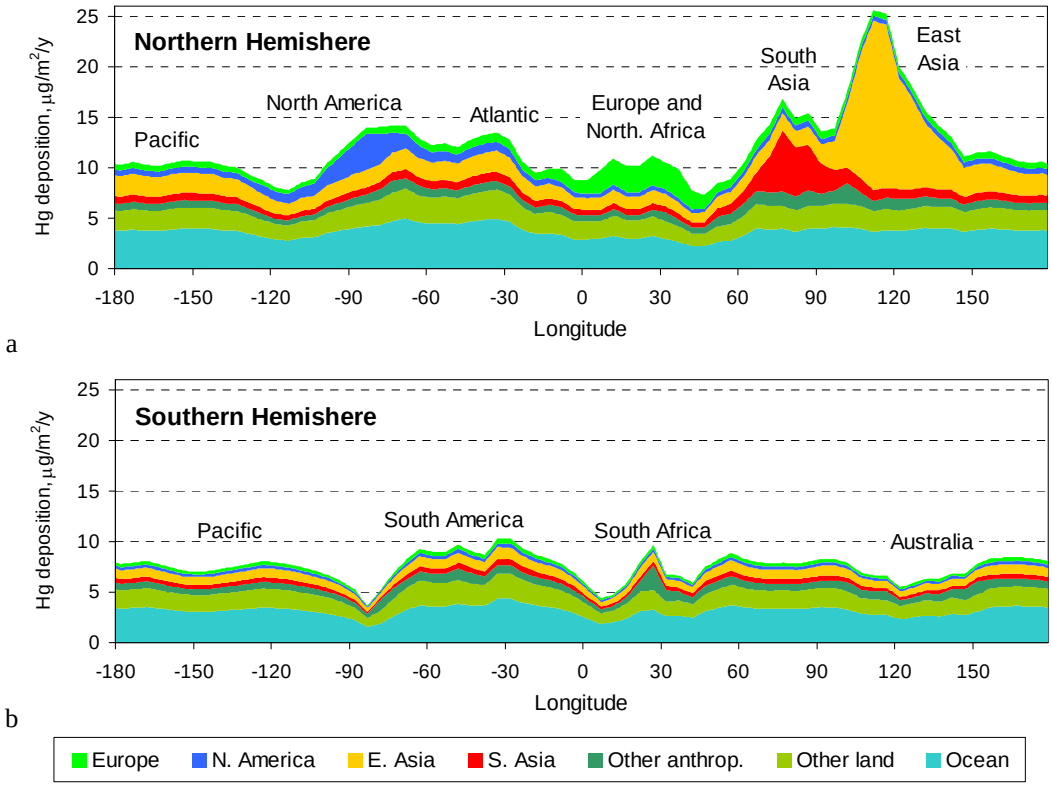

Fig. 1.8. *Area averaged mercury deposition flux in the Northern Hemisphere (a) and Southern Hemisphere (b) including contribution of different source regions*

As seen from Fig. 1.8a, mercury deposition fluxes are the highest in East and South Asia and somewhat lower in the western part of the Northern Hemisphere. Average deposition fluxes corresponding to longitudes of Europe are considerably reduced by very low deposition in Northern Africa. Contribution of the source regions to mercury deposition differs considerably in different parts of the Northern Hemisphere. Deposition from oceanic and terrestrial natural/secondary sources is relatively homogeneous over the whole hemisphere. The contribution of domestic sources prevails in each particular source region. It is the most pronounced in East and South Asia. Over the Pacific and Atlantic oceans the relative contributions of different source regions are rather even that reflects prevailing of the global mercury pool. In the Southern Hemisphere general level of deposition is noticeably lower (Fig. 1.8b). The minimum deposition fluxes correspond to the western coasts of South America and Africa as well as Australia characterized by low precipitation amount. The relative composition of deposition is markedly even over the whole hemisphere because of relatively small contribution of domestic anthropogenic emissions and the dominant role of the global pool. An exception is South Africa where significant anthropogenic sources are located.

Figure 1.9 illustrates contribution of intercontinental transport to mercury deposition in different parts of Europe. In Central Europe mercury deposition is dominated by domestic sources and contribution of intercontinental transport does not exceed 40%. In the United Kingdom, where mercury deposition is less affected by the continental Europe and the European contribution consists mostly of national sources, the contribution of intercontinental transport exceeds 60%. Relatively low deposition in Scandinavia consists of only 20% contribution of European sources and 80% contribution of intercontinental transport, which includes 27% from North America, East and South Asia in total, and about 6% from other anthropogenic sources. In the eastern part of the European territory of Russia the intercontinental transport also contributes about 80% of total deposition. However, in contrast to Scandinavia it includes large contribution of the 'Other anthropogenic' sources, which largely consists of emissions from the Eastern part of the country and from Central Asia.

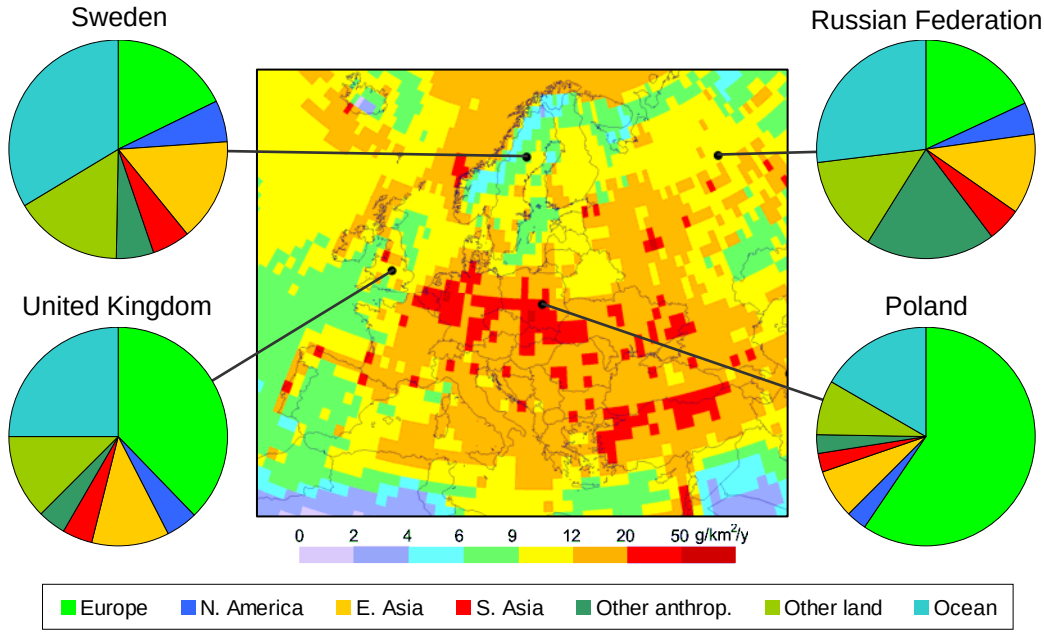

Fig. 1.9. *Contribution of intercontinental transport to mercury deposition in different parts of Europe. Background map presents total deposition flux of mercury. Diagrams relate to particular points of the map*

2. EMEP CONTRIBUTION TO HTAP 2010 ASSESSMENT REPORT

Within the framework of cooperation with the EMEP Task Force on Hemispheric Transport of Air Pollution (TF HTAP) MSC-E contributed to the preparation of HTAP 2010 Assessment Report (http://www.htap.org). In particular, the Centre coordinated activities of the modelling community in comparison of global scale chemical transport models for Hg and in conducting the multi-model assessment of mercury intercontinental transport. In cooperation with experts from the USA and Canada it also led publication of the multi-model experiment results in the HTAP 2010 Assessment Report. Major results of the multi-model assessment for Hg intercontinental pollution are presented below along with estimates of the simulation uncertainty and discussion of the key findings and recommendations.

2.1. HTAP multi-model experiment for mercury

As a part of the HTAP modelling study, the Hg multi-model experiment has a general goal to evaluate the global atmospheric dispersion of Hg, current levels concentration and deposition in different regions, and the role of the intercontinental transport in Hg contamination. The Hg multi-model experiment for Hg was conducted in two phases. The first phase included the reference simulation for 2001 and emission perturbation simulations that reduce anthropogenic emissions by 20% in Europe, North America, East Asia, and South Asia in order to estimate source-receptor relationships of Hg atmospheric transport between the continents. The second phase included the source attribution estimates for 2005 and forecasts of future Hg contamination changes for a number of emissions reduction scenarios.

Five global models (CTM-Hg, ECHMERIT, GEOS-Chem, GLEMOS, GRAHM) and one regional/hemispheric model (CMAQ-Hg) participated in the study. The models significantly differ in their formulation. In particular, they considerably vary in spatial resolution of the model grids, complexity of the chemical schemes, estimates of natural and secondary emissions, treatment of mercury cycling between the atmosphere and other media etc. Thus, comparison of the modelling results obtained with these models enables estimates of the uncertainty level of current state-of-the-art mercury modelling.

2.2. Global concentration and deposition levels

The spatial distribution and temporal variation of mercury concentration and deposition levels on a global scale were studied in the multi-model experiment. Figure 2.1 shows the model ensemble mean global distribution of a bulk atmospheric mercury species – gaseous elemental mercury (Hg^0) – in ambient air (Fig. 2.1a) as well as total Hg deposition flux (Fig. 2.1b). Circles on the figure represent long-term observations of Hg^0 concentration from several monitoring networks and individual sites.

As seen from the figure elevated concentrations (above 1.8 ng/m^3) are characteristic of the major industrial regions – East and South Asia, Europe, North America, South Africa**.** There is a pronounced gradient of the surface mercury concentration between the Southern and the Northern Hemispheres

resulting from the location of most emission sources in the Northern Hemisphere. Typical background levels of mercury concentrations are 1.2-1.4 ng/m^3 in the Southern Hemisphere and 1.5-2 ng/m^3 in the Northern Hemisphere. In general, this simulated pattern reproduces the long-term observations of Hg^0 concentration. However, it should be noted that the number and spatial coverage of available long-term measurements are not sufficient for comprehensive evaluation of the mercury dispersion models.

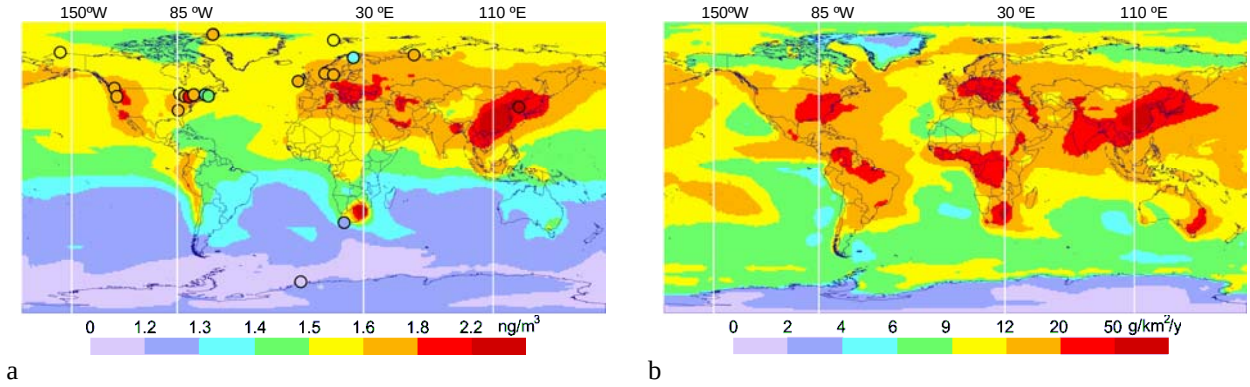

a b

Fig. 2.1. *Global distribution of ensemble mean annual Hg^0 concentration in ambient air (a) and total Hg deposition flux (b). Circles present long-term observations from the AMAP, EMEP, CAMnet networks and at some other monitoring sites (see caption to Fig. 1.4)*

Deposition of atmospheric Hg is mostly presented by wet scavenging and dry uptake of the oxidized forms (RGM and HgP). Depending on the origin of these Hg species, the deposition flux can be divided into two components: the first consists of deposition of primarily emitted short-lived forms; the second one is defined by *in-situ* oxidation of Hg^0 in the atmosphere. The former is prevalent in the vicinity of emission sources, whereas the later is dominant in remote regions. An additional process contributing to mercury deposition is air-surface exchange of Hg^0 (mainly with vegetated surfaces). Taking into account the relatively even global distribution of Hg^0 concentration (1.2-2.2 ng/m^3) one can expect that this process is rather defined by local surface conditions (land cover type, solar radiation, surface wetness and temperature, etc.) then by remoteness from the source regions.

Simulated global patterns of Hg deposition reflect the peculiarities mentioned above (Fig. 2.2b). High Hg deposition fluxes are obtained in major industrial regions and over some remote areas characterized by enhanced precipitation. In general, deposition fluxes are higher in low and mid latitudes because of higher concentration of the main oxidants and precipitation amount. Besides, elevated deposition levels are also characteristic of the Polar Regions where the Atmospheric Mercury Depletion Events (AMDEs) take place. The lowest deposition fluxes occur in the inland of Antarctica and Greenland.

The most significant deviations of the multi-model simulation results are characteristics of areas with large anthropogenic and natural and secondary emissions. One of the reasons for that is the uncertainty of emission data (particularly, natural and secondary emissions). Application of considerably different emission values by the models does not hamper reproducing the restricted number of available background observations where the inter-model deviation is relatively small. But the deviation increases significantly in the industrial regions and areas with large evasion fluxes. Another reason is substantially different spatial resolution of the participating models. Models with lower resolution fail to reproduce strong concentration gradients in the vicinity of emission sources and predict a smoother spatial distribution.

This is clearly seen in the set of concentration cross-sections presented in Fig. 2.2. The cross-sections through East Asia and South Africa (Figs. 2.2a,b) demonstrate significant differences between the models in these regions where the models with finer resolution predict considerably higher concentration peaks. On the other hand, the modelling results are quite consistent in remote regions where difference does not exceed 20%. An exception is high-latitude areas over the Southern Ocean where one of the models simulates essential decrease of annual mean concentration of Hg^0 due to its rapid oxidation and subsequent deposition during the AMDEs. Other models either predicted a much smaller effect of AMDEs in this area or did not take this phenomenon into account at all.

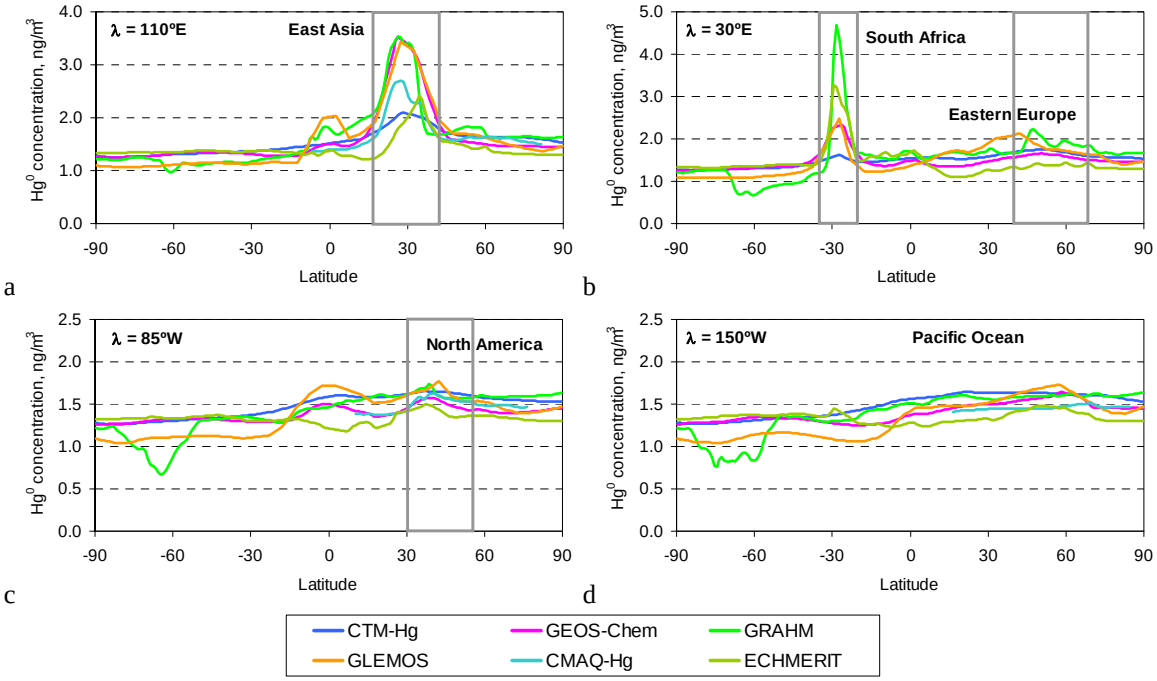

Fig. 2.2. *South-to-north cross-sections of simulated annual mean Hg^0 concentration in the ambient air corresponding to fixed geographical longitudes: (a) – λ = 110°E; (b) – 30°E; (c) – 85°W; (d) – 150°W. Directions of the cross-sections are delineated in Fig. 1.1*

2.3. Intercontinental transport of mercury

In order to evaluate the source attribution of Hg deposition all the participating models performed a number of perturbation runs zeroing out emissions in one of the eight source regions - Europe, North and South America, East, South and Central Asia, Africa and Australia with Indonesia. Besides, an additional model run was performed without any anthropogenic emissions to estimate contribution from natural and secondary emissions. Configuration of the source regions and the spatial distribution of anthropogenic mercury emissions in 2005 according *AMAP/UNEP* [2008] are given in Fig. 2.3a. Figure 2.3b presents the relative contribution of the source regions to global anthropogenic Hg emission. This shows that more than 45% of the total global mercury emissions in 2005 originated in East Asia.

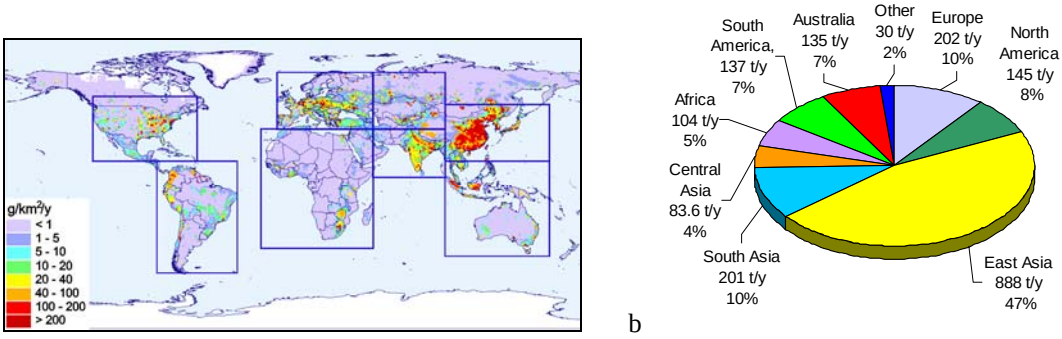

Fig. 2.3. *Global distribution of anthropogenic mercury emissions in 2005 (a) and the relative contribution of eight source regions to the global mercury emission (b). Rectangles show situation of the eight source regions*

Average levels of Hg deposition to a number of receptor regions in 2005 simulated by the four participating models are shown in Fig. 2.4 along with the source-attribution information. All the models predict Hg deposition levels comparable in Europe, North America and South Asia, and higher by a factor of 1.5 in East Asia. The inter-model deviation of the average deposition fluxes varies within 30-50% for different regions. It is particularly remarkable taking into account the fact that one of the models (GEOS-Chem) utilized completely different assumptions on Hg atmospheric chemistry. This model predicts higher deposition in comparison to the others but the difference is not extraordinary and falls within the common range of uncertainty. An exception is the Arctic where the inter-model deviation is much higher. The difference between the highest and the lowest estimates of annual Hg deposition to the Arctic exceeds a factor of 4. To explain this it should be mentioned that the lowest estimate (CMAQ-Hg) has been made without taking into account the effect of AMDEs on Hg deposition in the Arctic and, therefore, it is likely that it underpredicts real deposition levels in this region. On the other hand, the highest estimate (GEOS-Chem) presents the gross deposition to the Arctic, whereas two other models (GRAHM and GLEMOS) rather operate with net deposition that can be considered as a residual of gross deposition and prompt secondary emission.

In spite of the considerable difference in deposition estimates, the models are consistent in the evaluation of the source attribution. Relative contributions of the major source regions to Hg deposition are very similar among the models (Fig. 2.4). Typically domestic sources make the largest anthropogenic contribution to Hg deposition in the respective regions but the second largest contributor is East Asia contributing to 10-14% Hg deposition in other regions. In North America the contribution of the East Asian sources is even comparable with the contribution of domestic sources. Besides, the intercontinental transport from the European anthropogenic sources contributes to 2-5% to deposition in other regions, the South Asian sources – 2-3%, and the North American sources – 1-2%, respectively. In all the regions except for East Asia, more than half of total deposition consists of contribution from natural and secondary emissions. Aggregated contribution of the intercontinental transport from foreign anthropogenic sources is shown in Fig. 2.5. As seen the contribution of foreign emissions varies from 10% to 30% on average in different regions. Within the regions, the influence of anthropogenic intercontinental transport can be considerably lower in the vicinity of the local emission sources and somewhat higher at the periphery.

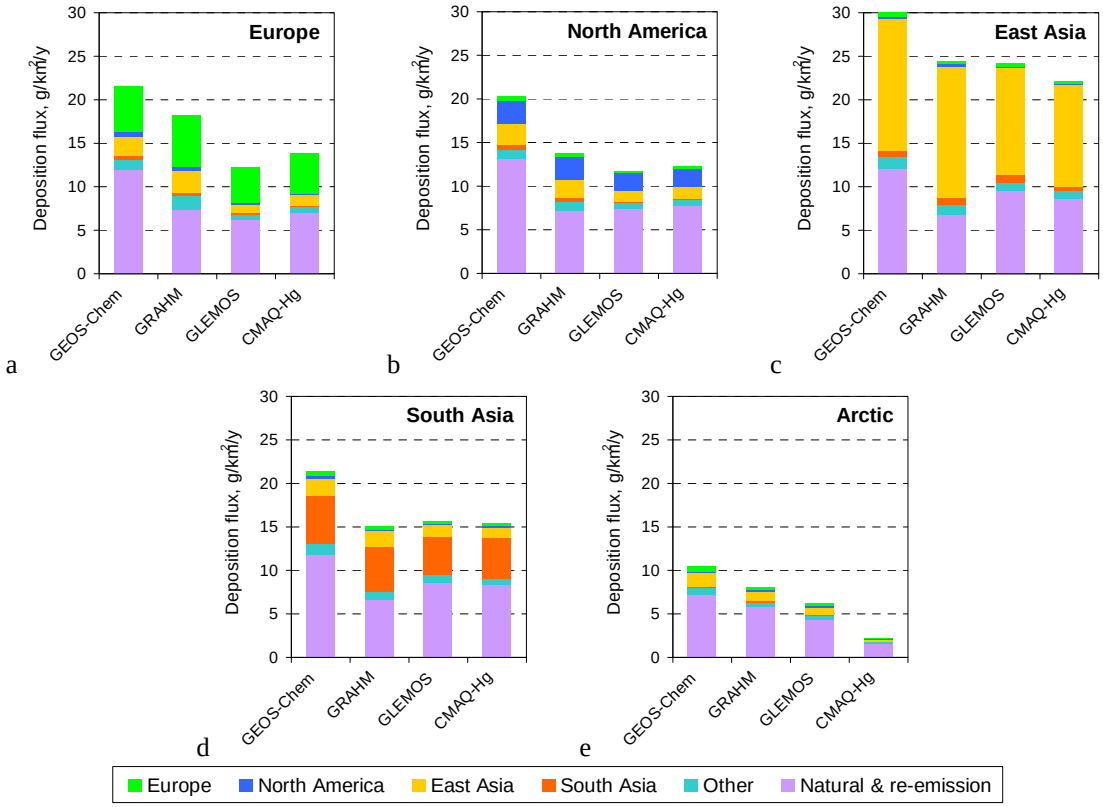

Fig. 2.4. *Simulated average Hg deposition fluxes and contribution major source regions to Hg deposition in Europe (a), North America (b), East Asia (c), South Asia (d), and Arctic (e) in 2005*

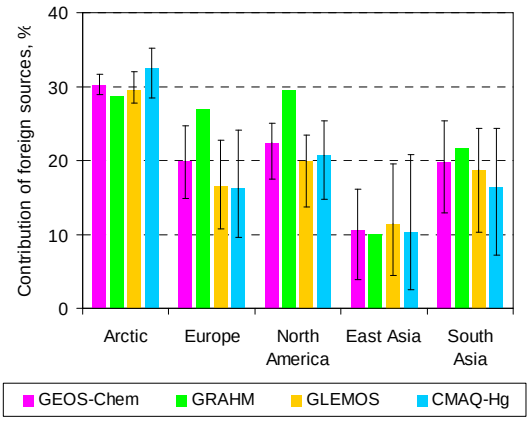

Fig. 2.5. *Contribution of foreign anthropogenic sources to Hg deposition in different receptor regions in 2005. Bars present average values, whiskers show 90%-confidence interval of the parameter variation over a region*

2.4. Future trends of mercury pollution

Future changes in mercury pollution levels and intercontinental transport due to expected emission changes were studied at the second stage of the HTAP multi-model experiment for Hg. For this purpose, gridded emission data based on the inventory for 2005 and three emission scenarios for 2020 [*AMAP/UNEP*, 2008] were used in the study. All model simulations were performed using meteorological data corresponding to the reference year 2005.

According to [*AMAP/UNEP*, 2008] the first scenario ('Status Quo', SQ) assumes that current patterns, practices and uses that result in mercury emissions to air will continue. Economic activity is assumed to increase, including in those sectors that produce mercury emissions, but emission control practices remain unchanged. For the second scenario ('Extended Emissions Control', EXEC) it is assumed economic progress at a rate dependent on the future development of industrial technologies and emissions control technologies, that is, mercury-reducing technology currently generally employed throughout Europe and North America would be implemented elsewhere. The third scenario ('Maximum Feasible Technological Reduction', MFTR) assumes implementation of all available solutions/measures, leading to the maximum degree of reduction of mercury emissions and its discharges to any environment; cost is taken into account but only as a secondary consideration. Figure 2.6 illustrates changes of total Hg emissions in four major source regions between 2005 and 2020 according to the emission scenarios. As seen the SQ scenario expects a moderate increase of emissions in all the regions except for North America. The EXEC and MFTR scenarios predict an emission decrease roughly by a factor of two and the difference between these two scenarios is not significant. A more detailed description is given in *AMAP/UNEP* [2008].

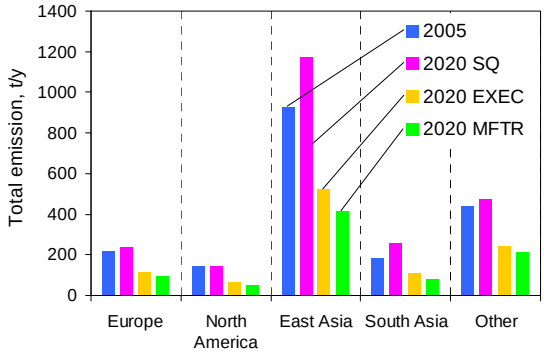

Fig. 2.6. *Changes of total Hg emission in four major source regions according to three emission scenarios for 2020 [AMAP/UNEP, 2008]*

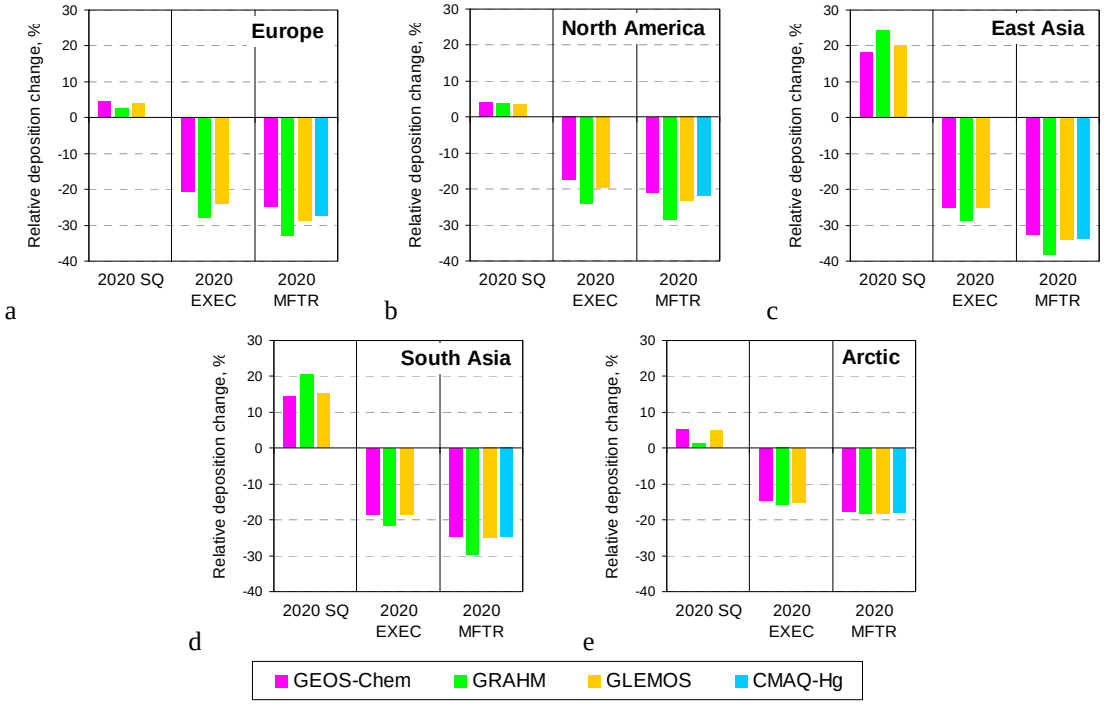

Fig. 2.7. *Relative change of Hg deposition between 2005 and 2020 in Europe (a), North America (b), East Asia (c), South Asia (d) and Arctic (e) according to three emission scenarios (SQ, EXEC, MFTR). Positive values correspond to increase of deposition*

Estimated deposition change between 2005 and 2020 in accordance with the three emission scenarios is illustrated in Fig. 2.7. The models agree well in the estimates of the relative deposition changes. According to the 'Status Quo' scenario, Hg deposition in Europe and North America will increase by 3-

5%. In South and East Asia the increase will amount to 15-20% and 18-25%, respectively. Two other scenarios predict a deposition decrease in all considered regions. For the 'Extended Emissions Control' scenario the largest deposition decrease is expected in East Asia (25-28%) and the smallest – in North America (18-24%). The 'Maximum Feasible Technological Reduction' predicts somewhat higher decrease of Hg deposition varying from around 25% in North America to 35% in East Asia. The Arctic represents a typical remote region that does not contain internal emission sources on its territory. Therefore, the deposition changes are less significant in this region: increase by 1.5-5% according to the SQ scenario, and decrease by 15% and 18% according to the EXEC and MFTR scenarios, respectively.

2.5. Uncertainty of model estimates

To estimate the modelling uncertainty the simulation results were evaluated against available long-term measurements. The analysis involved observations of Hg^0 from the AMAP, EMEP, and CAMnet monitoring networks as well as from some other monitoring sites: Look Rock, USA [*Valente et al.*, 2007]; Mount Bachelor Observatory, USA [*Jaffe et al.*, 2005b]; Cape Point, South Africa [*Baker et al.*, 2002], Kang Hwa, Korea [*Kim et al.*, 2002], Neumayer Station, Antarctica [*Temme et al.*, 2003]. For evaluation of wet deposition long-term measurements from the EMEP (Europe) and NADP/MDN (North America) monitoring networks were used. Limited geographical coverage of regular wet deposition measurements restrains evaluation of this parameter simulated by the models.

The suite of models participated in the HTAP experiment cover almost the complete range of uncertainties in emission estimates (anthropogenic, natural and secondary emissions), in atmospheric processes (chemistry, deposition, in-cloud transformation including Hg-particle interactions), and in model configurations (global vs. regional models, model grid resolution and initial/boundary conditions for the regional model). Therefore, the range of model results provides a reasonable estimate of combined uncertainty in the predicted quantities of atmospheric mercury and the source-receptor relationship.

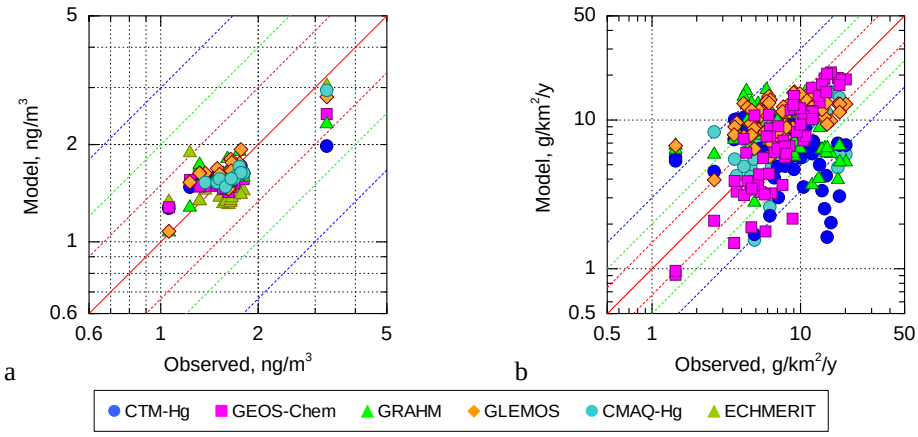

Fig. 2.8. *Comparison of simulated gaseous elemental mercury concentration in ambient air (a) and wet deposition flux (b) against long-term measurements. Red solid line depicts the 1:1 ratio; dashed lines show different deviation levels: red – by factor of 1.5, green – by factor of 2, blue – by factor of 3*

Figure 2.8 presents the model-to-observation comparison for annual mean Hg^0 concentration in the ambient air and wet deposition flux simulated by all participating models. It is clearly seen that scattering of the comparison points is much wider for wet deposition flux indicating larger deviations between the measurements and simulation results. This can be explained by larger effect of

uncertainties associated with the simulation of precipitation rates and Hg atmospheric chemistry on wet deposition modelling. Statistical analysis of the comparison results shows that uncertainty for Hg^0 concentration varies within the range 7-14%. Besides, 82-100% of modelling results agree with observations within a factor of 1.2. Uncertainty of wet deposition flux is considerably larger (39-74%), and for 57-91% of the comparison results the model-to-observation deviation does not exceed a factor of two.

Taking into account limited amount and scarce spatial coverage of available Hg observations additional information on the model uncertainty can be derived from analysis of the inter-model deviation of the simulation results. It is particularly relevant for evaluation of the simulation parameters which cannot be directly measured (total deposition, source attribution etc.). Estimates of the inter-model relative deviation (defined as the ratio of standard deviation to the model ensemble mean) of simulated Hg^0 surface air concentration and total deposition flux are presented in Fig. 2.9 for a number of selected receptor regions. The deviation of simulated Hg^0 concentration does not exceed 20% and is the largest in South Asia and the lowest over remote regions (North Atlantic, Pacific, and Arctic). The deviation of total deposition is considerably higher but does not exceed 80% in all the regions except for the Arctic where it reaches 120% because of the model uncertainties associated with parameterization of AMDE.

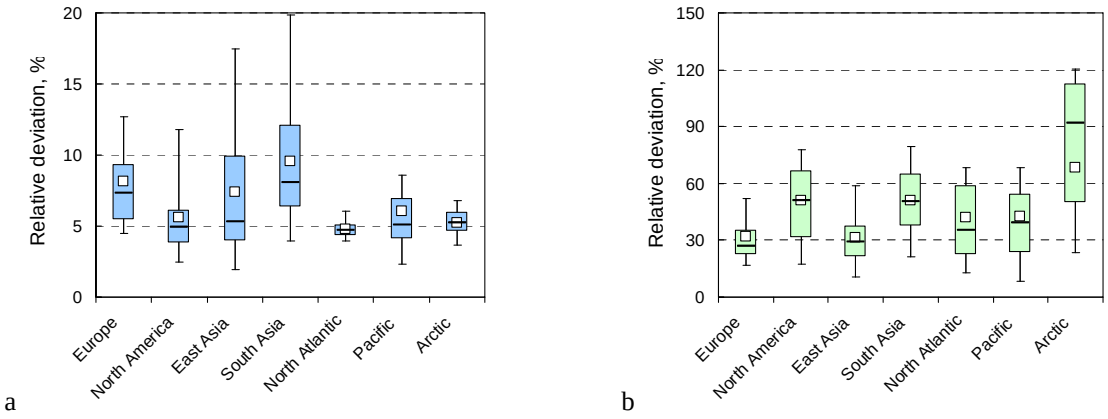

Fig. 2.9. *Inter-model relative deviation of simulated Hg^0 surface air concentration (a) and total deposition flux (b) in different receptor regions*

The multi-model source attribution simulations provide quantitative estimates of model uncertainty in evaluation of intercontinental transport. Figure 2.10 shows the inter-model deviation of simulated source attributions for Hg deposition in various receptor regions. The deviation of both absolute and relative contributions of the major source regions to Hg deposition flux is presented in the figure (Figs. 2.10ab, respectively). As seen the inter-model deviation of the absolute contribution of the sources is comparable with uncertainty of total deposition and varies within 10-80%. On the other hand, the deviation of relative source contributions is much smaller and commonly does not exceed 30%. This effect can be partly explained by long residence time of Hg in the atmosphere leading to significant mixing of emissions from different sources in the global Hg atmospheric pool. Therefore, transport pathways and physical-chemical processes have a lesser effect on relative source contribution to Hg deposition, particularly, in remote regions.

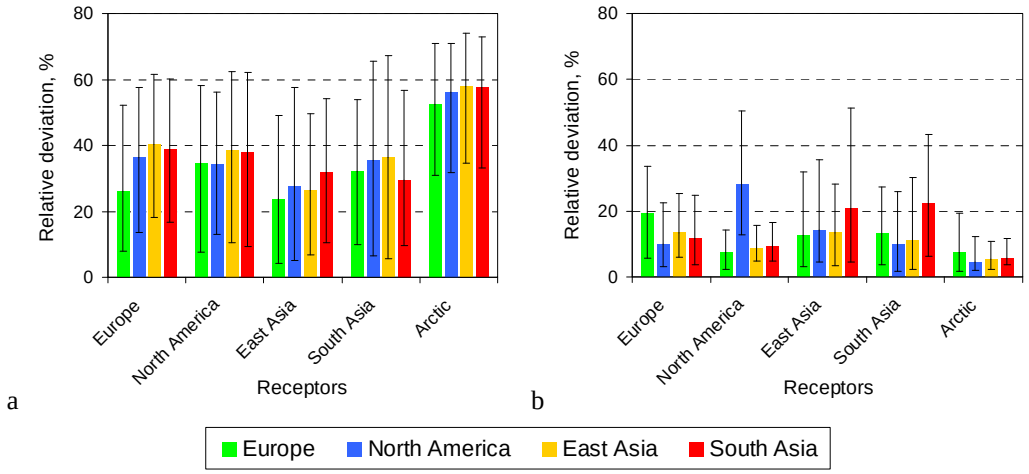

Fig. 2.10. *Inter-model relative deviation of absolute (a) and relative (b) contributions of major source regions to Hg deposition in various receptor regions. Bars present average values, whiskers show 90%-confidence interval of the parameter variation over a region*

2.6. Key findings and recommendations

Based on the analysis of the multi-model experiment results for mercury presented in the HTAP 2010 Assessment Report the following key findings were formulated along with recommendations for the further improvement of the scientific background and reliability of the model estimates of mercury atmospheric dispersion and intercontinental transport.

Process understanding and modelling uncertainties

a) Findings

1. Numerous studies using mercury transport models have been conducted in the past two decades on both global and regional scales for a variety of tasks including understanding of Hg processes in the atmosphere, evaluation of Hg levels, and assessment of source-receptor relationships. In many cases the models demonstrate satisfactory agreement with observations; however considerable variability of the model results indicates essential gaps in knowledge of Hg atmospheric processes. In spite of significant uncertainties, Hg models have proven to be a useful tool for assessing Hg pollution.
2. Ambient concentrations of elemental gaseous mercury, species responsible for long-range atmospheric transport, are reliably simulated by contemporary models. Model results are consistent with observations that show similar concentration gradients from the Southern Hemisphere to the Northern Hemisphere. However, spatial coverage of available long-term observations is not sufficient for constraining the models adequately.
3. Atmospheric Hg deposition is mostly defined by short-lived oxidized Hg species originating both from direct anthropogenic emissions and from in situ oxidation of elemental Hg in the atmosphere. Both dry and wet removal pathways are equally significant to the total deposition of mercury. Gaps in our knowledge of Hg atmospheric chemistry and emission speciation lead to significant uncertainties in simulated deposition fluxes.
4. The largest uncertainty of simulated atmospheric deposition of Hg is associated with dry uptake of various Hg forms by the surface because of the absence of systematic observations related to dry deposition of mercury. Model simulated wet deposition agrees with observations,

however available measurements of wet deposition are severely restricted in geographical coverage. The differences between models are largest in the regions of sparse measurements such as, the oceans, the Arctic, South Asia, and Africa.

5. The Arctic is a unique remote region because it does not have anthropogenic emission sources on its territory and undergoes a period of the atmospheric mercury depletion events (AMDEs) during springtime defining an important Hg load to the region. The models show significant deviation in estimates of Hg deposition to the Arctic due to the uncertainties in the model formulation of the processes related to AMDEs.
6. The models represented in this study cover almost the complete range of uncertainty in emission estimates and the model formulations therefore the range of model results provides a reasonable estimate of uncertainty in predicted quantities. The magnitudes of model uncertainties range from 20% for the simulated air concentration of Hg^0, up to 80% for the simulated total deposition. However, the simulation results for the relative source attribution have a smaller uncertainty at about 30%. This also indicates that different models have consistent results in predicting the source-receptor relationships.

b) Recommendations

1. There is a need for a comprehensive interoperable measurement network for mercury in the environment to constrain models and track future mercury trends. Extensive regular observations of speciated Hg concentrations are required for the full-scale model evaluation in different parts of the globe, in particular, in Asia, different regions of the Southern Hemisphere, over the oceans, and in the Polar Regions. Regular observations of wet and, in particular, dry deposition of Hg are highly required for the improvement of model formulation and Hg deposition estimates.
2. Better understanding of Hg chemistry through laboratory studies and field measurements are needed, particularly, for the gaseous and heterogeneous phase oxidation mechanisms, kinetics and products under different atmospheric conditions. The studied chemical mechanisms can be evaluated by application of self-consistent global chemical transport models in combination with extensive observational data.
3. Reliable assessment of intercontinental or global-scale dispersion of Hg requires development of multi-media biogeochemical models that take into account the entire cycle of Hg in the environment. It is particularly relevant for evaluation of long-term trends, future scenarios and the impact of climate change on mercury pollution. This is also important since the main exposure pathway of mercury to humans occurs through its bioaccumulation in biota in the aquatic environment.

Intercontinental transport and source-receptor relationships

a) Findings

1. Intercontinental transport of mercury can occur through two pathways. One is the direct transport of emitted mercury plumes from one continent to another. This pathway typically involves the lifting of mercury plumes to above the planetary boundary layer, followed by rapid atmospheric transport in the free troposphere. The other pathway is through the mercury emission input of a source region into the global mercury pool. This involves the release of Hg into air, dispersion in the atmosphere followed by oxidation and deposition removal as well as recycling in the environment.
2. The contribution of Hg intercontinental transport is significant, particularly in regions with few local emission sources. The models provide consistent estimates of intercontinental transport

and deposition. The contribution of foreign anthropogenic sources to annual deposition fluxes varies from 10% to 30%, on average anywhere on the globe. Besides, from 35 to 70% of total deposition to most regions consists of deposition contributed by global natural and secondary emissions. East Asia is the most dominant source region contributing to 10-14% Hg to deposition in other regions, followed by contributions from Europe (2-5%), South Asia (2-3%) and North America (1-2%).

3. Changes in emissions in one region affect mercury concentration and deposition in another region proportionally to the magnitude of source region's contribution to the receptor region. For example, 20% emission reduction in East Asia, Europe, South Asia, and North America separately results in 0.6-5.5%, 0.2-3.5%, 0.1-1.5% and 0.1-1.5% decrease of Hg deposition in other regions, respectively. The large contribution of natural sources and secondary emission of legacy Hg to deposition reduces the relative response of Hg deposition to the reduction in anthropogenic emissions. However, the response could be larger in the long-term perspective due to the lagged response of reduction of Hg recycling from planetary surfaces.

b) Recommendations

1. Model estimates of the effect of Hg intercontinental transport on regional pollution levels highly depend on the availability of reliable anthropogenic emissions data and, in particular, on speciation of Hg emissions. Therefore, further improvements of global Hg emission inventories are needed.
2. In light of the importance of natural emission and secondary emissions for Hg concentration and deposition over the globe under current and future conditions, more studies are required for quantitative and mechanistic understanding of Hg emissions from various surfaces (soils, water, and vegetation).

Future changes of Hg pollution

a) Findings

1. Three future emission scenarios for 2020 representing the status quo conditions (SQ), global emission controls similar to the present-day European controls (EXEC) and advanced global emissions control (MFTR) show significant changes in emissions in East and South Asia and smaller changes in European and North American emissions. The models considered in this study estimated consistent impact of the future emission scenarios on mercury deposition results with minimal uncertainty. Depending on the applied emission scenario the change of Hg deposition between 2005 and 2020 will increase by 2-25% for SQ and decrease by 25-35% for EXEC and MFTR in different industrial regions. In remote regions, such as the Arctic, the changes are expected to be smaller – from 1.5-5% increase (SQ) to 15-20% decrease (EXEC, MFTR).
2. Based on available mercury emission projections, the source-receptor relationships of anthropogenic emissions is not expected to change significantly in the next 20 years and the direction of changes depend on the assumptions of particular emission scenarios.

b) Recommendations

1. Few available projections of Hg anthropogenic emissions restrict model estimates of Hg concentration and deposition changes in the future. More efforts are needed for elaboration of future Hg emission scenarios as well as the application of chemical transport models in evaluating future changes of Hg pollution levels.

3. EMEP CASE STUDY ON HEAVY METAL POLLUTION ASSESSMENT

This chapter is devoted to the EMEP Case Study on heavy metal pollution assessment initiated by MSC-E and TFMM [ECE/EB.AIR/GE.1/2009/2]. The reasons to hold the Case Study, its general scheme, and expected output are described. Besides, current progress of this project is characterized. Special attention is given to contributions of countries-participants of the Case Study. Future plans are overviewed.

3.1. Objective

The main objective of the Case Study on heavy metals is to improve assessment of pollution levels in the EMEP domain on the base of the integrated analysis of factors affecting quality of the assessment including emissions, measurements, and modelling in individual countries. In the framework of this activity it is planned to collect country-specific emission data, monitoring information, geophysical information and carry out modelling of pollution levels with higher spatial resolution (e.g., 5×5 km^2 or 10×10 km^2) for individual countries. The Case Study is focused on priority heavy metals: lead, cadmium and mercury. It is planned to improve the assessment of heavy metal pollution levels over the entire EMEP region on the base of the results achieved for individual countries.

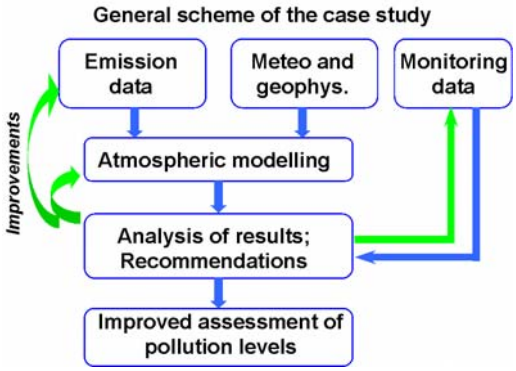

Fig. 3.1. *General scheme of the case study*

General scheme of the Study includes collection and preparation of necessary input information on emissions, measurements, and geophysical data (Fig. 3.1). On the base of these data modelling is carried out, the model results are analysed and the improvements concerning modelling, emissions and monitoring data are implemented.

General scheme of the Case Study consists of six work packages (WP):

WP1. Preparation of the emission data with high spatial resolution for modelling and analysis

WP2. Collection and analysis of monitoring data for pollution assessment

WP3. Preparation of input geophysical and meteorological data for modelling and modification of the model

WP4. Atmospheric modelling with high (5×5 km^2, 10×10 km^2) spatial resolution

WP5. Complex analysis of modelling results

WP6. Improved model assessment of pollution levels in a country

3.2. State of the art

Programme of the Case Study prepared by MSC-E was discussed at the TFMM meeting held in November 2009 in Ispra, Italy and now it is available in the internet [http://tarantula.nilu.no/projects/ccc/tfmm/index.html]. Special questionnaires were disseminated among countries in order to find out the availability of data. The form of this questionnaire can be found in the internet [http://tarantula.nilu.no/projects/ccc/tfmm/index.html].

Six countries-volunteers (the Czech Republic, the Netherlands, Croatia, Italy, Spain and Slovakia) expressed their wish to take part in the Case Study and filled in the questionnaire forms. Table 3.1 summarises responses of countries to questions concerning properties of the emission data, monitoring and geophysical information. As seen, all countries can provide the gridded emission data with 50-km resolution and most of countries – with finer resolution. The question regarding future emission scenarios and national-scale meteorological observations had not presented in the questionnaire and was requested at the recent TFMM meeting.

Table 3.1. *Availability of the emission data in countries for the case study*

Countries-volunteers	Czech Republic	Nether-lands	Croatia	Spain	Italy	Slovakia
Emission data						
Gridded, 50×50 km	✓	✓	✓	✓	✓	✓
Gridded, finer resolution (5-10 km)	+	✓	✓	+	+	-
Source category data	-	✓	✓	+	+	-
Large point source data	+	?	+	+	+	-
Detailed temporal resolution	-	-	-	+	+	-
Future emission scenarios	-	?	?	?	?	?
Monitoring data						
EMEP data	✓	✓	-	✓	✓	✓
Data from national networks	✓	✓	planned	+	+	+
Station's location characteristics	✓	+	+	+	+	+ (partly)
Meteo. data at stations	+	+ (partly)	+	+	+ (precip)	+ (partly)
Supplementary measurement data	+	?	-	+	-	-
Field campaigns	+	?	-	+	+	-
Geophysical data						
Land-cover information	+	+	-	+	+	+
Concentrations of HMs in topsoils and re-suspension of dust	+	?	+	+	-	-
Critical loads	+	?	-	?	-	-
Meteorological obs. data	+	-	+	+	?	?

'✓' – data submitted to MSC-E
'+' – data potentially available
'-' – data not available
'?' – availability is not known so far

3.3. Pilot results for the Czech Republic

Country-specific programme for the Czech Republic was prepared and considered at the joint expert meeting (Moscow, Russia, April , 2010). As a first step, it was agreed that the Czech Republic would provide measurement data on concentrations and wet deposition of cadmium from national monitoring network for 2007. MSC-E will prepare the model as well as input data for modelling and perform pilot calculations of pollution levels over the Czech Republic.

Contribution of the Czech Republic.

Measurement data on concentrations in air, in precipitation and wet deposition for 2007 have been provided by the Czech Republic. Map exemplifying measured levels of cadmium wet deposition is shown in Fig. 3.2. There are two stations in the Czech Republic which report regularly measurement information on heavy metals to CCC. However, there are about 30 stations measuring wet deposition of cadmium at national scale, which are a good basis for the evaluation and the analysis of modelling results. As seen from the map, the highest wet deposition levels take place in the northern and north-eastern parts of the country.

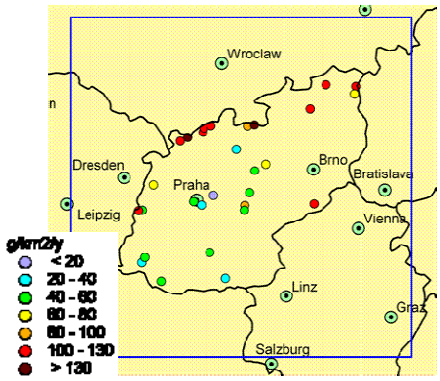

Fig. 3.2. *Measured wet deposition fluxes of cadmium in the Czech Republic in 2007*

Contribution of MSC-E

Meteorological data with fine resolution (10×10 km^2 and 5×5 km^2) were prepared for the Czech Republic. Finer resolution allows to reproduce more detailed fields of meteorological parameters. Example of maps of surface air temperature over the Czech Republic in 2007 with different spatial resolutions is given in Fig. 3.3.

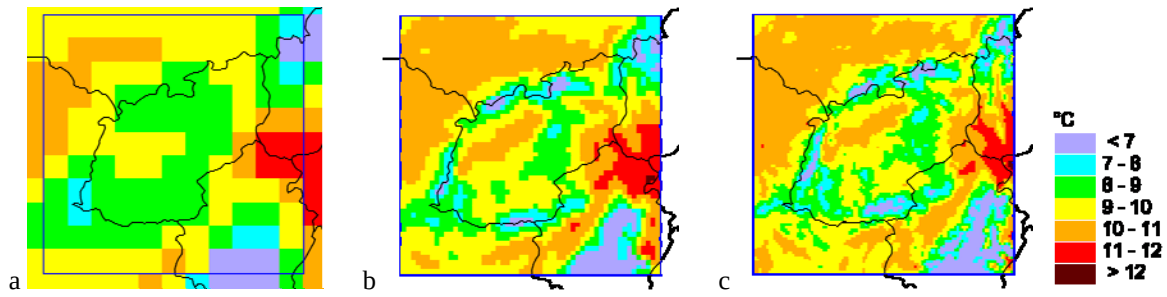

Fig. 3.3. *Annual mean surface air temperature in the Czech Republic with resolution 50×50 km (a), 10×10 km (b) and 5×5 km (c) in 2007*

Improvement of quality of meteorological data due to the increase of spatial resolution is demonstrated by the example of precipitation sums for the Czech Republic. Relative difference between modelled and observed precipitation decreases at the most of observation stations as the resolution increases (Fig. 3.4). When resolution is 50 km, for a half of stations relative deviation of modelled precipitation amounts from the observed one lies outside ±25% limits. For resolutions 10×10 and 5×5 km^2 the fraction of stations falling in these limits amounts to 22% and 14%, respectively. The better agreement between modelled and observed precipitation sums is seen also from the scatter diagrams (Fig. 3.5).

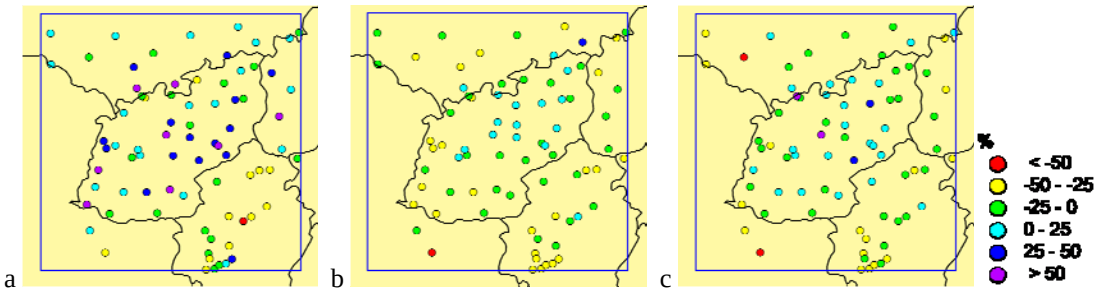

Fig. 3.4. *Relative difference (mm) between sums of annual precipitation calculated with resolution 50×50 km (a), 10×10 km (b) and 5×5 km (c) and observed at synoptic stations in the Czech Republic in 2007*

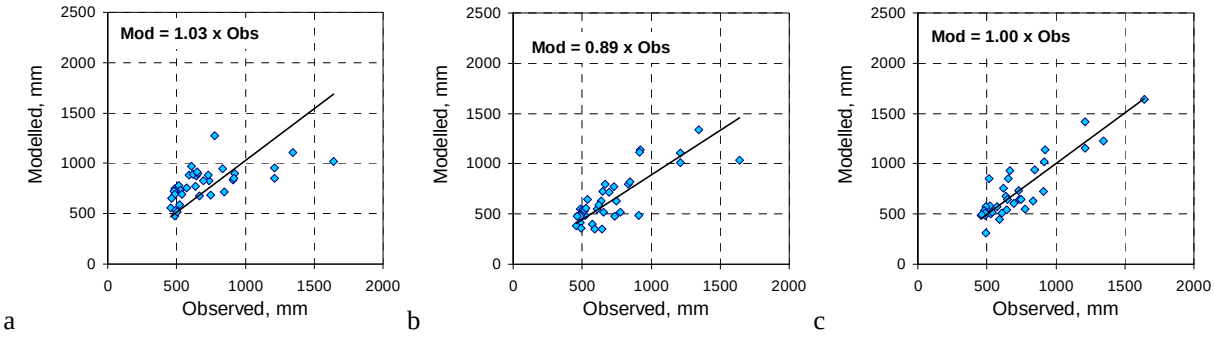

Fig. 3.5. *Modelled vs. observed annual precipitation sums in the Czech Republic inn2007 for resolution 50×50 km (a), 10×10 km (b) and 5×5 km (c)*

Table 3.2 summarises some statistical indexes confirming improvement of quality when resolution increases. For example, relative bias, which characterizes difference between two sets of data expressed in relative terms, decreases from 13% to 1% when resolution increases from 50 to 5 km. Spatial correlation coefficient also increased from 0.61 to 0.89.

Table 3.2. *Statistical indexes for comparison of calculated and observed precipitation amounts in the Czech Republic in 2007*

Spatial resolution, km	50 x 50	10 x 10	5 x 5
Relative bias, %	13	-9	1
Absolute bias, mm	87	-65	7
R_{corr}	0.61	0.80	0.89

Input geophysical information prepared for modelling with the resolution 10×10 km^2 includes data on land-cover and concentrations in soils. Land cover is important for the modelling of dry deposition. Besides, ecosystem-dependent deposition are needed for evaluation of critical loads exceedances. It is generated on base of MODIS satellite information [www-modis.bu.edu/landcover/] (Fig. 3.6a).

Wind re-suspension is significant factor of heavy metal pollution in Europe. Its contribution can exceed 50% in a number of countries [*Ilyin et al*, 2009]. Information on concentrations in topsoil is required to estimate wind re-suspension. Gridded concentrations of cadmium in top soils (10×10 km^2) in the Czech Republic are prepared by krigging of observational data (Fig. 3.6b). Topsoil observations of heavy metal concentrations are derived from the European-wide project FOREGS [www.gtk.fi/publ/foregsatlas/].

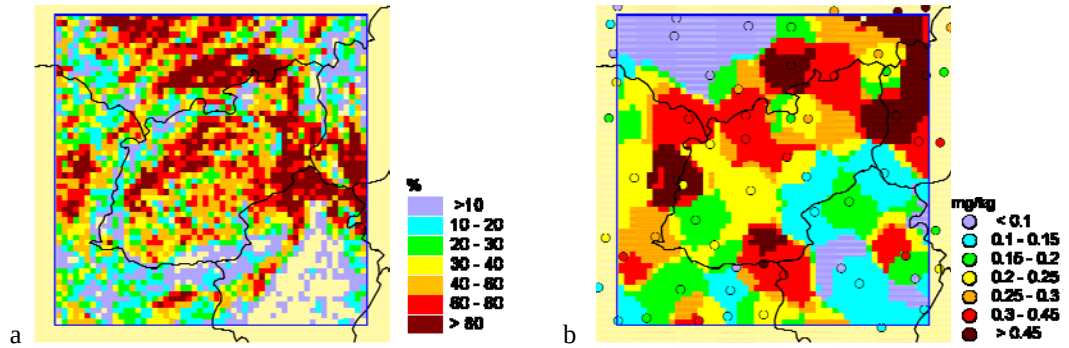

Fig. 3.6. *Spatial distribution of crop lands (a) and measured and gridded concentrations of cadmium in soils in the Czech Republic (b). Spatial resolution of the gridded parameters is with 10×10 km²*

Pilot calculations of pollution levels of cadmium over the Czech Republic with 10×10 km² and 50×50 km² resolution were carried out for 2007. The purpose of this modelling was to test the model adjusted to finer spatial resolution over the selected area. For this experimental modelling the emission data were prepared by interpolated of the emissions with 50-km resolution.

Spatial patterns of annual mean concentrations of cadmium in air calculated with different resolutions are similar in general (Fig. 3.7). It is not surprising keeping in mind that the emission data are actually identical. Nevertheless, there are also a number of differences in the two maps. For example, 50-km concentrations on the west of Prague do not exceed 0.5 ng/m³, and nearby Dresden – 0.3 ng/m³. However, 10-km concentrations lay within 0.5-1 ng/m³ limits in this region.

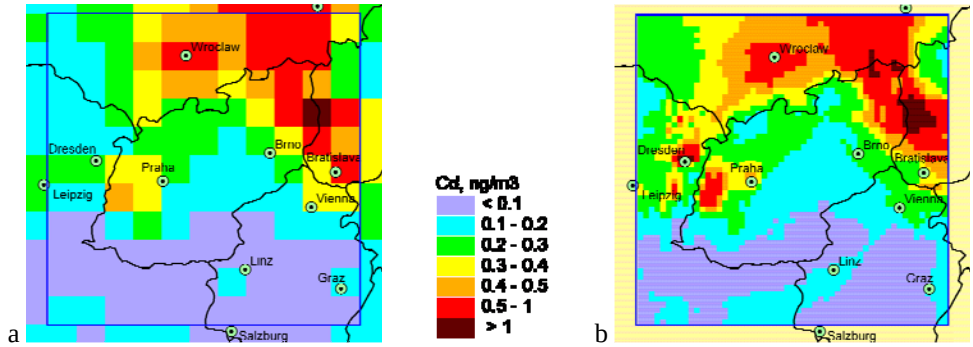

Fig. 3.7. *Concentrations of cadmium in air in the Czech Republic in 2007 with resolution 50×50 km² (a) and 10×10 km² (b)*

Similar peculiarities are noted for maps of total deposition flux of cadmium (Fig. 3.8). The patterns in general are quite similar. However, at finer-scale (local) levels the differences in two maps are distinguished. For example, the differences are well seen for regions nearby Wroclaw, Brno or Dresden. The differences in concentrations and deposition are totally caused by changes in spatial resolution of land cover, meteorological data, and wind re-suspension.

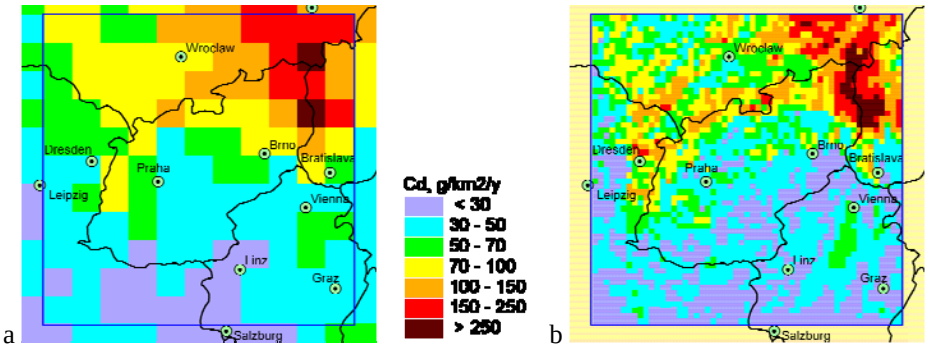

Fig.3.8. *Total deposition of cadmium in the Czech Republic in 2007 with resolution 50×50 km^2 (a) and 10×10 km^2 (b)*

Concluding remarks and future contribution for the Czech Republic

Information on concentrations and deposition observed at national monitoring network was submitted to MSC-E. The model was prepared for simulations of heavy metal pollution levels over the Czech Republic with fine (10×10 km^2) resolution. Pilot simulations of deposition and concentrations of cadmium were performed. Further calculations will include the following:

- Concentrations and deposition with high (10×10 km^2) resolution
- Contribution of neighbouring countries to pollution levels in the Czech Republic
- Contribution of source categories to pollution levels
- Contribution of large point sources to pollution levels in the Czech Republic
- Contribution of big cities to pollution levels in the Czech Republic (Prague, Ostrava region)

Furthermore, modelled pollution levels will be compared with national measurement data. Gridded meteorological data will be further validated via comparison with observed information from national synoptic network. The updated data based on soil concentration will be used for the improvements of wind re-suspension over the country.

3.4. Contributions to the Case Study of Croatia, Italy, Slovakia, Spain and the Netherlands

Countries-volunteers have started collection of input data for the Case Study. Viewpoints and ideas of the countries about the case study and current progress in this activity were presented and discussed at the TFMM meeting (Larnaca, Cyprus, May, 2010). Short overview of presentations of the countries is given in this section.

Croatia

Croatia has already gained significant experience in the national-scale modelling with fine resolution. In the framework of project EMEP4HR (2006-2009) high-resolution model has been developed. In the framework of the case study the country would like to obtain model-based information on pollution levels of heavy metals, namely, lead, cadmium and mercury over Croatia with high spatial resolution.

Processes controlling pollution levels will be investigated via combined use of modelling approaches, emission inventories and monitoring data.

Information on emissions and monitoring activities was presented at the meeting. Emission data on lead, cadmium and mercury are available for the periods since 1990. Country's emissions are presented as contributions of different source categories distributed with 10-km resolution over territory of Croatia (Fig. 3.9a). Road transport was a dominating source of lead emissions in nineties (Fig. 3.9b). At present the main contributors to emissions are road transport and production processes. It is important to note that the emission data on heavy metals with 10-km resolution have already been submitted to MSC-E.

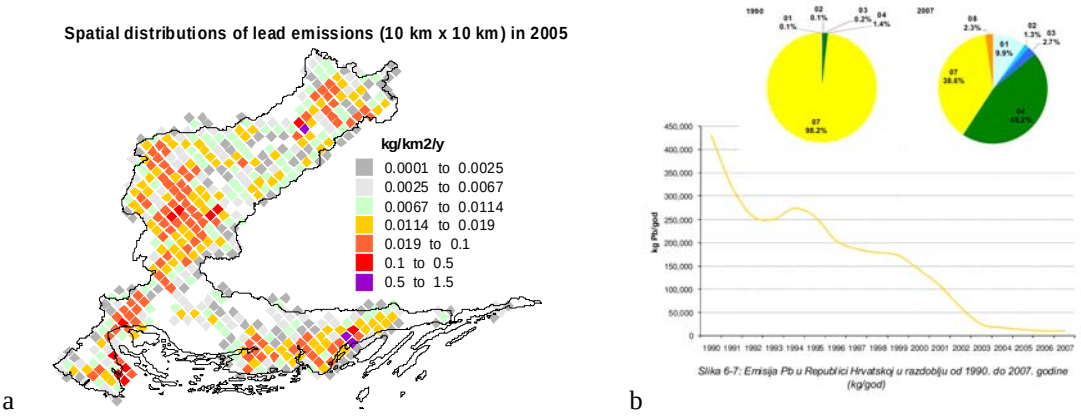

Fig. 3.9. *Spatial distribution of emission of lead in Croatia with 10×10 km^2 resolution (a) and long-term trend of emission and contribution of emission source categories to total emission of lead in Croatia (b)*

Development of national monitoring network of heavy metals in Croatia is ongoing. Currently there are four stations, located in Zagreb, Split, Sisak and Rijeka measuring heavy metals concentrations in air on daily basis. Example of monthly and annual mean values of cadmium concentrations monitored at these stations is presented in Fig. 3.10. Deposition measurements of heavy metals are carried out at stations in Zagreb, Rijeka, Split and Nasice. Besides, it is planned to establish 12 stations measuring concentrations of heavy metals in precipitation.

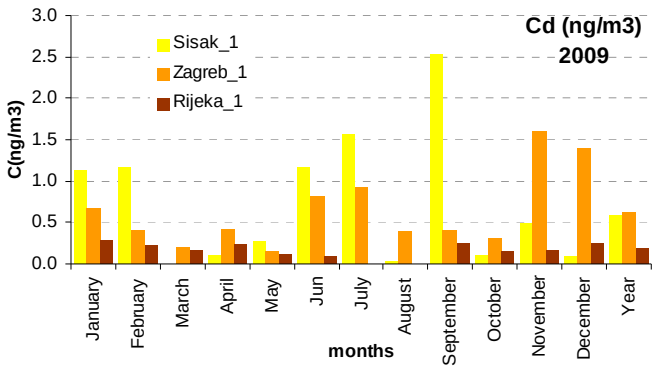

Fig. 3.10. *Monthly and annual mean concentrations of cadmium in air measured at stations in Zagreb, Split and Sisak in 2009*

Italy

Italy has presented information about available heavy metal emission data, monitoring activity and national-scale atmospheric modelling. Heavy metal emission inventories include country's total data split into different source categories. For example, main emission sources of lead, cadmium and mercury in Italy are industrial combustion, residential combustion and production processes (Fig. 3.11). Information on monthly, weekly and daily variability of the emissions as well as about spatial disaggregation of the emissions was presented.

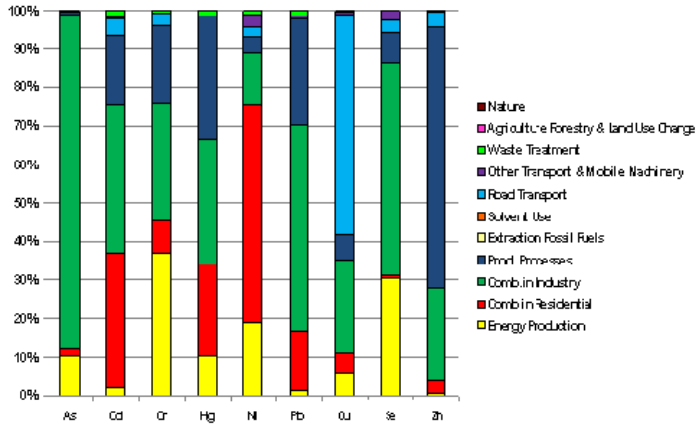

Fig. 3.11. *Contributions of different source categories to heavy metal emissions in Italy in 2005*

Monitoring of heavy metals is carried out at one EMEP station Montelibretti (Fig. 3.12) and at national monitoring networks. At present measurements of lead at urban, suburban and rural stations are available from 33 stations, and cadmium – from 19 stations located in the northern par of Italy.

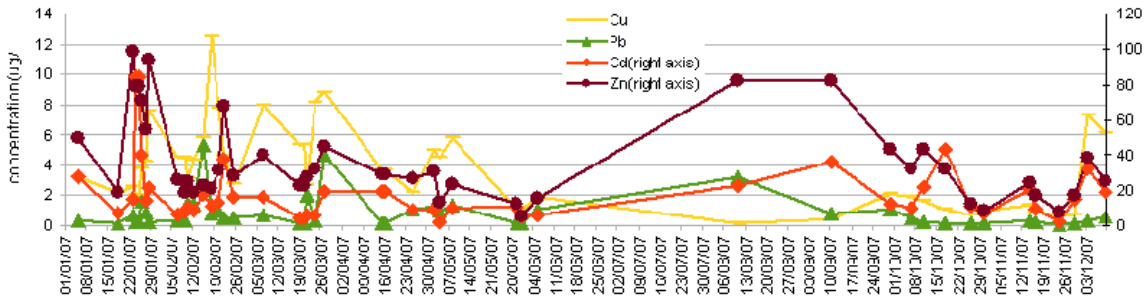

Fig. 3.12. *Measurements of heavy metals in precipitation at station Montelibretti in 2007*

Comparison of modelling results obtained by the EMEP MSCE-HM model and national models is assumed to be one of activities within the case study. Italy presented national modelling system MINNI, consisting of meteorological, emission and atmospheric transport sub-systems. Atmospheric chemical transport model FARM takes into account such processes as dispersion, wet and dry removal, treatment of fine and coarse fractions of aerosols, and detailed gaseous and aqueous chemical mechanisms.

Slovakia

Overview of national heavy metal monitoring and emission data was presented by Slovakia. There are four EMEP background stations performing monitoring of heavy metal concentrations (including lead and cadmium) in air on weekly basis and concentrations in precipitation on monthly basis (Fig. 3.13). Besides, six urban stations carry out monitoring of concentrations in air every second day.

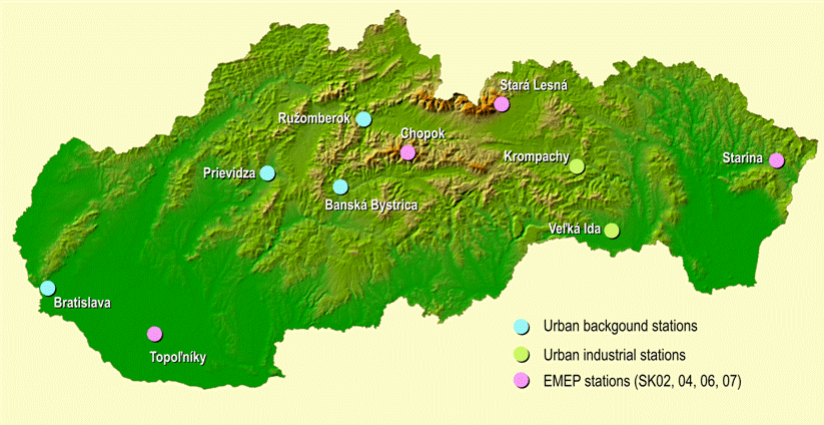

Fig. 3.13. *Location of monitoring stations in Slovakia*

Emissions of different source categories of lead and cadmium were presented. Temporal changes of contributions of source categories to national total value were analyzed. For example, total emission of lead in Slovakia in 1990 made up around 150 tonnes (Fig. 3.14). The highest contribution (more than 40%) to this value was made by road transport. By 2008 the emissions of lead declined almost twice. The main emission sources in 2008 were agglomeration of iron ore and waste incineration, while the role of road transport reduced to 3% of total value. In case of cadmium the main source category for the entire period of 1990 - 2008 was glass production, which contribution remained almost the same and amounted to 70 – 75%.

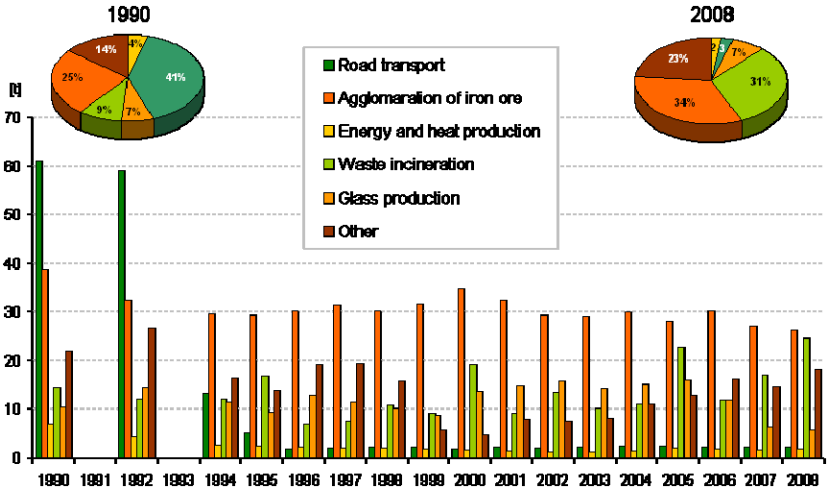

Fig. 3.14. *Emission from main source categories of lead in 1990 – 2008 in Slovakia*

Spain

Development and testing of national atmospheric transport model for heavy metals was presented by Spain (CIEMAT). It is based on the CHIMERE chemical transport model and operates over two domains: European domain with coarse (0.5° x 0.5°) resolution and finer-scale domain (resolution 0.2° x 0.2°) covering Spanish territory.

Emissions of lead and cadmium used in modelling are data officially reported to EMEP. They split in different emission source categories. For each category monthly, weekly and daily variations of emissions are introduced. Map of total emissions of lead and cadmium in Spain used in modelling is demonstrated in Fig. 3.15.

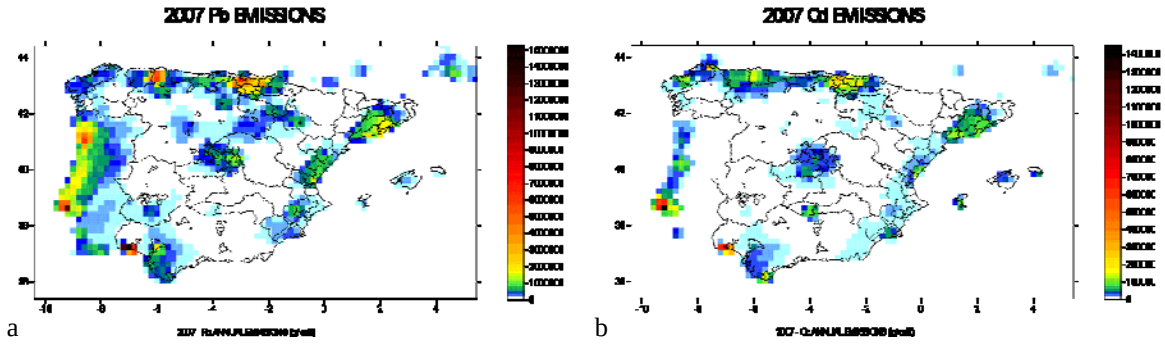

Fig. 3.15. *Maps of lead (a) and cadmium (b) emissions in Spain in 2007*

On the base of the official emission data and meteorological information for 2007 maps of concentrations and deposition were generated. The highest simulated concentrations of lead and cadmium in air are noted for regions known for significant emission sources (Fig. 3.16), namely northern, south-western and north-eastern coasts and the central part of the country.

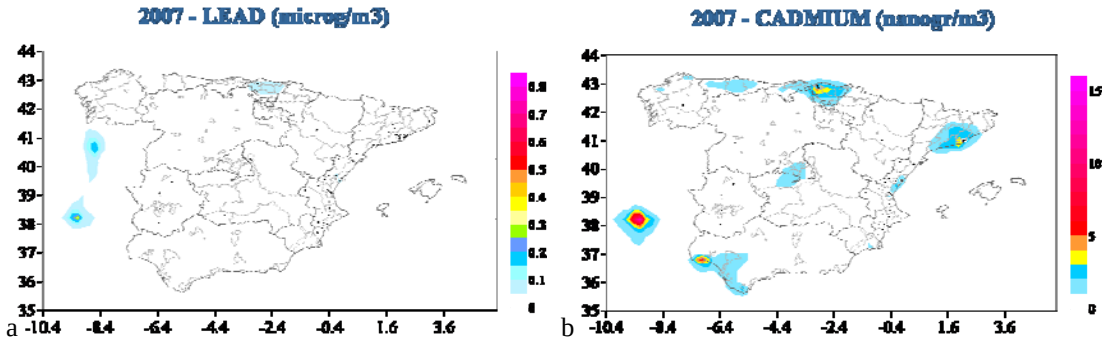

Fig. 3.16. *Maps of modelled annual mean air concentrations of lead (a) and cadmium (b) in Spain in 2007*

The model was tested via comparison of modelled values with observations. Both EMEP data and measurement information from national networks was involved into the comparison. The observed levels of lead and cadmium were reproduced by the model reasonably well.

Netherlands

The aim of the Netherlands to participate in the case study was to have an up-to-date assessment of current pollution levels of heavy metals (concentration and deposition). It is planned to use the outcome of the case study in the assessment of the monitoring program of heavy metals in the Netherlands. To achieve this aim it is planned to contribute gridded emission data with high (5×5 km^2) resolution and the data from national monitoring network.

Detailed gridded emission data with fine resolution have already available in the Netherlands. For the EMEP purposes these data are converted to 50-km resolution. For this case study the data on lead, cadmium and mercury were transformed to 5×5 km^2 resolution (Fig. 3.17) and submitted to MSC-E.

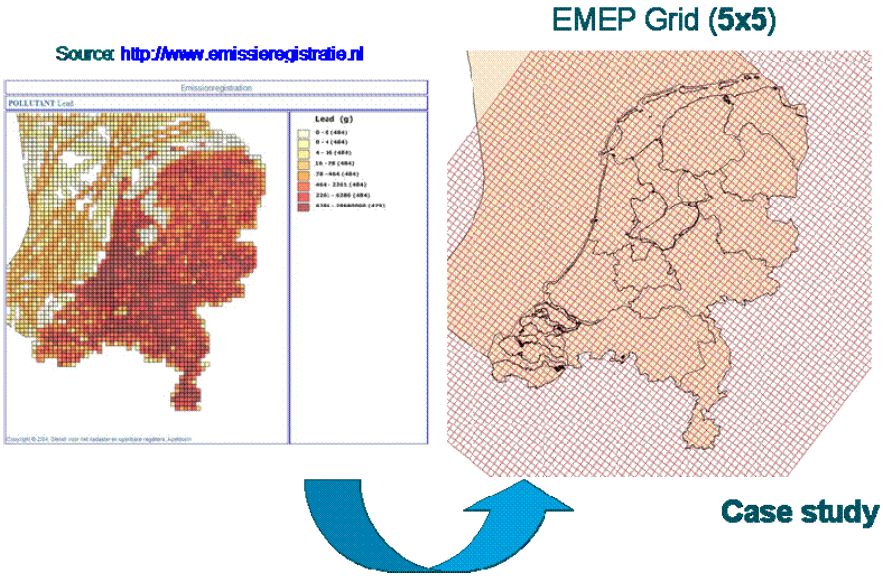

Fig. 3.17. *Preparation of the Dutch emission data with 5×5 km^2 resolution*

Monitoring information in the Netherlands is available from 6 stations measuring concentrations in air and 4 stations – in precipitation. Concentrations in air are measured every second day. Frequency of measurements in precipitation is one week (Fig. 3.18).

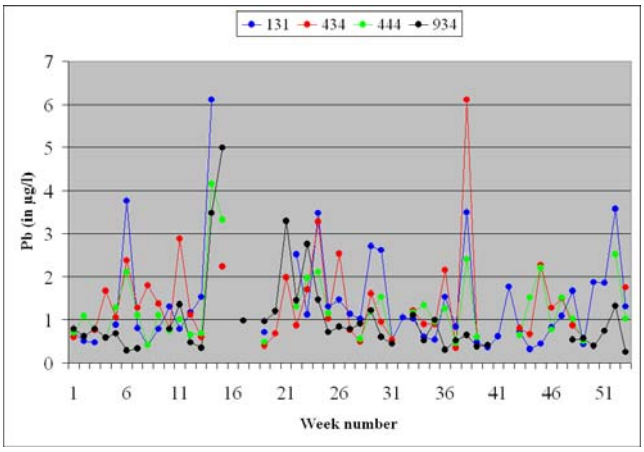

Fig. 3.18. *Measured concentrations of lead in precipitation at the Dutch stations in 2007*

3.5. Further activities

MSC-E will continue to tightly cooperate with all six countries-volunteers of the Case Study next year.

Taking into account that Croatia and the Netherlands have already provided MSC-E with the emission data on lead, cadmium and mercury with high resolution and monitoring data, country-specific programmes for these countries will be developed in close cooperation with the national experts. Model calculations are planned to be started in autumn, 2010.

Following the request of Italy information on boundary concentrations of mercury for national-scale model will be generated and delivered to ENEA in autumn, 2010.

Further work with other countries on the Case Study depends on the submission of their input data. On the base of the results obtained for the individual countries-volunteers the model assessment of pollution levels in the entire EMEP domain will be improved.

4. ASSESSMENT OF HEAVY METAL POLLUTION WITHIN EMEP REGION

This chapter is focused on the integrated assessment of heavy metal (Pb, Cd, Hg) pollution levels in the EMEP region in 2008. Monitoring activity, emission data and meteorological conditions are considered. Besides, concentration and deposition, and transboundary transport issues are described. Finally, special attention was given to the uncertainties of the integrated assessment of pollution.

4.1. Monitoring of heavy metals in EMEP

Measurement network

Heavy metals were included in EMEP's monitoring program in 1999. However, earlier data has been available and collected, and the EMEP database [http://ebas.nilu.no] thus also includes older data, even back to 1987 for a few sites. A number of countries have been reporting heavy metals within the EMEP area in connection with different national and international programmers such as HELCOM, AMAP and OSPAR.

Detailed information about the sites and the measurement methods are found in EMEP/CCC's data report on heavy metals and POPs [*Aas and Breivik*, 2010]. In 2008, there were 35 sites measuring heavy metals in both air and precipitation, and altogether there were 70 measurement sites, which were 4 more sites than in 2007. There were 26 sites measuring at least one form of mercury which is an increase of 4 sites from the previous year. 11 sites were measuring mercury in both air and precipitation. The measurement obligations set by the EMEP monitoring strategy [*UNECE*, 2009] and the EUs air quality directives [*EU*, 2004, 2008] have clearly improved the site coverage the last years, though there is still a lack of measurements in some parts of Europe, especially for mercury.

Observed concentration level of Pb, Cd and Hg in 2008

Annual averages of Pb, Cd and Hg concentrations in precipitation and in air in 2008 are presented in Fig. 4.1-4.6. Note that Cyprus with measurements of heavy metals in air is outside the map domain. The lowest concentrations for all elements in air as well as precipitation are generally found in northern Scandinavia. An increasing gradient can in general be seen southeast, but the concentration levels are not evenly distributed, there are some "hotspots" for some elements. I.e. an extremely high annual concentration of cadmium in precipitation (2.4 ng/L) is seen at IT01, which most likely must be due to local influence from sources in the Rome area. Portugal has also high level of cadmium, but this is due to high detection limit, so these data are not shown in Fig. 4.4. For cadmium in air the highest levels are seen in Slovakia, Belgium and Latvia. For lead in precipitation, the highest levels are observed in Spain, Latvia and Slovakia, while in air the highest level is in the BeNeLux, Slovakia and at Cyprus. The spatial distribution of elemental mercury in air does not follow a general pattern; the highest annual average is seen in Norway (1.71 ng/m^3), and lowest in Poland, Great Britain and Northern Finland. The concentration at GB91 is half the level compared to the general average, but it is not known the reason for this.

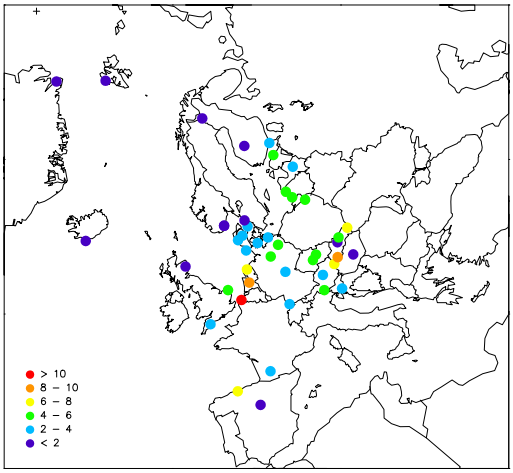

Fig. 4.1. *Pb in aerosol, ng/m^3*

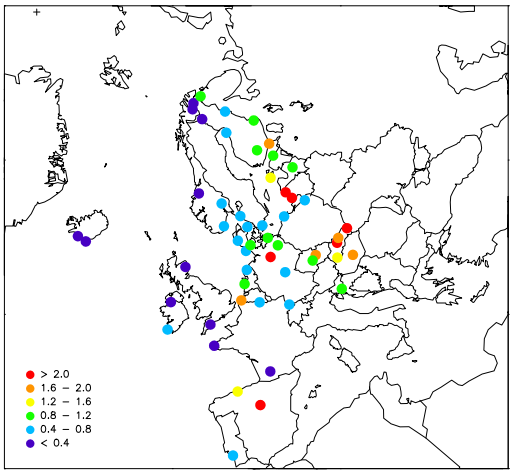

Fig. 4.2 *Pb in precipitation, μg/L*

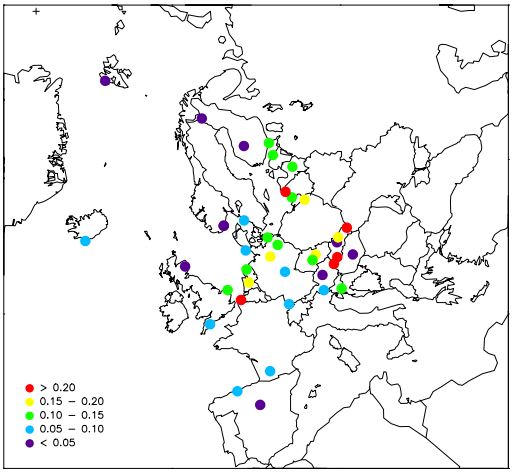

Fig. 4.3*. Cd in aerosol, ng/m^3*

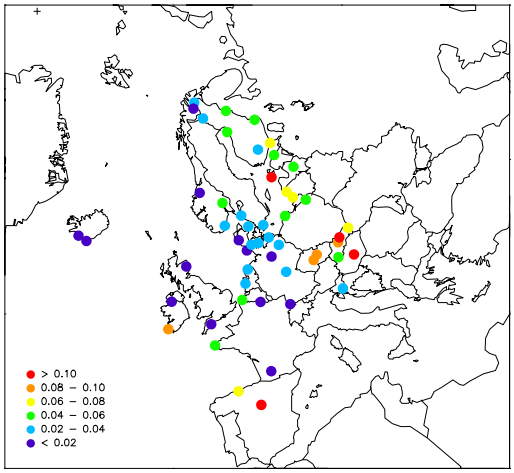

Fig. 4.4. *Cd in precipitation, μg/L*

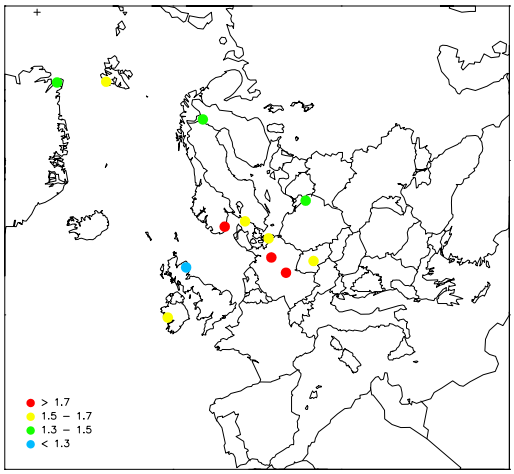

Fig. 4.5*. Hg (g) in air, ng/m^3*

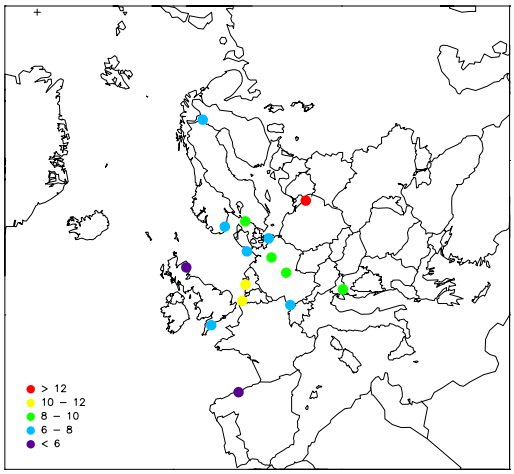

Fig. 4.6. *Hg in precipitation, ng/L*

Data quality

The quality of the measurements depends on many factors, i.e. the methodology used, though it is difficult to assess and quantify the uncertainties based on this information unless parallel measurements or intercomparisons have been performed. Further, the measurements may be influenced by local sources or contaminations both in field and in the laboratories which is difficult to detect.

Usually is the uncertainty in the analytical performance is of less importance compared to the overall uncertainty in the measurements. If we look at the analytical uncertainty as assessed in the annual EMEP laboratory intercomparison, several laboratories have less than 5% deviations from the expected value for many elements. However there are exceptions, some laboratories have problems with some elements and the uncertainty depends upon concentration. The data quality objectives (DQO) in EMEP states that the accuracy in the laboratory should be better than 15% and 25% for high and low concentrations of heavy metals, respectively

There are some countries/laboratories reporting measurements data without participation in the laboratory intercomparison: Ireland, Lithuania, Cyprus, Portugal, and Spain. Data from these countries are of unknown quality; and it is therefore strongly recommended that they take part in the annual laboratory intercomparison. Sweden and Iceland were not participating because these measurements were analysed in Norway. The performance for most elements and labs are satisfactory for lead and cadmium which are the priority metals, though some labs should look into their QA/QC routines.

Intercalibration of acidified water samples are not necessarily representative for a real air and precipitation samples and the total uncertainties is therefore expected to be higher. E.g. the digestion techniques are of importance to ensure that all the metals are dissolved before analysis, this is especially important for nickel that often forms oxides which needs strong digestion techniques to be dissolved. *W.Aas et al.* [2009] showed that the uncertainty in wet deposition for As, Cd and Pb is about 20%, but more than 30% for Ni. It is expected that the uncertainty in air measurements should be of the same order, though few large scale field intercomparison has yet been performed.

Table 4.1. *Average per cent error (absolute) in low and high concentration samples, results from the laboratory intercomparison representative for the 2008 data. DQO is EMEPs data quality objectives*

	As		Cd		Cr		Cu		Pb		Ni		Zn	
Lab nr	low	high	low	high	low	high	low	high	low	high	low	high	low	high
1 AT	2	8	8	2	5	1	1	1	0	2	5	1	2	1
2 BE	13	5	23	4	8	0		8	15	7	10	1	10	14
3 CZ	0	5	4	4	0	8	4	7	7	2		0		0
4 DK		17		6		4		7		4		5		
5 FI	11	14	8	10	34	14	3	8	6	10	8	8	2	8
159 FR	4	5	29	11	17	4	6	4	5	1	12	5	2	6
168 FR90	27	43	8	3	11	21	11	12	14	7	42	7	19	3
8 DE	3	2	8	5	2	4	5	5	7	9	7	6	3	3
10 HU			30	2					14	11				
13 IT			8	26			9	32	22	10			23	6
14 NL	11	2	23	4	10	6	6	3	3	1	3	3	10	2
15 NO	4	1	4	2	1	5	4	2	1	4	11	9	7	1
16 PL04			4	8	0	0	25	0	0	14	0	0	0	1
39 PL05			15	0	0	0	11	0	7	0	15	0		1
23 GB	18	3	23	9		8		9	14	4		11		
31 SK	0	0	4	2	3	1	2	5	4	6	12	1	12	8
33 LV	4	4	0	5	2	5	0	4	0	4	2	4	2	0
36 SI	4	3	7	1	10	3	3	2	10	6	12	1	10	14
38 EE		31		0		4	17	4	46	2		25		6

not participated/reported | 1/2 - 1 DQO | 1 - 2 DQO | > 2 DQO

4.2. Emission data for model assessment

The data on emission totals from the EMEP countries for 2008 used for modelling this year were based on the official data received from the EMEP Centre on Emission Inventories and Projections (CEIP) [http://www.emep-emissions.at/ceip/]. If countries did not report their national emission data, emission totals for 2008 were estimated by interpolation between 2000 and 2010 of non-official estimates and projections made by the Dutch TNO institution [*Denier van der Gon et al.,* 2005]. Information about spatial distribution of heavy metal emissions at least for one year of the period 1990-2008 was provided by 28 countries (Austria, Belarus, Belgium, Bulgaria, Croatia, Cyprus, Czech Republic, Denmark, Estonia, Finland, France, Germany, Hungary, Ireland, Italy, Latvia, Lithuania, Netherlands, Norway, Poland, Portugal, Slovakia, Slovenia, Spain, Sweden, Switzerland, Ukraine and the United Kingdom). Gridded data for the countries Austria, Belarus, Denmark, Estonia, Germany, Ireland, Lithuania, Netherlands, Portugal, Spain, Switzerland and Ukraine were provided by CEIP. For the other countries the spatial distribution was prepared by MSC-East.

In 2008 total anthropogenic emission of lead from the EMEP domain made up around 7210 tonnes, which was 250 tonnes lower than that for 2007. Emission from the European part of the EMEP domain (excluding part of Kazakhstan territory) equalled to 6050 tonnes, and from the extended part (Kazakhstan, Kyrgyzstan, Tajikistan, Turkmenistan, Uzbekistan, the eastern part of Russia) - 1160 tonnes. The highest decrease of emission values (in absolute terms) took place in Ukraine (95 tonnes), Portugal (92 tonnes), Poland (23 tonnes) and Turkey (48 tonnes).

Total emission of cadmium in Europe and Central Asia in 2008 (318 tonnes) was almost the same as that in 2007. This value included 270 tonnes from emission sources located in European countries and 48 tonnes – from the Central Asian region. Compared to emission values used in modelling for 2007, emissions in Spain, the Czech Republic, Cyprus declined by 2.7, 2.2 and 1.1 tonnes. Significant increase of the emission values was noted for Romania (2.4 tonnes), Poland (2.1 tonnes) and Slovakia (1.7 tonnes).

Emission of mercury in the European and Central Asian countries in 2008 amounted to 227 tonnes. European emissions were 165 tonnes, and the emissions from Central Asia and the Asian part of Russia – 62 tonnes. The changes of emissions for the EMEP domain as a whole between 2007 and 2008 were minor. Most significant increase of emission values in individual countries took place in Romania and Slovakia (7.4 and 1.4 tonnes, respectively). The highest decrease was in France, Spain, Cyprus and the United Kingdom (2.7, 1.3, 1.2, and 0.9 tonnes, respectively).

The official information on emissions for the Asian part of the EMEP domain was not available. Therefore, emission data for this region were based on non-official emission estimates. Lead emission totals for Kazakhstan and Kyrgyzstan were derived from the TNO emission inventory [*Denier van der Gon et al*., 2005] using the interpolation between 2000 and 2010. Lead emissions in Turkmenistan, Tajikistan and Uzbekistan for 2008 were taken from the global inventory for 1990 [*Pacyna et al*., 1995; *http://www.ortech.ca/cgeic/index.html*] expecting the same emission reduction in these countries between 1990 and 2006 as in the Russian Federation according to the recent EMEP official data. Total emission of lead from the Asian part of Russia was assessed using the official emission data for the European part of the country in 2008 and keeping the ratio between the European and the Asian parts obtained from the global lead inventory. Besides, the global emission data were also used for the other Asian and African countries, falling fully or partly into the EMEP domain, assuming the same emission reduction between 1990 and 2008 as for Turkey. Turkey was selected for this purpose because it was the only country located in Asia, for which non-party estimates of lead emission changes were available. Spatial distribution of lead emissions from all these countries was obtained by interpolation of the global gridded emissions with 1°×1° spatial resolution into the model grid.

Mercury emissions for the Asian part of the EMEP domain and for the northern African countries were derived from global mercury inventory for 2005 [*AMAP/UNEP*, 2008]. It was assumed that the emissions were not changed significantly between 2005 and 2008.

Global emission inventories for cadmium are currently not available. Therefore cadmium emission data for the Asian part of the EMEP domain and for the north of Africa were obtained on the basis of the available non-party estimates for cadmium emissions. Spatial distribution was assumed to be similar to that used in the global mercury inventory [*AMAP/UNEP*, 2008]. For this purpose, cadmium emission was assumed to be proportional to emission of mercury with a coefficient depending on a region: $E_{Cd} = \alpha \cdot E_{Hg}$. For the eastern part of Russia the proportionality coefficient (α) was taken the same as for the European part (1.14). The coefficient for the remaining Central Asian countries was assumed to be the same as that for Kyrgyzstan (0.56). For the other Asian countries and Africa the coefficient was taken equal to that for Turkey (0.91). All coefficients were estimated on the basis of the TNO inventory [*Denier van der Gon et al*., 2005].

Spatial distributions of lead, cadmium and mercury emissions used in the modelling are shown in Fig. 4.7. Temporal and vertical distribution of the emission data and speciation of mercury emissions, employed in the MSCE-HM model, are described in [*Travnikov and Ilyin*, 2005].

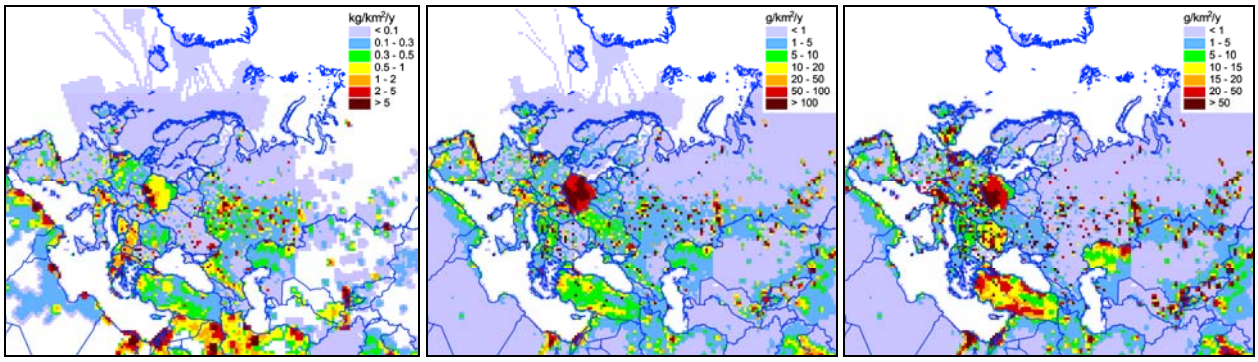

a b c

Fig. 4.7. *Spatial distribution of lead (a), cadmium (b) and mercury (c) emissions over the extended EMEP domain in 2008*

4.3. Meteorological conditions

Meteorological data, along with emission values, are one of the key parameters influencing pollution levels in Europe and Central Asia. When annual changes of the emission values in countries are relatively small, long-term variability of pollution levels is mostly controlled by variability of meteorological parameters. An increase of precipitation amounts favours higher wet deposition, and vice versa. Higher temperatures lead to faster chemical reactions of mercury oxidation and can lead to more intensive mercury removal from the atmosphere. Changes in wind pattern can affect source-receptor relationships. Therefore, it is very important to compare meteorological conditions of current (2008) and previous (2007) years. Moreover, understanding of fate of atmospheric pollution levels in response to long-term climatic changes of meteorological variables is becoming actual and challenging task.

Meteorological conditions in 2008 vs. 2007

Atmospheric circulation pattern in Europe is often characterized by so-called North Atlantic Oscillation (NAO) index [*Hurrel et al.*, 2003]. The value of this index characterises fluctuation of pressure gradient between Icelandic Low and Azores High. Positive index means that the gradient between these two centres is higher than normal, stronger atmospheric transport, mild and wet conditions in the northern part of Europe and relatively dry conditions in its southern part. Negative index implies weaker atmospheric transport and relatively dry conditions in the northern and relatively wet conditions in the southern part of Europe. Time series of winter (December, January, February, March) and summer (May, June, July, August) NAO index for the period 1990 -2009 based on the data of Climatic Research Unit (http://www.cru.uea.ac.uk) are exemplified in Fig (4.8).

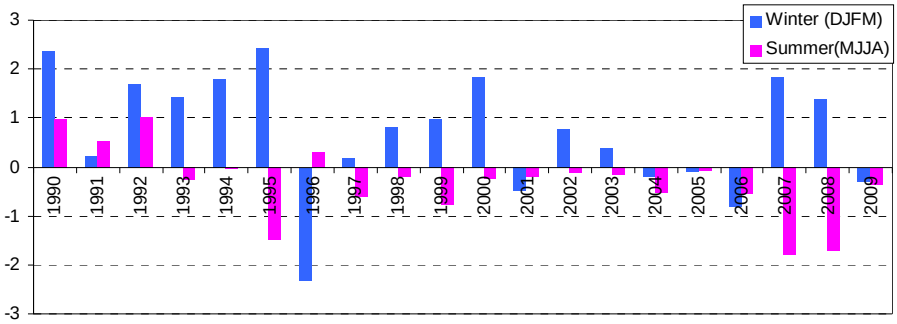

Fig. 4.8. *NAO summer and winter index (base on the data from http://www.cru.uea.ac.uk)*

Winter of 2008 was characterized by positive phase of NAO, indicating strong westerly air flows, while in summer period meridional flows were more pronounced (Fig. 4.8). Negative phase of NAO in summer favoured penetration of the cold air from the Arctic into the north-eastern, central and southern Europe [*Peterson and Baringer*, 2009]. Comparison of NAO indexes of 2007 and 2008 showed that for Europe as a whole both summer and winter pairs of indexes were similar. Hence, principle features of atmospheric circulation patterns in 2007 and 2008 over Europe as whole should be similar. However, on shorter time scales, as well as for particular regions the differences can be significant and should be specially analysed.

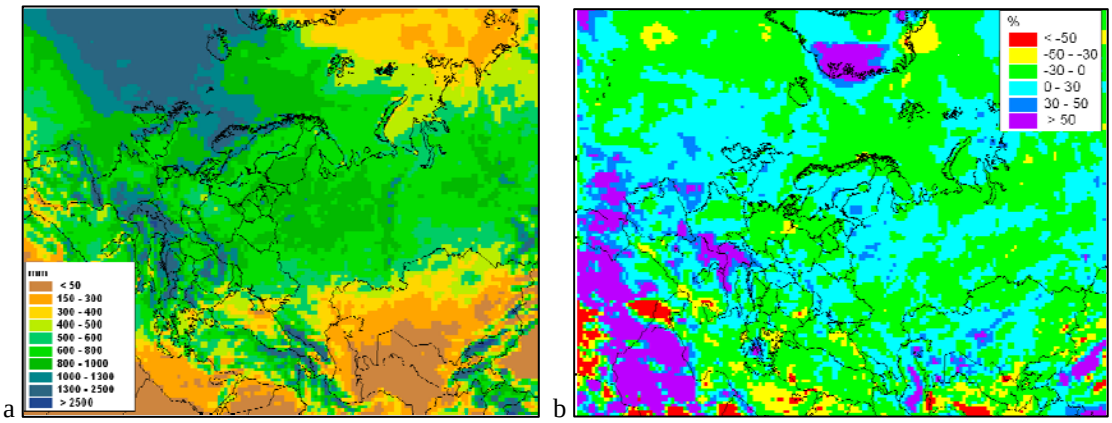

Fig. 4.9. *Annual precipitation amounts in 2008 (a) and relative difference between precipitation in 2008 and 2007 (b)*

The highest precipitation in 2008 took place over the Northern Atlantic, north of the British Isles, the west of the Balkan region (Fig. 4.9a). Besides, high precipitation also occurred in mountainous regions:

western slopes of Scandinavian mountains, the Alps, Caucasus, Pamir, and Tien Shan mountains. Compared to 2007, precipitation significantly increased over the Alps, southern France, Iberian Peninsula, Bay of Biscay, the Caspian Sea, central part of Kazakhstan (Fig. 4.9b). Therefore, an increase of deposition could be expected in these regions. Over the central and south-eastern part of Europe (Germany, Poland, Romania, Bulgaria), the eastern part of the Mediterranean, and the southern part of Central Asia precipitation decreased. This would favour decrease of deposition in these regions in 2008 in comparison with 2007.

Winter (January, February, March) of 2008 was colder than that of 2007 over most part of Europe and Central Asia (Fig. 4.10a). The difference between surface air temperatures made up -0.5 - -1.5 °C over Central and Southern Europe, and below -1.5 °C over the Central Asian region. The exceptions were Scandinavia, the northern part of Russia, and the Iberian Peninsula. Summer (June, July, August) of 2008 was warmer than that of 2007 in the central and western parts of Europe as well as over the Central Asia (Fig. 4.10b). The eastern part of Europe was characterized by cooler summer, caused by meridional air transport from the Artic.

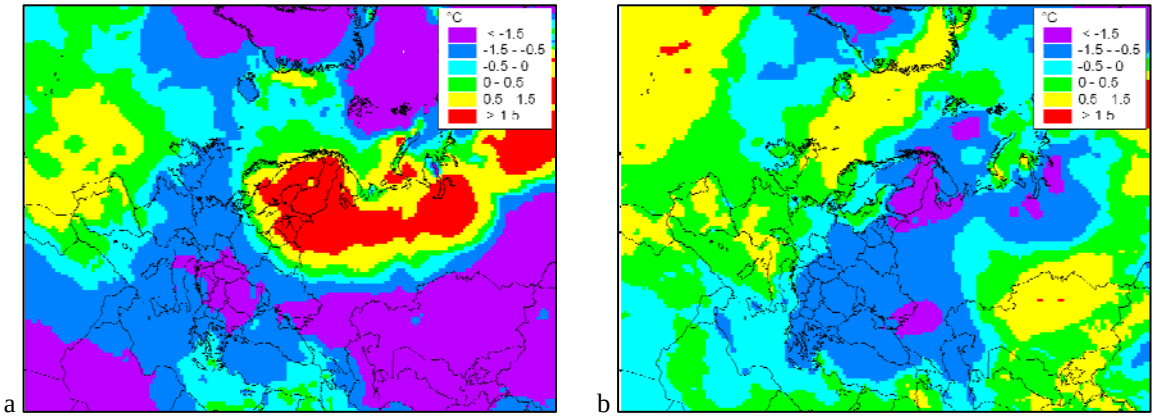

Fig. 4.10. *Difference between winter mean temperatures (a) and summer mean temperatures (b) in 2008 and 2007*

Sensitivity to meteorological parameters associated with climate change

The work aimed at linking of changes in climatic variables and pollution levels was initiated in MSC-E. At this stage the changes of pollution levels were compared with the variability of meteorological parameters at current climatic conditions. For this purpose a development of statistical approach based on application of regression analysis was started.

The idea of the method is as follows. It is assumed that a pollution parameter of interest (so-called target parameter) is influenced by one or several meteorological parameters (factors). The numerical relationship (regression) between deposition and the factors is evaluated following step-by-step approach. At first step the factor with the highest influence is selected. At the further step the regression is constructed for the pair of factors etc. As a result of the analysis the statistical relationship (multiple regression) between the target parameter (e.g., deposition) and meteorological variables is established. First of all, this approach allows to determine the importance of meteorological parameters with regard to pollution levels. Besides, the established numerical relationship between pollution level and meteorological variables makes possible to estimate the level in response of known changes of meteorological parameters (e.g., because of climate change). More detailed information on this approach is available in MSC-E Technical report [*Ilyin et al.*, 2010].

This approach can be applied for various atmospheric contaminants, including heavy metals and persistent organic pollutants. Its pilot application to heavy metals is considered below. Country-averaged total deposition of lead in the Czech Republic, Finland, Italy and the United Kingdom were considered as target parameters. Meteorological factors involved in the regression analysis were country-averaged precipitation amount (P), air temperature (T), friction velocity (U_{fric}), and wind speed (V). Besides, averaged wind speed over countries of Europe (V_{Eur}) was also considered.

Precipitation controls wet scavenging of particulate heavy metals like lead. Friction velocity is one of the key parameters affecting dry deposition. Country-averaged wind speed influence the amount of pollution emitted by national sources which are transported outside the country. European-scale wind speed characterizes transboundary transport to a considered country from other regions of Europe.

Total deposition was calculated for the period from 1990 to 2007. The emission data used in calculations was the same for the comparability of the results. Monthly sums of deposition of the same months of each year were regressed via corresponding meteorological parameters. In other words, deposition of Januaries of 1990 – 2007 period were compared with meteorological parameters form the same periods, etc.

Application of this approach was demonstrated by some examples. According to the regression analysis the main meteorological parameter affecting the deposition in the Czech Republic was country-averaged wind speed. The coefficient of determination was 0.52, which meant that 52% of variability of deposition was explained by the variability of the wind. The estimated deposition were reproduced based on the regression analysis (Fig. 4.11a). As seen, temporal variability of the two deposition time series (modelled and estimated by regression analysis) was quite similar. However, in the beginning of the time series, relating to early nineties the difference between the two deposition was obvious. It meant that other parameters, in addition to wind speed, should be involved into the analysis. As other considered parameters were added, multiple coefficient of determination rose to 0.68. It means that the use of all the considered meteorological parameters in the regression analysis allowed to explain 68% of variability of modelled deposition in the Czech Republic in January (Fig. 4.11b).

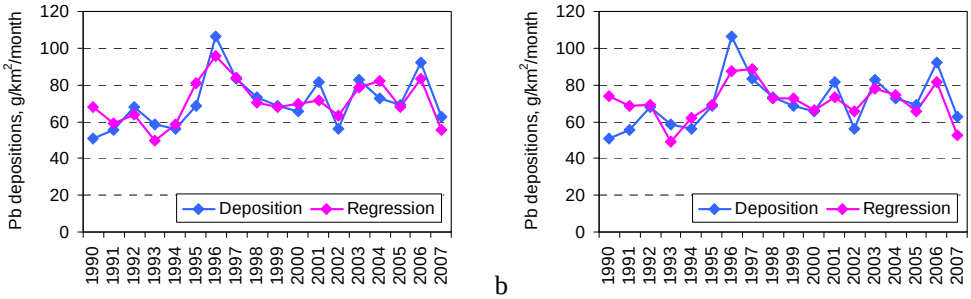

Fig. 4.11. *Deposition of lead in the Czech Republic in Januaries calculated by the model and estimated via regression analysis using: (a) the main influencing meteorological parameter (country-mean wind speed) and (b) combination of all considered meteorological parameters*

The ability of this approach to estimate deposition levels via multiple regression differed largely depending on a country and month. For example, for Finland in June the coefficient of determination was almost 0.8, while in February it is below 0.2 (Fig. 4.12). Low value of the coefficient implied that the set of meteorological parameters selected for the analysis is incomplete, and some other factors (parameters) are missing. At further stages of the development of this approach more attention will be paid to the selection of the influencing factors.

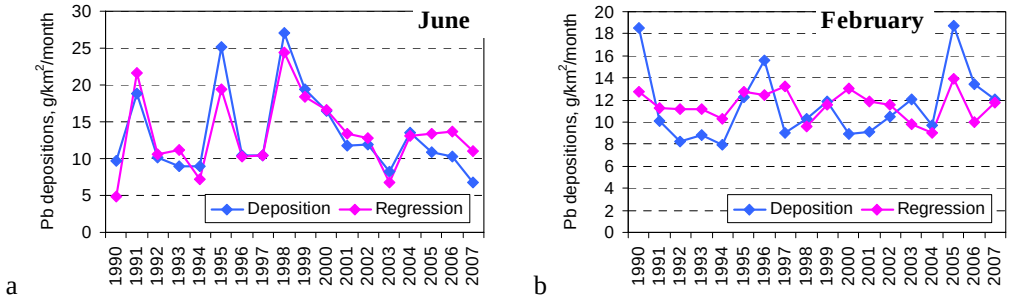

a b

Fig. 4.12. *Deposition of lead in the Finland in Januaries calculated by the model and estimated via regression analysis using all considered meteorological parameters in June (a) and in February (b)*

Priority of meteorological parameters varied for different country and month. In the table below ranks of the parameters were summarized for each country for all months as a whole (Table 4.2). The rank equalled to unity means that this parameter was most important, equal to two – less important etc. As seen from the table, precipitation amount was the main factor affecting the deposition levels in all selected countries except for the United Kingdom. For this country the main parameter is country-averaged wind speed. The prevalence of this factor could be explained by relative remoteness of the United Kingdom from main pollution sources. At lower velocity pollution emitted by the British sources is deposited within country's territory, while at higher – transported outside the country. At the same time, at higher wind speed only relatively little amount of pollution comes to the United Kingdom by transboundary transport due to the remoteness and "upwind" position of this country relative to main European emission sources.

Table 4.2. *Ranking of the importance of meteorological factors for deposition of lead*

Country	P	T	U_{fric}	V	V_{Eur}
Italy	1	5	3	2	4
Finland	1	2	4	5	3
United Kingdom	2	3	4	1	5
Czech Republic	1	3	4	2	5

The results demonstrated by this approach should be considered as preliminary. In the framework of the further development of this approach the set of factors possibly affecting pollution levels will be revised. First of all, more detailed description of wind patterns is needed. For example, averaged wind speeds can be replaced or supplemented with density of back trajectories ending in a country. Besides, other parameters affecting deposition (e.g., land-cover distribution, Monin-Obukhov length scale) may need consideration.

4.4. Analysis of heavy metal pollution levels in 2008

This section deals with the analysis of pollution levels of lead, cadmium and mercury based on modelling and monitoring information for 2008. Modelling results were obtained by the MSCE-HM model. Measurement data were submitted to CCC database by the EMEP countries. Spatial distribution of heavy metal deposition and concentration, description of the pollution level changes between 2007 and 2008, and source-receptor relationships in Europe and Central Asia are considered. Finally, evaluation of the atmospheric loads to the regional seas is presented.

LEAD

Both modelling results and monitoring data were used for the assessment of pollution levels over the EMEP region. Over major part of Europe and Central Asia annual mean concentrations of lead lay within 1-10 ng/m^3 limits (Fig. 4.13). Relatively high concentrations took place in regions with significant emission sources where concentrations exceeded 10 ng/m^3, and in some regions – even 20 ng/m^3. In the central, western and northern parts of Europe both modelled and measured concentrations demonstrated similar pattern. In particular, in Germany, Slovakia and the Czech Republic the modelled and observed concentrations varied from 3 to 10 ng/m^3, in the Benelux region they could exceed 10 ng/m^3 at some stations.

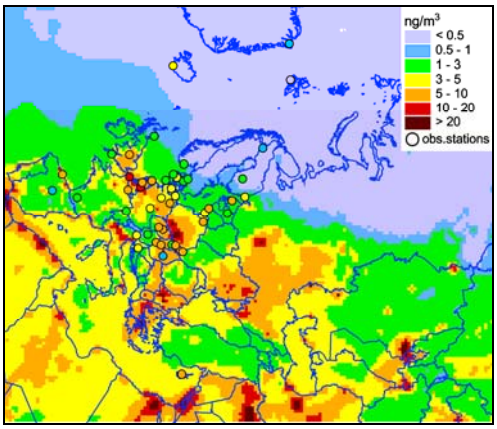

Fig. 4.13. *Calculated and measured surface concentrations of lead in air over Europe and Central Asia in 2008*

Relatively high calculated concentrations were indicated for the Balkan region, the eastern part of Ukraine and the European part of Russia. However, because of scarce measurement network in these regions it was not easy to confirm this finding. The lowest concentrations were obtained for Scandinavia and the northern part of Russia.

Another measurable parameter was wet deposition flux. The combined map of modelled and measured wet deposition fluxes of lead in 2008 is demonstrated in Fig. 4.14. Since periods of observations at stations often did not cover entire year, for comparability the modelled and observed wet deposition fluxes were depicted as daily mean sums. Spatial distribution of modelled wet deposition first of all reflected distribution of the emissions and precipitation patterns. In particular, relatively high deposition occurred in the central part of Russia, the eastern part of Ukraine, southern Poland, Slovakia, northern Italy, the Benelux region, and over the Balkans. Comparatively low deposition took place in parts of the EMEP region remote from main emission sources: in the Arctic, over Scandinavia, Iceland. Besides, low deposition was found over Africa and the desert regions of Central Asia. Measured deposition mostly followed this pattern. Relatively high (1.5 – 5 g/km^2/day) deposition was indicated for Slovakia and the Benelux region. In Germany, Denmark, Poland and France modelled and measured wet deposition mostly laid within 0.8-2.5 g/km^2/day. Smaller wet deposition fluxes were measured in Finland and Iceland. However, in some regions the measured values considerably exceeded the modelled ones. For example, these regions were Spain, Latvia, and the southern part of Norway.

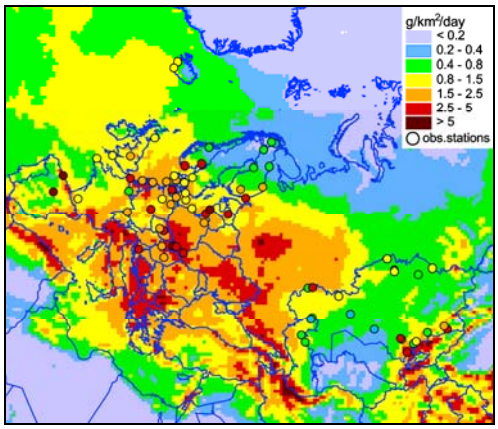

Fig. 4.14. *Calculated and measured daily sums of wet deposition fluxes of lead over Europe and Central Asia in 2008*

Low (0.2 – 0.8 g/km^2/day) wet deposition of lead over the central part of Kazakhstan were confirmed by the monitoring data were submitted to MSC-E by national experts from this country. (Fig. 4.14). In the south-eastern mountainous part of the country the deposition exceeded 2.5 g/km^2/y because of higher precipitation (Fig. 4.9a) and emission values (Fig. 4.7a).

Spatial pattern of total deposition was similar to that of air concentrations and wet deposition. Relatively high deposition levels (1-2 kg/km^2/y) were associated with location of main sources of anthropogenic emission or wind re-suspension, the lowest deposition occurred in areas remote from regions with significant emission (Fig. 4.15). In addition to magnitude and spatial distribution of atmospheric sources of lead, deposition levels in Europe and Central Asia depended on meteorological peculiarities, first of all precipitation and wind patterns, and on properties of the underlying surface.

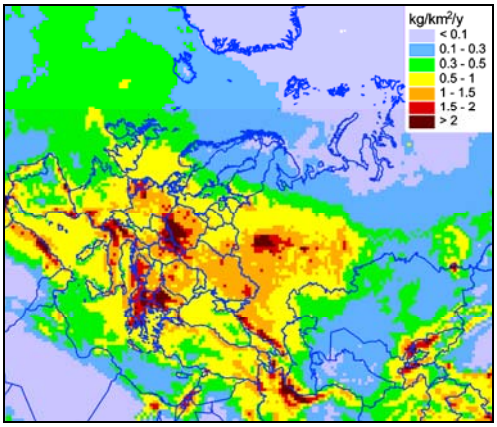

Fig. 4.15. *Total annual deposition of lead in Europe and Central Asia in 2008*

There are three sources of origin of heavy metal total deposition: anthropogenic sources, wind re-suspension of historical accumulated deposition and transport from non-EMEP sources (transport through the EMEP domain boundaries and the emission from the northern Africa and parts of Middle East and eastern Asia within the EMEP domain). Change in one of these sources does not always result to the same relative change in deposition. For example, significant reduction of anthrogenic emission in a country can lead to smaller changes in deposition if re-suspension and transport from non-EMEP sources remains the same, and vice versa.

Total deposition of lead to the European and the Central Asian countries from anthropogenic sources amounted to 5570 tonnes. Deposition to Europe was 4445 tonnes, and to the Asian part (five central Asian states and the eastern part of Russia) - about 1125 tonnes. Compared to 2007, deposition to the EMEP domain declined due to the decrease of emission values used in modelling. Total deposition to Europe and Central Asia from all sources (anthropogenic, wind re-suspension and non-EMEP sources) amounted to 11870 tonnes. This value was almost two tonnes (14%) lower than that in 2007, because of lower estimated re-suspension flux and anthropogenic emissions in Europe and Central Asia.

The deposition resulted from wind re-suspension is subject to high uncertainty. For example, re-suspension of lead estimated by the British national experts for the United Kingdom amounted to 40.8 tonnes, versus 266 tonnes used in the MSC-E estimates [*K. Vincent*, personal communication]. This significant difference between the estimates confirms that further investigation of this process is needed.

The most significant (15-30%) decline of the deposition took place in the southern, central and western parts of Europe. Smaller (5-15%) decline occurred in the eastern and south-eastern part of Europe. These changes were caused by several reasons. First of all, anthropogenic emission values of lead used in modelling for 2008 were lower than those for 2007. For example, emission values of lead used for Ukraine decreased 1.5 times, in Portugal – 3 times. Besides, re-suspension in 2008 was also lower over most part of Europe compared to 2007. In addition to this, in some parts of Europe precipitation amounts declined (e.g., Germany, Serbia, Bulgaria). In some countries, such as the western part of the United Kingdom and Ireland the deposition of lead rose between 2007 and 2008. The main reason for this was the increase of precipitation over this region, and in case of Ireland – also some increase of the emissions (around 10%). Increase of deposition in the southern, eastern and south-eastern parts of Russia and in the central part of Kazakhstan was caused by the increase of wind re-suspension flux in these regions. Besides, growth of precipitation amount in the central part of Kazakhstan favoured the increase of lead deposition.

The highest country-averaged fluxes of lead total deposition (about 2 kg/km^2/y) were obtained for Monaco, Bulgaria, Slovakia and the FYR of Macedonia, the lowest (about 0.2 kg/km^2/y) – for Iceland, Turkmenistan and Norway (Fig. 4.16). The contribution of wind re-suspension to deposition varied from 20% to 75%. In 22 countries (of total 50) its contribution to total deposition exceeded 50%. It was important to mention that re-suspended lead was represented by both natural component and by historical deposition, while the latter was likely to predominate. The contribution of non-EMEP sources was relatively small. In majority of countries it made up less then 15%. High contribution of non-EMEP sources (about 50%) was noted for few countries which national emission was relatively low and which were located close to the EMEP boundaries (e.g., Armenia, Azerbaijan, Turkmenistan).

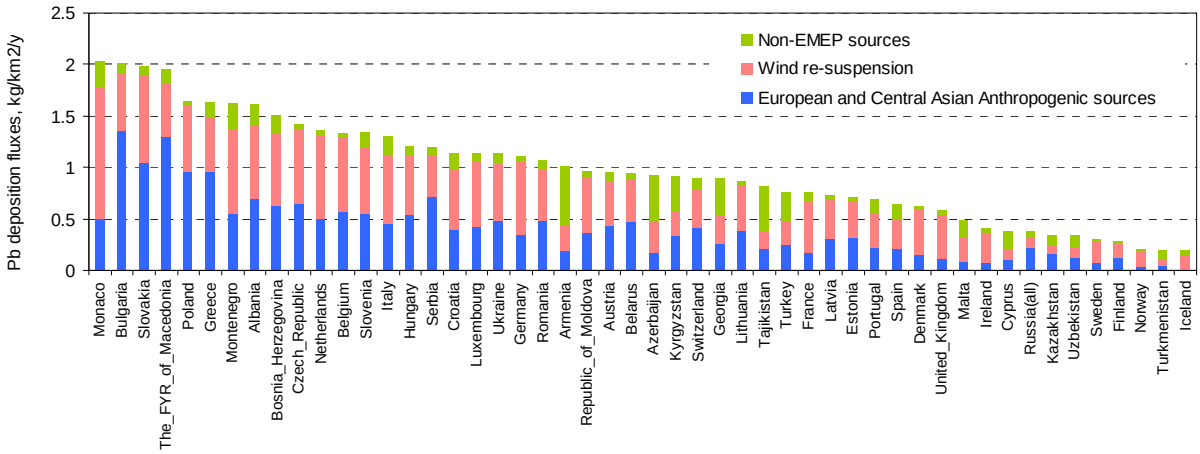

Fig. 4.16. *Country-averaged deposition fluxes of lead from the European and Central Asian anthropogenic, natural/historical and non-EMEP sources in 2008*

Relative contribution of the transboundary transport to anthropogenic deposition of lead ranged from almost 100% in Monaco and 97% in Croatia to 15% in Spain (Fig. 4.17). In 38 countries this contribution exceeded 50%, and in 21 country – 80%. The highest contribution of transboundary transport was typical for countries with small territory and relatively low country-averaged emission. Therefore, high contribution of transboundary transport took place in Montenegro, Republic of Moldova, the Baltic countries. Even for relatively big Scandinavian countries, Belarus, Germany and France the contribution exceeded 60% due to low density of national emissions of lead and influence of neighbouring countries with significant emissions. In countries possessing vast territory (e.g., Kazakhstan, Russia) the contribution was below 50%. Because of large territory emitted pollutant was deposited within a country not reaching the state borders. Besides, the contribution was low in countries with relatively high emission density (Belgium, Bulgaria, Greece, Poland). In some countries (e.g., Portugal, the United Kingdom, Spain) the contribution was relatively low because of their “upwind” position relative to main emission regions.

Contribution of countries to transboundary pollution was evaluated as the mass of the pollutant, emitted by national sources and transported outside country’s territory. The highest contribution was noted for Russia (615 tonnes), followed by Kazakhstan (about 440 tonnes) and Greece (380 tonnes) (Fig. 4.18). Over most of countries the fraction of emitted lead transported outside the country varied from 60% to almost 100%. It meant that only less than a half of the emitted lead was deposited within a country, and most of it was transported outside the country and deposited elsewhere. The exception was Russia. This fraction in Russia in 2008 was about 24%. The reason for this was a large territory of the country, and location of most national sources relatively far from the state borders.

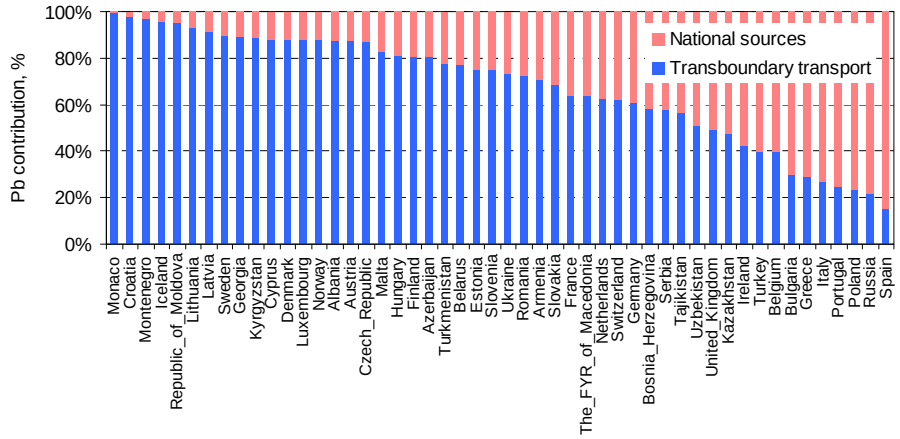

Fig. 4.17. *Relative contribution of the transboundary transport and national sources to anthropogenic lead deposition in the European and Central Asian countries in 2008*

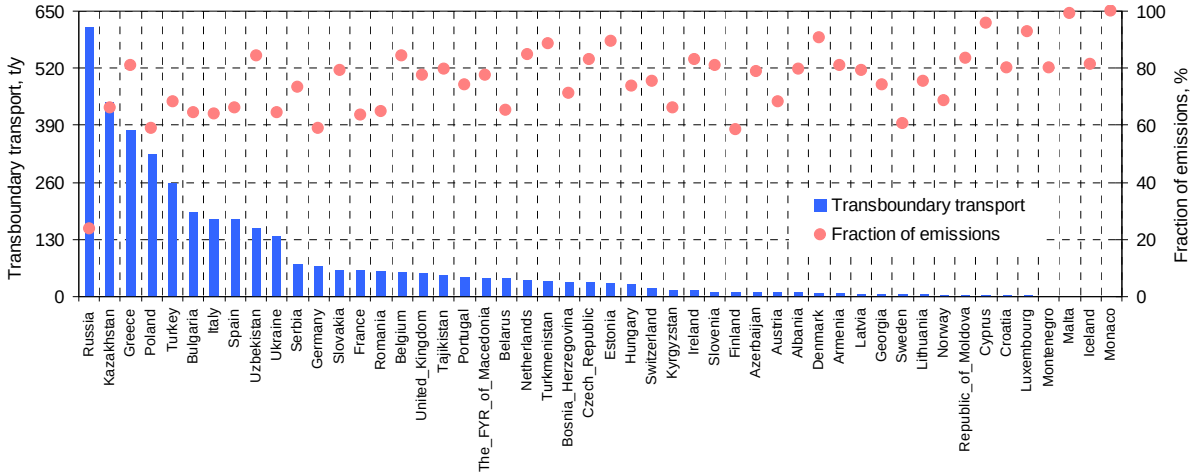

Fig. 4.18. *Absolute contribution of the European and Central Asian countries to lead transboundary transport in Europe and Central Asia in 2008 and relative fraction of national emissions involved into the transboundary pollution*

CADMIUM

Annual mean calculated and observed concentrations of cadmium in air in 2008 varied between 0.01 – 0.3 ng/m^3 over most part of Europe (Fig. 4.19). The highest calculated concentrations were associated with regions with significant emission sources (Poland and adjacent regions, the Benelux countries, the Balkans). The lowest concentration levels were noted for the Scandinavian countries, the north-eastern part of Russia and the Arctic region.

Monitoring network covered territory of the central, western and northern parts of Europe, while in eastern, south-eastern Europe and Central Asia

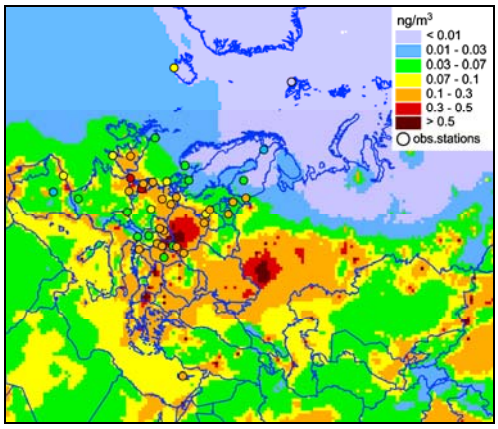

Fig. 4.19. *Calculated and measured surface concentrations of cadmium in air over Europe and Central Asia in 2008*

background monitoring data were not available. Therefore, pollution levels over these areas were assessed only by means of modelling.

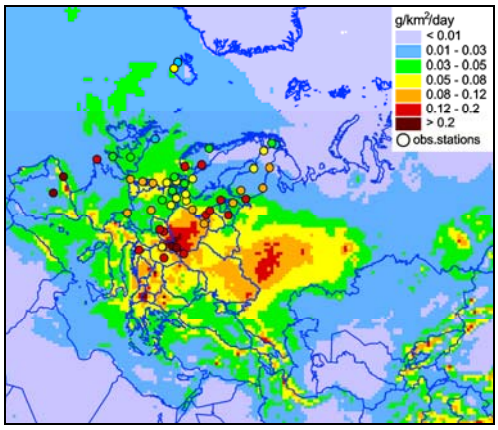

Fig. 4.20. *Calculated and measured daily sums of wet deposition fluxes of cadmium over Europe and Central Asia in 2008*

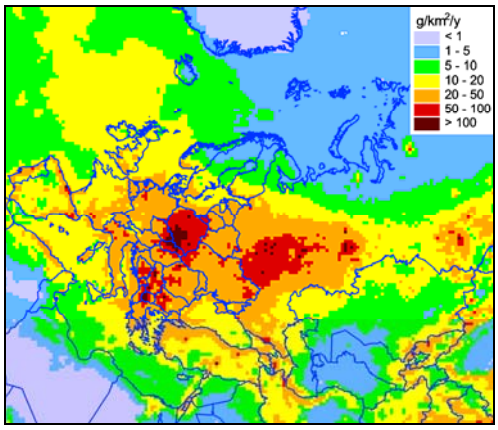

Fig. 4.21. *Total annual deposition of cadmium in Europe and Central Asia in 2008*

Pattern of cadmium wet deposition was distributed across Europe similar to that of concentrations in air: regions with higher emissions were characterized by higher deposition levels. Since measured deposition fluxes did not always represent entire year both modelled and monitored deposition were expressed as daily mean sums (Fig. 4.20). Relatively high measured and modelled wet deposition fluxes (0.05 – 0.2 g/km^2/day) were noted in or nearby regions known for high emissions: in Poland, Slovakia, Belgium, the Netherlands. Relatively small measured and calculated levels were indicated for the United Kingdom (0.2 – 0.4 g/km^2/day), Germany and Denmark (0.3 – 0.8 g/km$^{2/}$day). However, over a number of regions, e.g., Scandinavia, Spain, Hungary and Baltic countries, calculated levels were lower than the observed ones.

Total deposition of cadmium in 2008 ranged from 5 to 50 g/km^2/y over most part of Europe and Central Asia (Fig. 4.21). In most polluted areas (south of Poland, the FYR of Macedonia, central regions of Russia) the deposition exceeded 100 g/km^2/y. The lowest levels were typical for the Scandinavian countries because their national emission sources were relatively low and these countries were remote from the main emission sources. Low deposition in the Central Asian counties such as Uzbekistan and Turkmenistan were explained by low precipitation amounts typical for arid regions.

Total deposition of cadmium from all sources (anthropogenic, wind re-suspension, and non-EMEP sources) to the European and the Central Asian countries (including eastern part of Russia) in 2008 made up 416 tonnes, including 313 tonnes related to Europe and 103 tonnes – to Central Asia. Compared to 2007, deposition in 2008 was about 10% lower. The decline was mainly explained by the lower wind re-suspension flux in the EMEP domain. It was important to note that the uncertainty of re-suspension of heavy metals was quite high. For example, estimates of the re-suspension of cadmium in the United Kingdom made by the British experts were 0.5 tonnes while similar estimates employed in MSC-E – 4.7 tonnes [*K. Vincent*, personal communication]. The difference between these two estimates meant insufficient knowledge about this process and hence, necessity to further investigates this process.

Deposition decline in individual countries was explained by various reasons such as smaller wind re-suspension, lower values of cadmium emissions in countries, and annual meteorological variability. Significant reduction (20-30%) occurred in the western, southern and central parts of Europe (France, Germany, Spain, Italy etc). Small growth of deposition in Ireland and on the western part of the United Kingdom was caused by the increase of precipitation amounts. The same reason referred to the

increase of cadmium deposition in the central part of Kazakhstan, Slovakia, southern part of Greece and Norway, and the central part of Sweden.

The highest country-averaged deposition of cadmium in 2008 took place in the FYR of Macedonia and amounted to about 140 g/km^2/y (Fig. 4.22). The lowest levels (4 – 10 g/km^2/y) were found for some Central Asian countries (Turkmenistan, Uzbekistan) and for Scandinavia (Finland, Sweden, Norway, Iceland). Similar to lead, deposition of cadmium stemmed from three types of sources: anthropogenic emissions, wind-re-suspension and non-EMEP sources. In the majority of countries the major contribution to deposition was made by anthropogenic sources. However, in some countries the contribution of wind re-suspension exceeded 50% (Germany, the United Kingdom, Iceland). The contribution of non-EMEP sources was the lowest in countries with relatively high national emissions and located far from the EMEP domain boundaries, and vice versa. Therefore, it ranged from 1-2% in Poland, Slovakia, the Czech Republic, and the FYR of Macedonia to 40 - 50% in Armenia, Turkmenistan and Tajikistan.

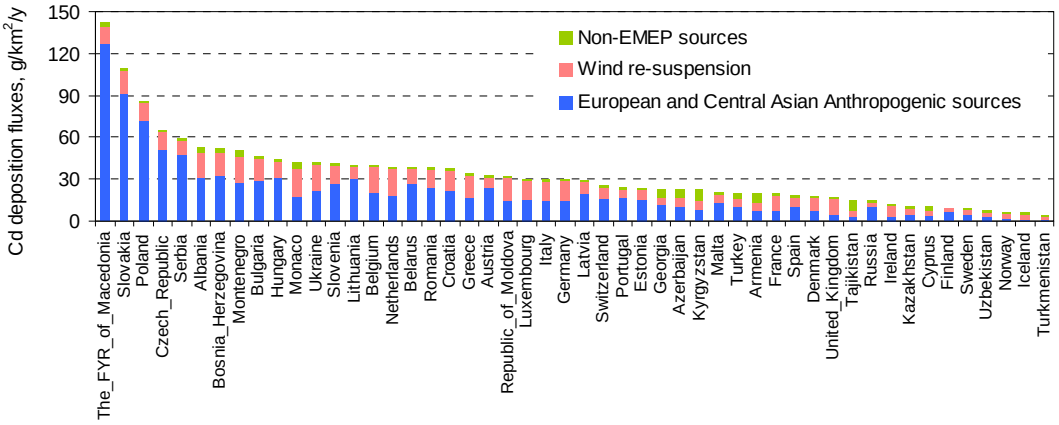

Fig. 4.22. *Country-averaged deposition fluxes of cadmium from the European and Central Asian anthropogenic, natural/historical and non-EMEP sources in 2008*

The contribution of transboundary transport of cadmium to deposition from anthropogenic sources varied from 97% in Monaco to 12% in the FYR of Macedonia (Fig. 4.23). This contribution was also quite high (more than 90%) in Lithuania, Latvia, Republic of Moldova, Montenegro and other countries. In 35 countries of Europe and Central Asia the contribution exceeded 50%, in 19 countries – 80%. The reasons governing the ratio between deposition from transboundary and national sources were similar to those of lead.

Amount of cadmium emitted by countries and transported outside country's territory ranged largely between countries of Europe and Central Asia. In absolute terms, the highest contribution to transboundary transport was made by Russia (28 t/y), followed by Poland (24 t/y) (Fig. 4.24). Fraction of the emitted cadmium leaving country's territory ranged between 60% and 90% for most of countries. The exception was Russia. Because of large territory and location of major national emission sources relatively far from the state borders (central regions, the Urals) most of emitted cadmium was deposited within the Russian territory.

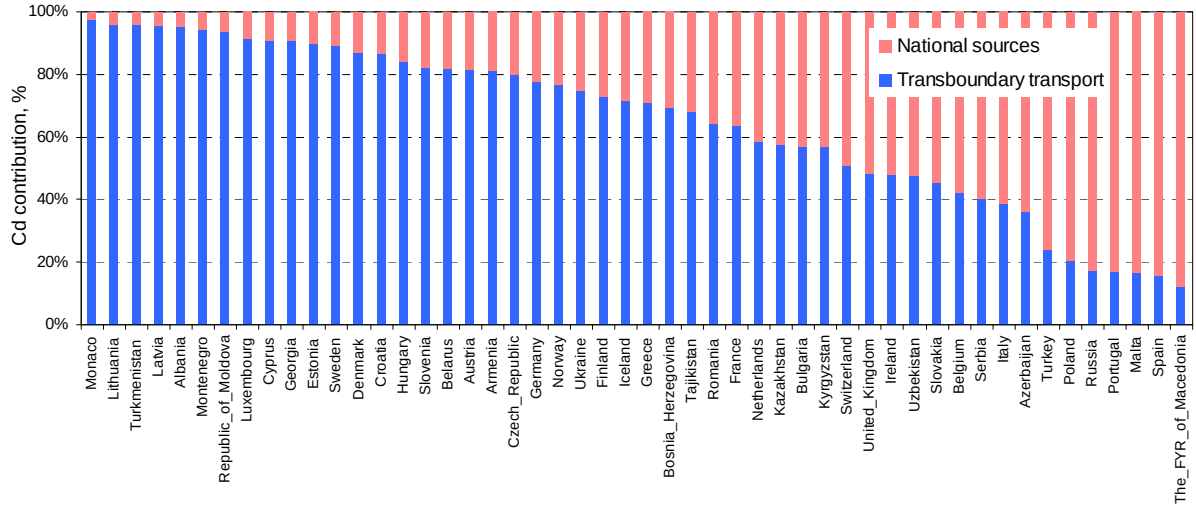

Fig. 4.23. *Relative contribution of the transboundary transport and national sources to anthropogenic cadmium deposition in the European and Central Asian countries in 2008*

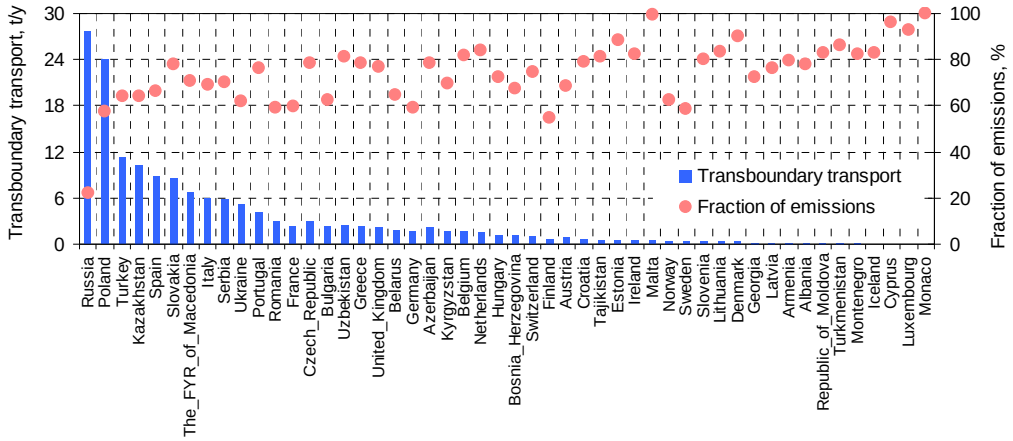

Fig. 4.24. *Absolute contribution of the European and Central Asian countries to cadmium transboundary transport in Europe and Central Asia in 2008 and relative fraction of national emissions involved into the transboundary pollution*

MERCURY

Spatial distribution of mercury concentrations in air was smoother compared to that of lead and cadmium (Fig. 4.25). It is explained by the fact that mercury life time in the atmosphere is about one year. This time is sufficient for almost complete mixing over the globe. It implies that mercury is a global pollutant. Over major part of Europe and Central Asia annual mean modelled and observed concentrations of mercury in air varied between 1.4 to 1.7 ng/m^3. In some regions of Europe known for significant mercury emission sources (southern Poland, north of Italy, Hungary, Romania) the concentrations exceeded 1.7 ng/m^3.

Gaseous oxidized and particulate mercury are the forms which readily washed out from the atmosphere. These forms present in the anthropogenic emissions as well as they originate in the atmosphere due to mercury chemical transformations. Therefore, map of mercury wet deposition reflects combined effect of emission distribution, precipitation patterns and regional distribution of oxidizing properties of the atmosphere. Spatial distribution of mercury wet deposition was more inhomogeneous compared to that of concentrations in air (Fig. 4.26), especially in the vicinity of

regions with large emissions. Over most of the European and Central Asian territory wet deposition fluxes in 2008 ranged from 0.01 to 0.05 g/km^2/day. Observed levels lay in the same range. The highest deposition levels took place in regions known for large emission sources (northern part of Italy, Poland, the Balkan region). The lowest deposition fluxes were noted in the Arctic region and in the arid regions of Central Asia.

Map of total annual deposition of mercury was similar to that of wet deposition. Higher deposition typically occurred in regions with significant emission sources and high precipitation (Fig. 4.27). Typical regional-scale deposition values in 2008 varied from 7 to 20 g/km^2/y, and in most polluted areas (southern Poland, the Balkans, Kyrgyzstan) they exceeded 20 g/km^2/y.

Total deposition to the European and Central Asian countries were 234.4 tonnes (157.9 to Europe and 76.5 to Central Asia and Eastern Russia). It was almost the same as deposition in 2007. Most of deposition in 2008 were caused by non-EMEP sources (155 t), while the anthropogenic sources contributed 76 tonnes and natural sources within the EMEP domain - only 4 tonnes. Predominant contribution of deposition from the non-EMEP sources reflected the fact that mercury was a global pollutant. It meant that sources of mercury located far (thousands km) from the receptor regions could significantly contribute to mercury pollution levels of the receptor. In order to specify the contribution of global sources and intercontinental transport to pollution in the EMEP region global-scale models (e.g., GLEMOS) are needed.

Over the most countries the country-averaged deposition between 2007 and 2008 changed within ±15%, which was consistent with the changes of deposition caused by annual variability meteorological conditions. For example, the increase of precipitation amount between 2007 and 2008 over the most part of Scandinavia, north-west of Italy and the central and north-western parts of Russia resulted in some increase of total deposition in these regions. Rise of precipitation in Spain was compensated by simultaneous decline of emissions, which finally led to minor changes in deposition in this country. In some countries the deposition changes were more significant. For example, deposition to Denmark declined by almost 20%, to Cyprus – by 45%. The

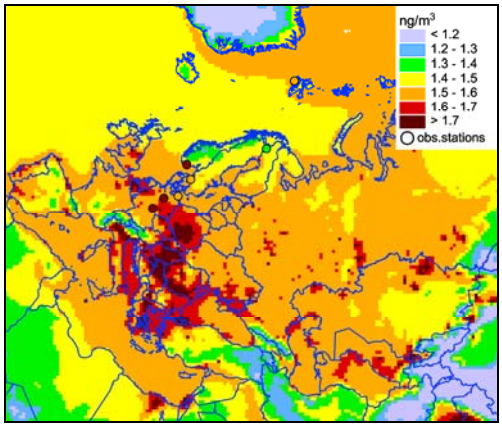

Fig. 4.25. *Calculated and measured surface concentrations of mercury in air over Europe and Central Asia in 2008*

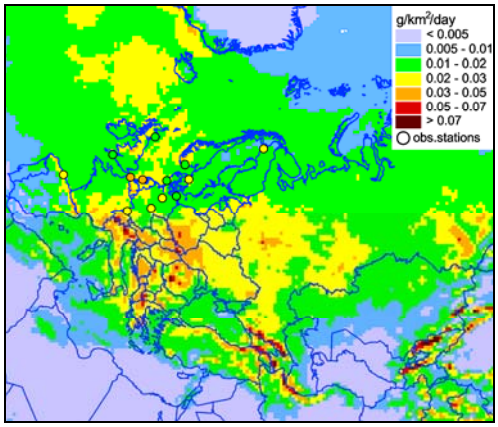

Fig. 4.26. *Calculated and measured daily sums of wet deposition fluxes of mercury over Europe and Central Asia in 2008*

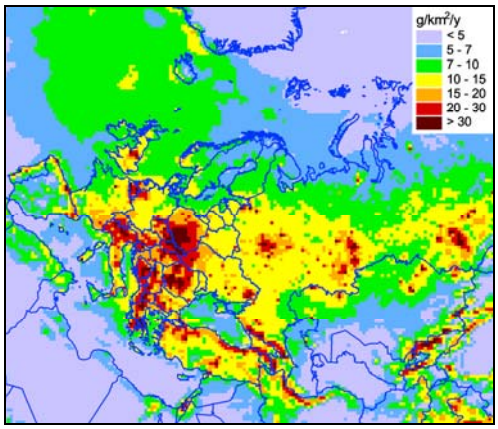

Fig. 4.27. *Total annual deposition of mercury in Europe and Central Asia in 2008*

reason for this was the fact that the emissions in 2008 reported by these countries were substantially lower than those in 2007. Similar reason led to the decrease of total deposition of mercury in some other countries, e.g., Germany, France, or Norway. In Slovakia and Romania the deposition increased by about 25% and 35%, respectively, because of the increase of emissions.

Country-averaged deposition of mercury in 2008 varied significantly across Europe and Central Asia. The highest deposition was obtained for Slovakia (33.4 t), and the lowest – for the Central Asian countries Uzbekistan and Turkmenistan (Fig. 4.28). As a rule, higher deposition was associated with regions with high emission. Low country-averaged deposition in the Central Asian countries was explained by low precipitation amounts in these countries. In 35 countries of 50 non-EMEP sources were the major contributor to deposition. The largest contribution (more than 80%) of non-EMEP sources to total mercury deposition in countries was estimated for Scandinavian countries (Iceland, Norway, Finland, Sweden) and some Central Asian countries (Tajikistan, Kyrgyzstan, Turkmenistan). In countries of the central and south-eastern Europe, known for significant mercury anthropogenic sources, the contribution of global sources was the lowest (30 – 35%). These countries were Slovakia, Belgium Poland, Greece, Serbia, Hungary, and the Czech Republic.

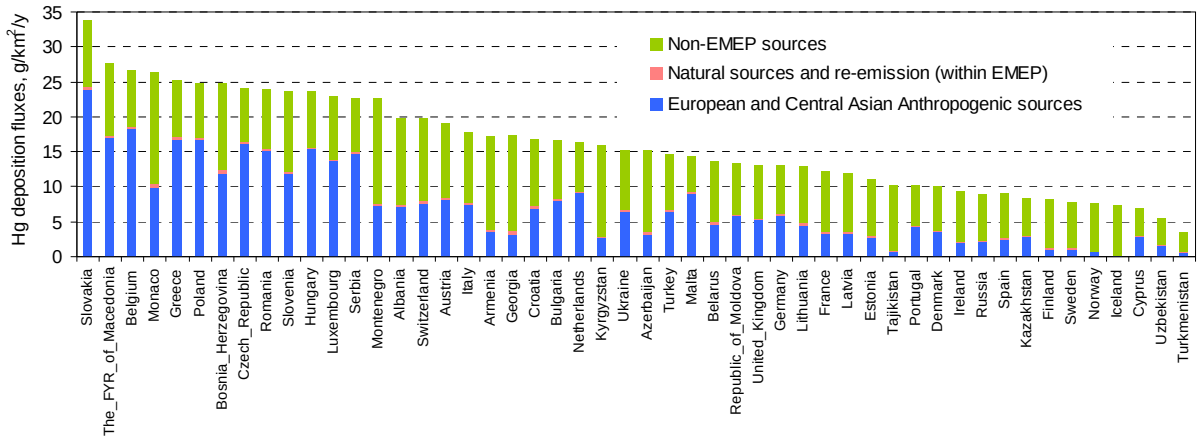

Fig. 4.28. *Country-averaged deposition fluxes of mercury from the European and Central Asian anthropogenic, natural/historical and non-EMEP sources in 2008*

The highest contribution of transboundary transport to anthropogenic deposition of mercury in Europe and Central Asia was obtained for countries with relatively low national emissions (Iceland, Lithuania, Turkmenistan, Latvia etc). In these countries the contribution of transboundary transport was around 90% or more (Fig. 4.29). Lowest contribution (below 25%) of transboundary transport to anthropogenic deposition took place in countries with significant mercury emissions (e.g., Turkey, Greece, Poland, Italy) or for countries remote from main emission sources (e.g., the United Kingdom, Spain, Malta). In 27 countries the contribution of transboundary transport exceeded 50%, and in 9 countries – exceeded 80%.

The largest contribution to transboundary transport of mercury emitted in a country was made by Russia (29 tonnes) (Fig. 4.30). Other significant contributors were Kazakhstan (23 tonnes), Turkey (17 tonnes), Poland (12 tonnes). The fraction of mercury emitted by national sources and transported outside the country was quite similar for all countries and ranged between 80% and almost 100%. Because of the vast territory Russia was an exception: the fraction was 63%. Compared to lead and cadmium, the fraction of mercury transported outside the country was higher. It was explained by the fact that considerable part of the emitted mercury was represented by elemental form which was slowly removed from the atmosphere and thus readily entered long-range and global transport.

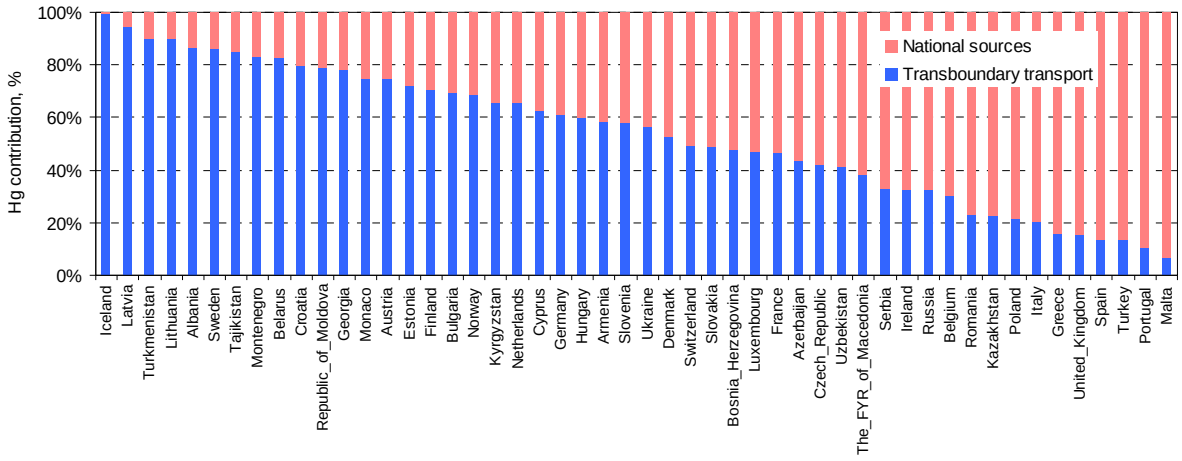

Fig. 4.29. *Relative contribution of the transboundary transport and national sources to anthropogenic mercury deposition in the European and Central Asian countries in 2008*

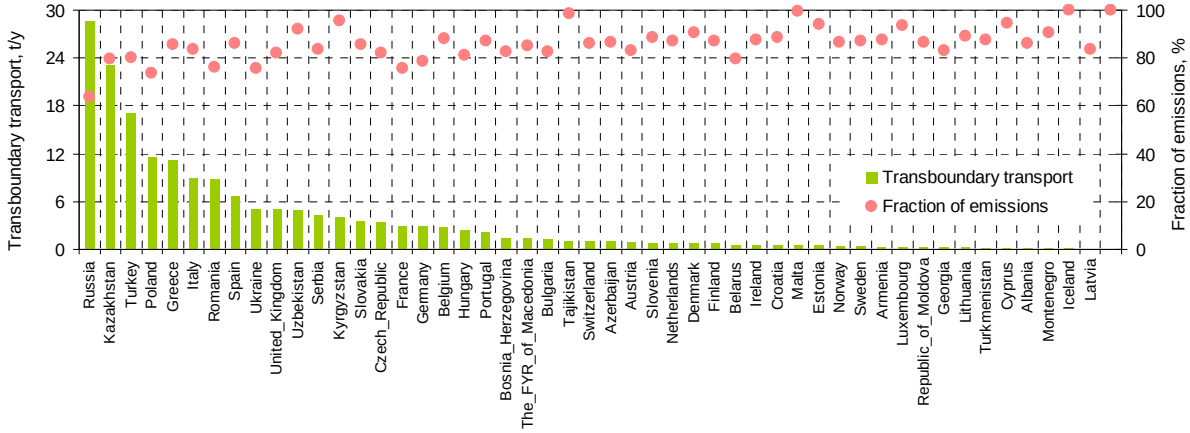

Fig. 4.30. *Absolute contribution of the European and Central Asian countries to mercury transboundary transport in Europe and Central Asia in 2008 and relative fraction of national emissions involved into the transboundary pollution*

Deposition to regional seas

According to the workplan MSC-E performed calculation of atmospheric deposition of lead, cadmium and mercury to the seas surrounding Europe: the Black (with Azov), the North, the Mediterranean, the Baltic and the Caspian. The Black Sea was characterized by the highest deposition of lead (0.65 kg/km^2/y) and cadmium (19.5 g/km^2/y) (Fig. 4.31). The highest mercury deposition (9.1 g/km^2/y) was evaluated for the North Sea.

Compared to 2007, deposition of lead and cadmium in 2008 declined by 5 – 25% for all seas expect the Caspian Sea. Deposition to the Caspian Sea changed insignificantly. The decrease of deposition over the seas was explained mostly by lower wind re-suspension of lead and cadmium from land,

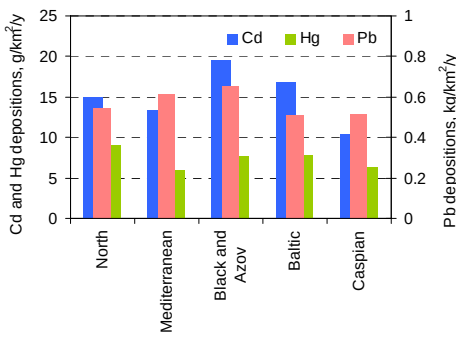

Fig. 4.31. *Averaged deposition fluxes of lead, cadmium and mercury to regional seas in 2008*

and also by lower emission values in some countries used in modelling for 2008. In case of mercury the changes of deposition were minor over all seas except the Caspian Sea. The deposition of mercury to the Caspian Sea increased in 2008 by about 12% because of the increase of precipitation amount in 2008 compared to 2007.

Contribution of all individual countries to deposition of lead, cadmium and mercury to the considered seas was evaluated. Fig. 4.32 demonstrates the example for the Caspian Sea. As seen from the figure, the main contributors of heavy metal deposition to this sea were Russia, Kazakhstan, Azerbaijan, Turkey and Uzbekistan. For cadmium and mercury Ukraine was also among the main contributors. Russia and Kazakhstan were the main sources of anthropogenic deposition of lead, and their contributions were 38% and 36%, respectively (Fig. 4.32a). More than 80% of anthropogenic deposition of cadmium was caused by Russia, Kazakhstan and Azerbaijan (Fig. 4.32b). As for mercury, the main contributor to deposition was Kazakhstan (62%), followed by Azerbaijan and Russia (Fig. 4.32c). Deposition of heavy metals from different countries to the Caspian Sea was governed by a number of factors including magnitude of emission sources, their proximity to the sea, wind and precipitation patterns. It was also worth mentioning that deposition only to the sea surface was considered. For more detailed evaluation of marine pollution it is necessary to take into account deposition to basins of rivers flowing into the sea and their consequent transport to the sea with surface runoff.

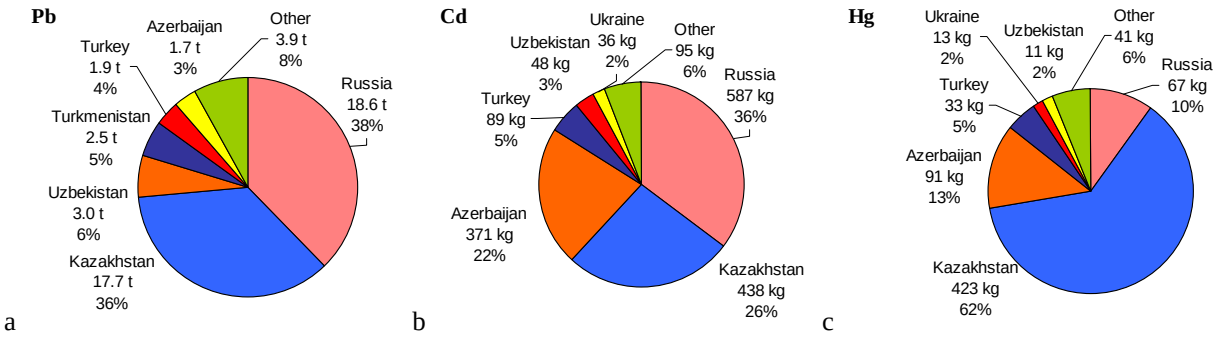

Fig. 4.32. *Contribution of different countries to anthropogenic deposition of lead(a), cadmium(b) and mercury (c) to the Caspian Sea in 2008*

4.5. Uncertainties of the pollution assessment

Quality of the air pollution assessment can be characterized on the base of integrated approach which takes into account uncertainties of the model, emission data and measurements. This section summarizes the available estimates of the uncertainties of the emission and monitoring data. These uncertainties are compared with the deviation between modelled and observed concentrations and deposition.

Emissions

Uncertainties of the emission data were discussed in depth at the joint TFMM/TFEIP Workshop held in Larnaca, Cyprus, in May, 2010. It was noted that the uncertainties of the emission estimates could be caused by missing of source categories, insufficient data on activities, current knowledge on emission factors etc. Official information of total emission data uncertainty of heavy metals in 2008 was available

for Denmark, Finland, France, Sweden and the United Kingdom (Table. 4.3). As seen from the table, the uncertainty of country totals of heavy metal emission can reach hundreds of per cents, but typically is about 30 – 60%. Most likely, this is stochastic uncertainty, and it does not include systematic uncertainty of the emissions caused by missing emission sources.

Table. 4.3. *Uncertainties of the heavy metal emission totals for 2008, %*

	Denmark [*Nielsen et al*., 2010]	Finland [*SYKE*, 2010]	France [*CITEPA*, 2010]	Sweden [*SEPA*, 2010]	United Kingdom [*Murrells et al*., 2010]
Lead	332	±27	61	15	-30 to +50
Cadmium	195	±29	60	47	-20 to +50
Mercury	142	±25	48	99	-30 to +40

Monitoring

Uncertainties of measurement data also contribute to the discrepancies between modelling results and observations. Intercomparisons of national laboratories involved in the analysis of lead and cadmium measurements sampled at the EMEP stations are carried out regularly. These intercomparisons demonstrate that the accuracy for most of the laboratories is better than ±25% (See chapter 3) for lead and cadmium in precipitation.

Laboratory intercomparisons provide evaluation of the accuracy of analytical methods. Overall measurement accuracy can be estimated by field campaigns. Field comparison of measurements of total gaseous mercury concentrations held in May, 2005, demonstrated that the results of most of the laboratories, participated in the comparison, fall within ±30% range, and for concentrations in precipitation - within ±40% range [*Aas*, 2006]. Uncertainty of wet deposition of lead and cadmium, estimated on the base of the results of 2006-2007 field campaign, was around 20% [*Aas et al*., 2009]. However, these estimates do not take into account the effect of representativeness of station location.

Modelling

Uncertainty of the model assessment of pollution levels can be characterized via comparison of the modelled and measured values, keeping in mind the uncertainties of observations mentioned above. Fig. 4.33 demonstrates scatter plots showing deviation of the modelled concentrations in air and wet deposition fluxes from the observed parameters. As seen from the Figure, for most of stations the deviation of the modelled value from the measured one is within a factor of two. However, there are some stations for which the discrepancies are significant. For example, the model underestimates wet deposition of lead and cadmium by a factor of three or more at Spanish sites, and some Scandinavian stations.

Concentrations of mercury in air are known for low spatial variability, which is of the same order of magnitude as their measurement uncertainties. Therefore, all modelled and measured concentrations are grouped within a range of 1.4 – 1.8 ng/m^3.

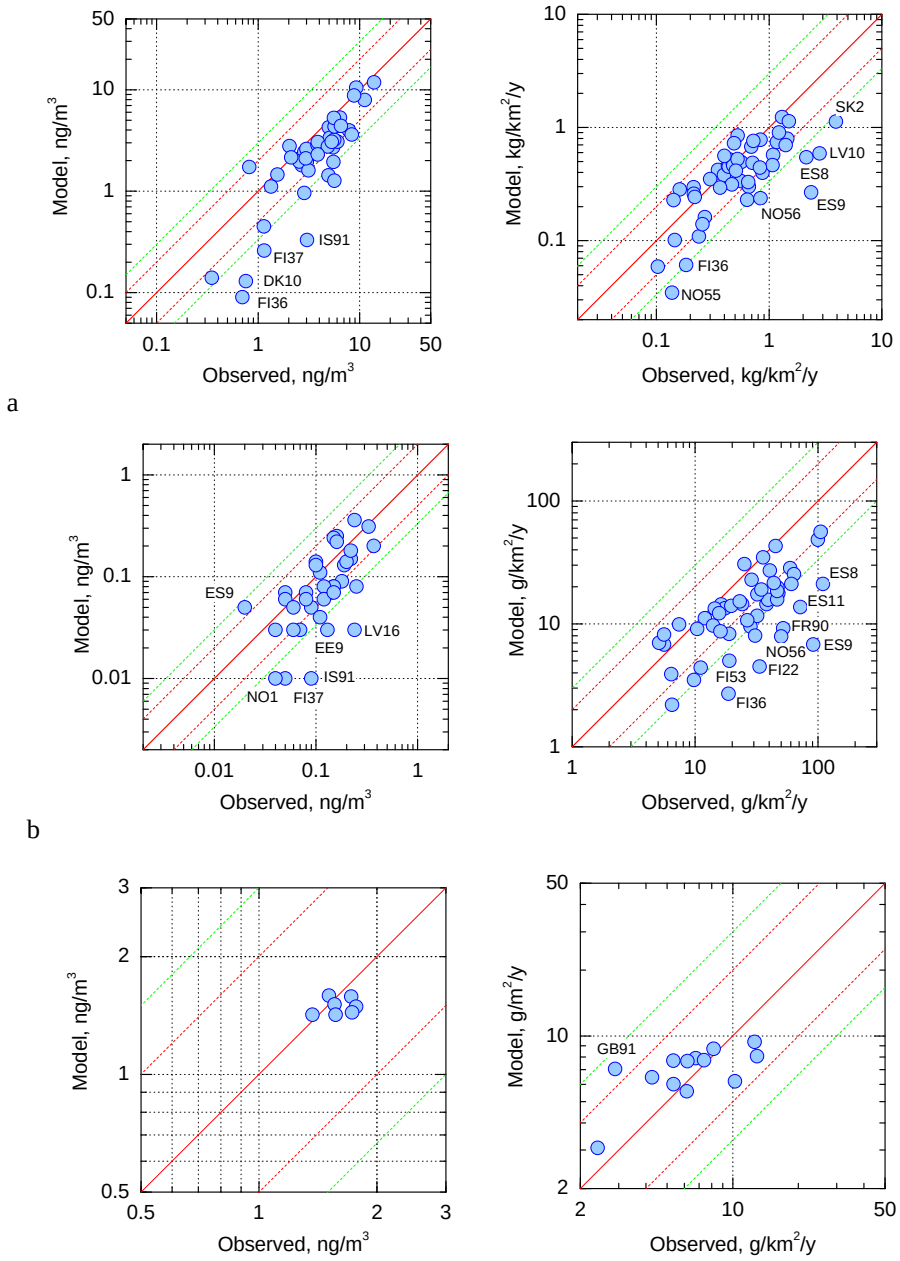

Fig. 4.33*. Modelled vs. observed concentrations of lead (a), cadmium (b) and mercury (c) in air (left) and wet deposition fluxes (right). Solid red line depicts 1:1 ratio; dashed lines: deviation within factor 2 (red) and factor of 3(green)*

Table 4.4 summarizes statistical metrics which characterize the model uncertainty. They include Root Mean Square Error (RMSE), correlation coefficient (R_{corr}), mean normalized bias (MNB) and a fraction of stations for which the ratio between modelled and measured value falls within a certain factor. For example, F2 relates to two-fold deviation, F3 – three-fold deviation.

As seen, RMSE for air concentrations and deposition fluxes of heavy metals is around 50%. Keeping in mind uncertainties of the emissions (Table 4.1) and measurements data, this result seems satisfactory. At around 70% of stations modelled and observed lead and cadmium concentrations in air and wet deposition fluxes of lead agree within a factor of two. For wet deposition of cadmium this fraction is around 50%. The MNB indicates that the model has some tendency to underestimate the observed lead and cadmium values. However, the extent of the underestimation is comparable with the emission

and measurement uncertainties. Correlation coefficients for all parameters are higher than 0.5 except for mercury in air. Low correlation for this species is explained by low spatial variability of elemental mercury comparable with the uncertainties of its measurements.

It is necessary to note that these statistical parameters are strongly affected by high discrepancies between modelled and values obtained at few stations. Relatively high observed values at these stations can be caused by measurement errors, the influence of local emission sources, peculiarities of geographical location of the stations etc. and should be investigated separately in cooperation with CCC and national experts. These investigations could be undertaken in the framework of the EMEP Case Study project, focused on in-depth analysis of pollution levels in individual countries (Chapter 3).

Table 4.4. *Statistical parameters of the model-to-observation comparison for concentrations in air and wet deposition fluxes*

Parameter	Pb, in air	Pb, wet dep.	Cd, in air	Cd, wet dep	Hg in air	Hg, wet dep
RMSE*, %	47	45	56	54	10	49
F2, %	70	75	69	47	100	92
F3, %	89	86	85	82	100	100
R_{corr}	0.88	0.58	0.68	0.62	0.2	0.62
MNB**, %	-31	-39	-25	-55	-7	1

$^{*}RMSE = \sqrt{\frac{1}{N}\sum_{i}^{N}\left(\frac{M_i - O_i}{O_i}\right)^2} \cdot 100\%$ $^{**}MNB = \frac{(\overline{M} - \overline{O})}{\overline{O}} \cdot 100\%$

M_i , O_i –modelled and observed values at i[th] station. $\overline{M}$, $\overline{O}$ - averaged modelled and observed values

In order to better understand the reasons which can lead to the discrepancies between modelled and measured values, the comparison of modelled and observed time series for each station is carried out. Back trajectory analysis is applied to investigate the periods of the significant discrepancies. For example, comparison of temporal variability of the measured and observed wet deposition at the Czech station CZ3 indicated that for some periods the model well matched the observed values while for other periods the underestimation was significant (Fig. 4.34).

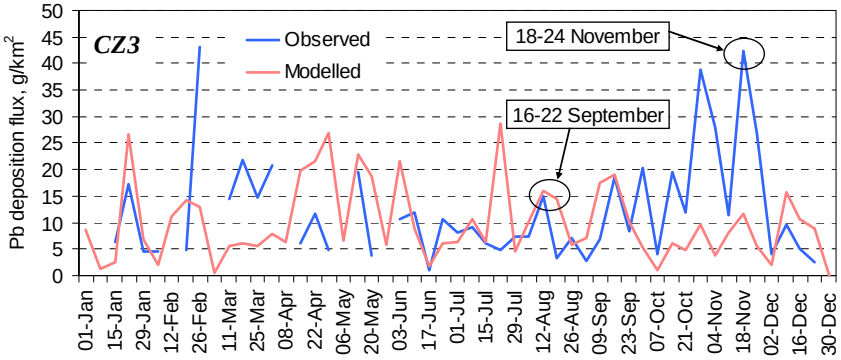

Fig. 4.34. *Modelled and observed concentrations of lead in precipitation at Czech station Kosetice (CZ3) in 2008*

Back trajectory analysis was applied to the periods when the modelled values agreed well with measurements and when the discrepancies between measured and modelled values were high. For example, in the period from 18 to 24 November the model significantly (around 3.5 times) underestimated measured pollution fluxes at CZ3. In this period and also other periods in October and

November the prevailing transport of air masses was from the west (Fig. 4.35a). When the eastern transport from territory of Slovakia or Poland took place (e.g., in 16th – 22nd of September), the levels agreed satisfactory (Fig. 4.35b). Precipitation amounts derived by meteorological pre-processor and observed at the station were similar. The discrepancies can be explained by uncertainties of national or external emission data, e.g., unaccounted possible short-term temporal variability, or by the influence of local sources. Uncertainties of modelling and measurements also contribute to the discrepancies. Case Study on heavy metal pollution assessment is aimed at integrated analysis of factors affecting agreement between modelled and measured values. Detailed analysis of emission, measurement data and modelling results will be carried out in cooperation with experts from the Czech Republic.

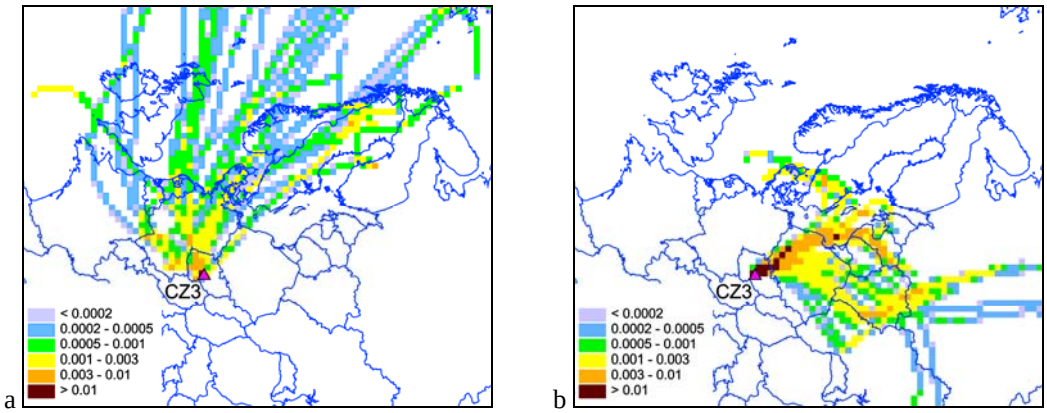

Fig. 4.35. *Density of back trajectories crossing grid cells for the Czech station Kosetice (CZ3) for the period of 18th – 24th of November (a) and 16th – 22nd of September (b)*

Another example demonstrating the application of back trajectories is given for the analysis of cadmium concentrations in air at the Czech station CZ1 (Svratouch) (Fig. 4.36). For some peak periods (e.g., 25th of April, 28th of May, 5th of June, 29th of July) the transport of air masses took place through territory of Poland (Fig. 4.37a). Poland is known for high cadmium emission (Fig. 4.7b). Threfore, both modelled and measured values in this period were high compared to other periods. The exception was the period of 5th of June. This and previous days were characterized by significant precipitation which led to scavenging of cadmium in air and hence, to relativity low modelled air concentrations.

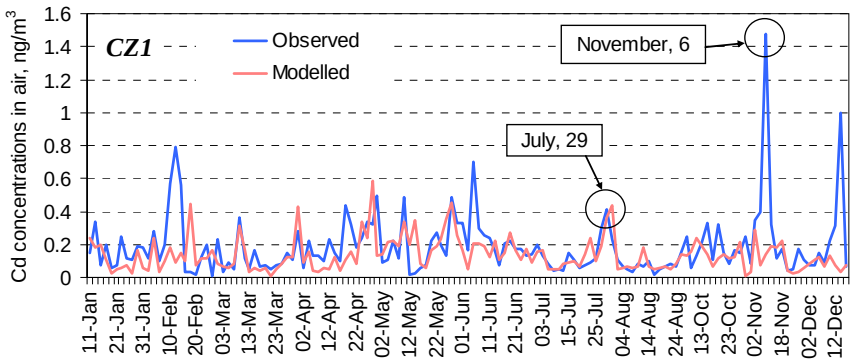

Fig. 4.36. *Modelled and observed air concentrations of cadmium at Czech station Svratouch (CZ1) in 2008*

However, some extremely high peaks can hardly be explained by transport from Poland. For example, in 6th of November (Fig. 4.37b) air masses arriving to the station passed over Austria and southern part of Europe (Italy, Croatia, and other countries). The agreement between modelled and observed

concentrations of cadmium at Austrian stations is satisfactory, so it is hardly possible that emissions in Austria or other countries in this region were so drastically underestimated. Most likely, local sources significantly contributed to levels measured at this station. These situations can be analysed in more detail in the framework of the Case Study in cooperation with national experts and applying modelling at finer resolution (e.g., 10×10 km^2).

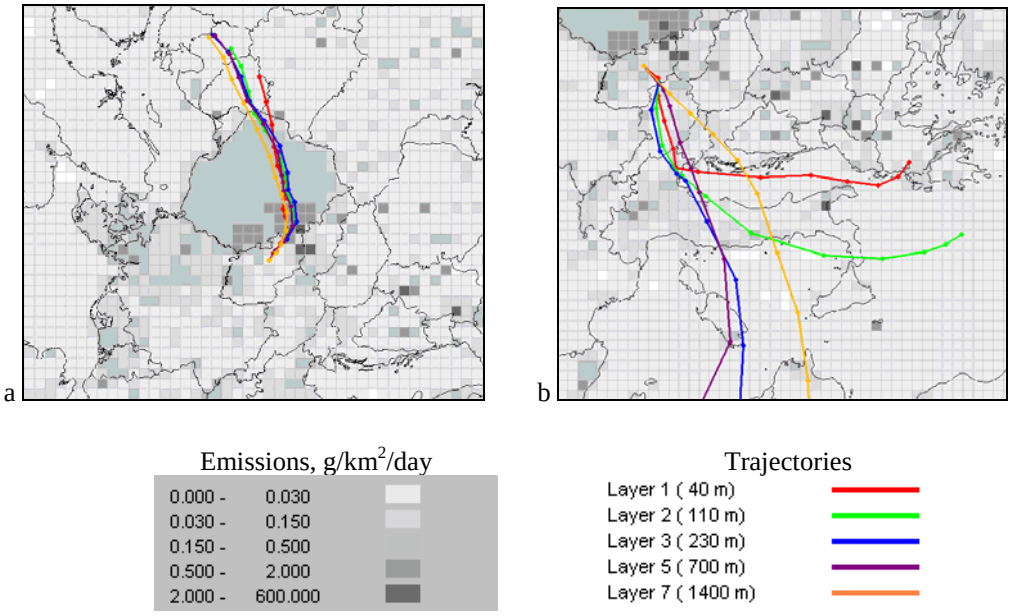

Fig. 4.37. *Back trajectories crossing grid cells for the Czech station CZ1 for the period of 29th of July (a) and 6th of November (b) and overall (anthropogenic emission and wind re-suspension) of atmospheric input of cadmium*

5. COOPERATION

In the framework of evaluation of heavy metal pollution levels MSC-E and CCC closely cooperated with the WGE, TFMM and TFEIP. In particular, at the joint workshop of TFMM and TFEIP (Cyprus, Larnaca, May, 2010) information on uncertainties of heavy metal emissions and model assessment was presented. Contribution to the TF HTAP activity is given in Chapter 2. MSC-E took part in the project in support of the revision of the Heavy Metal Protocol. Cooperation with national experts, with the emphasis on EECCA countries, and with international organizations (HELCOM, AMAP, OSPAR, UNEP etc) was continued.

5.1. Contribution to the project in support of the revision of the CLRTAP Protocol on Heavy Metals

MSC-E contributed to the project in support of the revision of the Heavy Metal Protocol initiated by the Dutch Ministry of Hosing, Spatial Planning and the Environment (VROM). Information on deposition and concentrations of lead, cadmium and mercury was prepared on the base of four scenarios of heavy metal emissions. Data on deposition of lead, cadmium and mercury were submitted to Coordinating Centre for Effects (CCE) to determine the exceedances of critical loads for ecosystems and human health. The results of this project are planned to be reported to the Working Group on Strategies and Review (WGSR).

Emission data

TNO has developed four scenarios of lead, cadmium and mercury emissions in Europe:

- 2010 current legislation and current ratification of the HM Protocol (Scenario 1)
- 2020 full ratification of the HM Protocol (Scenario 2)
- 2020 full ratification of the amended HM Protocol option 1 for dust plus Hg measures (Scenario 3)
- 2020 full ratification of the amended HM Protocol option 2 for dust plus Hg measures (Scenario 4)

Emissions for modelling over the EMEP domain were prepared jointly by TNO and MSC-E. It is worth mentioning that emission expert estimates, prepared by TNO differ from the emission data used in modelling under EMEP for 2008. The preparation of the EMEP emission data for modelling is described in Section 4.2 of this report. Fig. 5.1 demonstrates lead emission totals of these two data sets. In some countries the emission values are quite comparable. For example, in the Netherlands, Belgium, the Czech Republic, Italy, Sweden the difference between the two sets lies within ±15%. However, in other countries the differences reach several times, and in some cases, e.g., in Greece – almost 40 times.

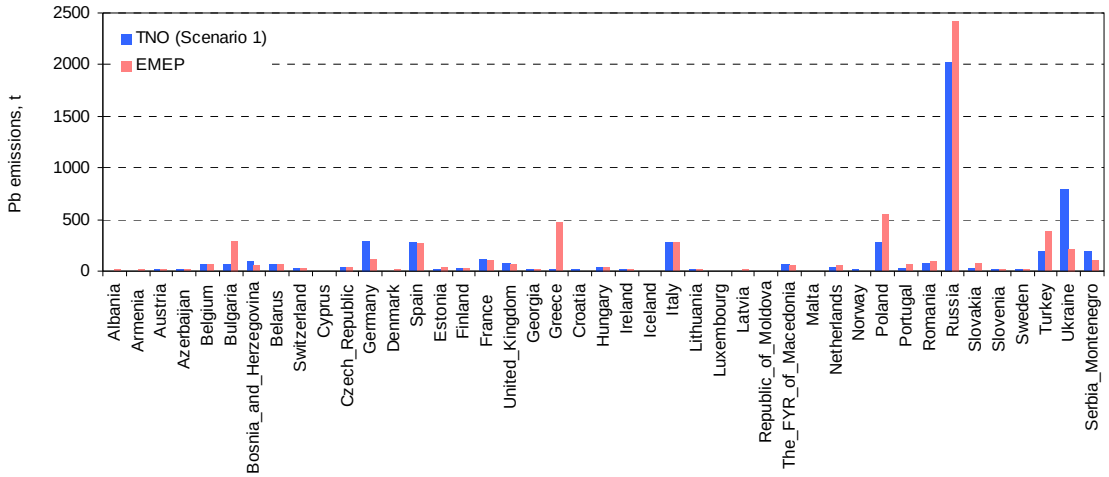

Fig. 5.1. *Country-averaged emission of lead prepared by TNO for Scenario 1 (current legislation, 2010) and used in modelling by EMEP for 2008*

The comparison of the two emission data sets reflects significant uncertainties associated with the existing heavy metal emission data. From modelling viewpoint, it would be useful if countries report not only one total value, but also estimate possible range (maximum and minimum) of uncertainties of national emission totals. In addition to this, in-depth comparison of the official data and emission expert estimates is recommended to harmonize the datasets and to remove major discrepancies between them.

Modelling results

Comparison of country-averaged deposition simulated on the base of different emission scenarios demonstrates that the most significant changes in heavy metal pollution levels are projected for countries located in the south-eastern and the eastern parts of Europe. This fact is exemplified by lead (Fig. 5.2), but for cadmium and mercury the situation is quite similar. In countries of the central, western and northern parts of Europe the differences in deposition are relatively small. For example, the difference in country-averaged deposition of lead, cadmium and mercury based on four emission scenarios is within ±20% in Austria, Germany, France, etc. However, in the FYR of Macedonia, Russia, or Ukraine the differences can be 1.5 - 2 times.

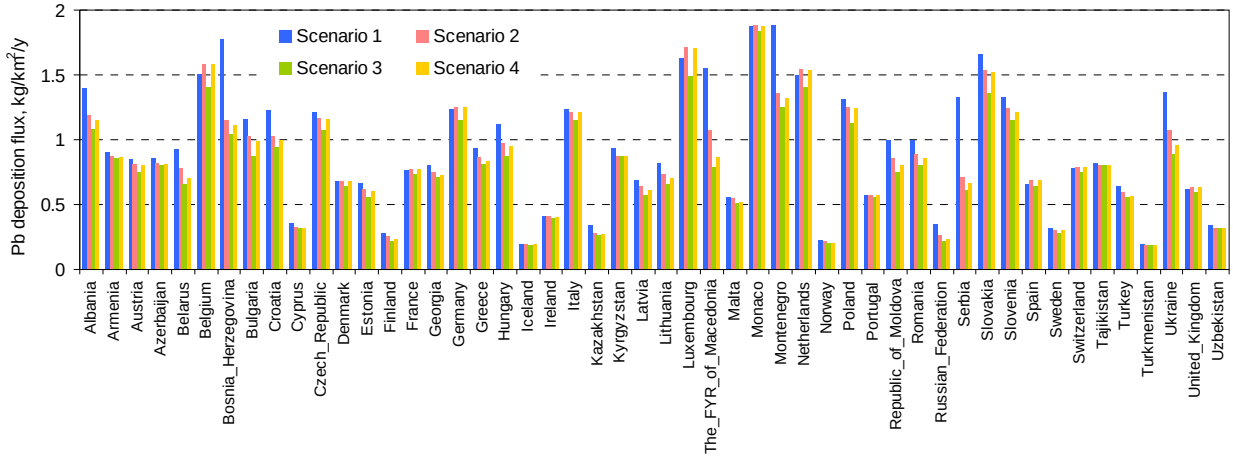

Fig. 5.2. *Country-averaged deposition fluxes of lead to countries of Europe and Central Asia calculated on the base of different TNO emission scenarios*

The reason for this is connected with the scenarios of the emissions used in this study. Most of countries in the central, western and northern parts of Europe have already ratified the Protocol on Heavy Metals, and their emissions have already declined following the requirements of the Protocol. Therefore, according to the considered scenarios the long-term changes of the emissions in these countries are relatively low. Hence, changes of deposition in these countries are expected to be insignificant. A number of countries of the south-eastern and eastern Europe (e.g., Bosnia and Herzegovina, Montenegro, Kazakhstan, Russia, Ukraine, etc.) have not yet joined the Protocol. Since TNO emission scenarios for 2020 assume full implementation of the Protocol in all EMEP countries, significant changes in emissions, and consequently, in calculated pollution levels of heavy metals are expected.

There are three sources of deposition: anthropogenic emissions, wind re-suspension of historically accumulated metals and transport from non-EMEP sources. Therefore, the change of one of the sources results to smaller change of the deposition. Total anthropogenic emission reduction for Europe and Central Asia as whole is 52%, and for deposition over this region – 24%. However, the decline of total atmospheric input (anthropogenic, re-suspension, sources in Asia and Africa) of lead between 2010 and 2020 (Scenario 3) makes up 25%, which is consistent with the reduction of deposition. The magnitude of re-suspension and non-EMEP sources used in the modelling of deposition has not changed for all the scenarios, and thus the relative changes of deposition are smaller than the changes of anthropogenic emissions.

Spatial distributions of deposition calculated on the base of various emission scenarios look quite similar in countries where differences in total emissions are relatively small, and vice versa. Fig. 5.3 exemplifies maps of lead deposition based on Scenario 1 (2010, current legislation) and Scenario 3 (2020, full Protocol implementation option 1). The most distinguished changes in deposition are seen in the central part of Russia, the eastern part of Ukraine, in the south-eastern part of Europe (e.g., Romania, Bulgaria, Serbia, Croatia). In the western, central and northern parts of Europe the changes in deposition fields are minor.

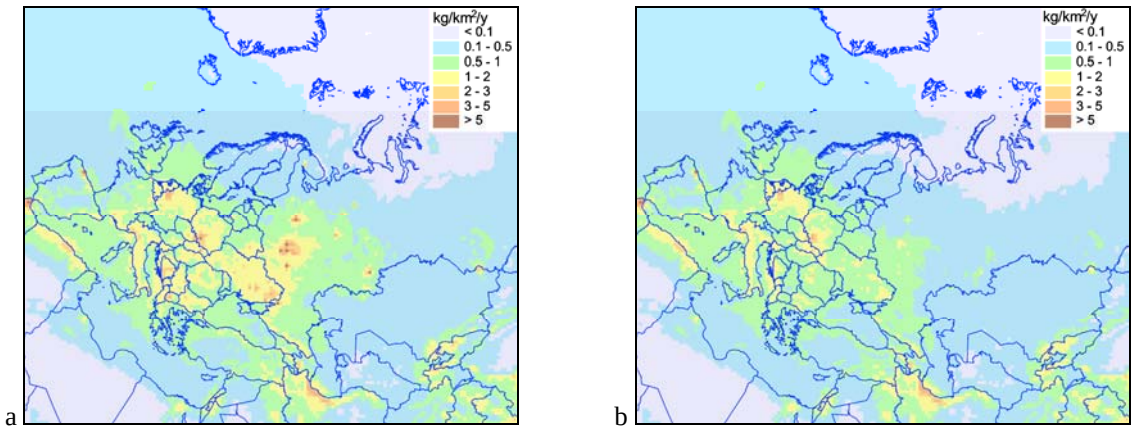

Fig. 5.3. *Spatial distributions of total deposition of lead based on emission scenario 1 (a) and scenario 3 (b)*

On the basis of the analysis it is possible to conclude that the reduction of total deposition of lead to countries of Europe and Central Asia as a whole between 2010 and various scenarios for 2020 range within 15 - 24 % depending on the considered scenario. These changes are resulted from the reduction of anthropogenic emission in this region within 33 - 52%. The corresponding reduction for total atmospheric input is 16 - 25%. For cadmium the reduction of deposition ranges from 15 to 27% for Europe and Central Asia as a whole. For mercury the deposition changes vary between growth of 4% to the reduction of 5%. Relatively low changes of mercury deposition are explained by the significant influence of intercontinental transport. The changes for individual countries are highly variable because of the influence of transboundary transport.

5.2. ICP-Vegetation (Working Group on Effects)

Mosses are often used in monitoring of atmospheric pollution, and, in particular, of heavy metals [*Harmens and Norris*, 2008]. Extensive pan-European moss surveys are carried out every five years. ICP-Vegetation of the Working Group on Effects (WGE) is responsible for coordination of this activity.

Detailed analysis of pollution levels involving modelled deposition and measured concentrations of heavy metals in mosses was initiated last year [*Ilyin et al.*, 2009]. ICP-Vegetation provided MSC-E with the data on concentrations in mosses of heavy metals surveyed in 1990, 1995, 2000 and 2005/2006. Spatial variability of total deposition and concentrations in mosses in Europe were compared, long-term trends of the deposition and concentrations were analyzed. Besides, correlation coefficients between the deposition and concentrations were calculated for each country for each survey. This year more detailed analysis of factors affecting correlation between deposition and concentrations in mosses has been performed.

Four factors were considered. First of all, the effect of type of deposition was analyzed. Concentrations in mosses were compared separately with modelled wet and dry deposition fluxes. Second factor considered was the period of averaging of the deposition. Furthermore, the effect of modelled wind re-suspension on the comparison was evaluated. Finally, the influence of variability of measured moss concentrations within the EMEP grid cells and density of sampling network was characterized.

The experiments demonstrated that both wet and dry deposition fluxes were important for the comparison of concentrations in mosses and deposition. Similar conclusion could be made for wind re-suspension: both anthropogenic sources and re-suspension were significant for the comparison. Period of averaging of modelled deposition had minor effect on the correlation between total deposition and concentrations in mosses. The main reason of this was small changes in annual deposition patterns from one year to another.

More interesting results were obtained in the final set of experiments. The purpose of the experiments was to evaluate the effect of spatial variability of moss measurements within the EMEP grid cells on the correlation between concentrations in mosses and deposition. Density of moss measurements varied largely across Europe. It means that number of moss sampling plots falling in each EMEP grid cell differs among the grid cells. In most of the EMEP grid cells there are one, two or three sampling plots. In the quarter of the grid cells number of moss sampling plots equals or exceeds five.

Concentrations in mosses within the EMEP grid cells varied significantly. Fig. 5.4a depicts ratio of maximum to minimum measured concentrations of lead in mosses within the EMEP grid cells. High variability was noted for Switzerland, Germany, Slovakia, and the Balkan region. Relatively small ratio in France and the United Kingdom was explained by the fact that sampling density in these countries was 1 – 2 plots per grid cell.

In more than a half of grid cells the ratio was higher than 1.5, and in 1/3 of grid cells – more than 2 (Fig. 5.4b). In the analysis of pollution levels modelled deposition was compared with concentrations in mosses averaged over a grid cell. If a number of moss sampling plots within a grid cell is small (e.g., 1 or 2) it is not possible to be sure if moss measurements characterize higher or lower or medium pollution levels within a grid cell.

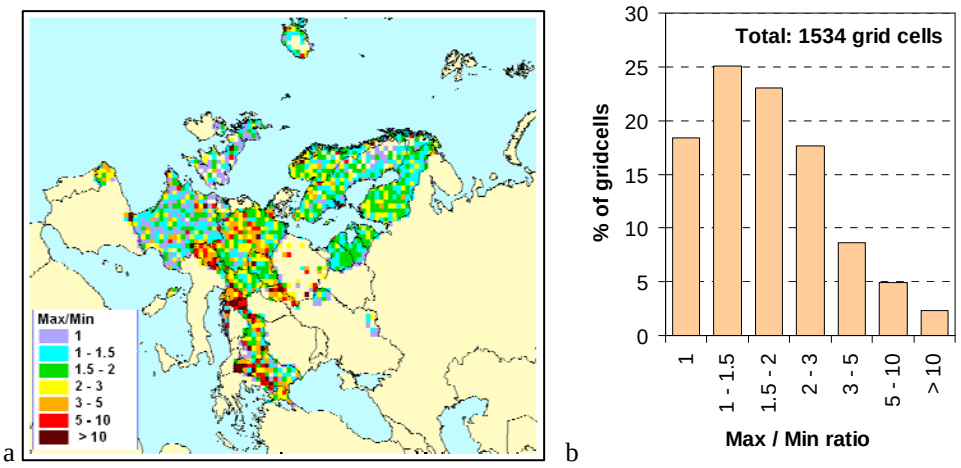

Fig. 5.4. *Ratio of minimum-to-maximum concentration of lead in mosses sampled in 2005 (a) and frequency distribution of the ratio (b)*

Therefore, spatial correlations were estimated for two cases. In the first case deposition was compared with grid-cell averaged concentrations in mosses obtained in all grid cells where moss measurement data were available (so-called base case). In the second case modelled deposition was compared with grid cells where three or more sampling plots were located.

Correlation between total deposition and concentrations in mosses was better for areas with higher sampling density. For example, in case of lead surveyed in 2005 significant increase of correlation coefficient was noted for France, the United Kingdom, Ukraine and other countries (Fig. 5.5). Similar results were obtained for the moss surveys held in other years and for cadmium.

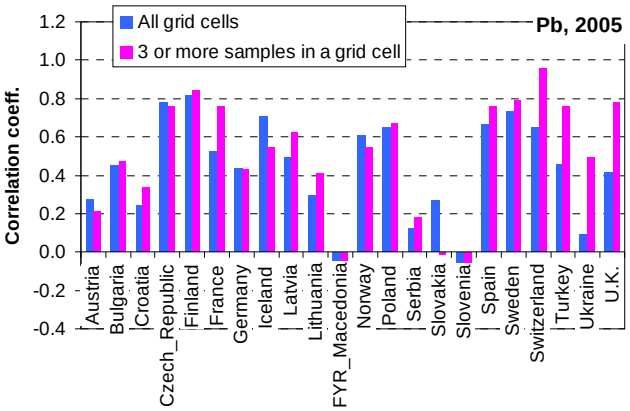

Fig. 5.5. *Spatial correlation coefficients between modelled deposition and grid-cell averaged concentrations of lead in mosses surveyed in 2005*

Modelled deposition was averaged over 50-km gridcells. Samples of mosses were collected of individual plots. These plots did not always characterize the entire 50-km grid cell from viewpoint of local variability of natural conditions. Besides, some samples could be taken in regions affected by local contamination [*Harmens and Norris*, 2008]. However, the more moss sampling plots were available within a grid cell, the more variability of natural conditions was embraced. Therefore the use of grid cells with big number of sampling points gave higher correlation compared to the base case.

The results of this analysis can be used by countries involved in moss survey activity when places of moss sampling are considered.

5.3. Cooperation with Arctic Monitoring and Assessment Program

MSC-E took part in preparation of the AMAP Assessment 2010 for mercury [*AMAP, 2011, in prep*]. In particular, the Centre participated in drafting and discussion of the assessment parts relating to the multi-model assessment of mercury atmospheric transport to the Arctic. Besides, MSC-E performed collection and processing of the modelling results for the multi-model assessment of the Arctic pollution with mercury. Some results of the multi-model assessment are presented below. More details are available in [*AMAP, 2011, in prep*.].

The mercury transport models participated in the multi-model assessment (GRAHM, GEOS-Chem, GLEMOS, DEHM) include detailed description of major physical and chemical processes governing mercury fate in the atmosphere. However, parameterizations and chemical schemes implemented into the models differ significantly. In particular, all the models include explicit treatment of the Atmospheric Mercury Depletion Events (AMDEs) taking place in the Polar Regions but major assumptions, chemical kinetics and input data utilized in the simulation are considerably different between the models. These differences demonstrate essential gaps in the current understanding of mercury processes in the atmosphere (such as oxidation, dry and wet removal, air-surface exchange) and, in particular, of the processes responsible for AMDEs.

Figure 5.6 presents estimates of mercury deposition flux over the Arctic performed by different chemical transport models. In general, the simulated spatial patterns of Hg deposition agree in identification of areas with high and low Hg loads. All the models predict general north-to-south gradient of Hg deposition reflecting the absence of significant emission sources within the Arctic. The lowest deposition levels are characteristics of Greenland because of its high elevation and snow cover of the surface. High deposition fluxes are typical for the European sector of the Arctic (North Atlantic and Barents Sea) because of the relative proximity of emission sources. In other parts of the Arctic simulated spatial patterns exhibit noticeable discrepancy. Scarce measurements of mercury deposition fluxes in the Arctic are not sufficient for reliable constraining the models.

Estimates of total mercury deposition to the Arctic (within the Arctic Circle, 66.5°N) vary within 110-221 t/y. However, among these estimates the one model (GEOS-Chem) reports the gross deposition, whereas three others – the net deposition flux (deposition minus re-emission). It should be noted that the prompt re-emission of mercury from snow is essential process characterizing periods of AMDEs and leading to decrease of mercury accumulation in snowpack [*Kirk et al*., 2006; *Johnson et al*., 2008; *Ferrari et al*., 2008]. Therefore, the net deposition flux appears to be more proper from the view point of evaluation of mercury accumulation in the Arctic environment and negative impact on the vulnerable ecosystems. The multi-model estimates of the total net deposition to the Arctic are more consistent and amount to 140±30 t/y.

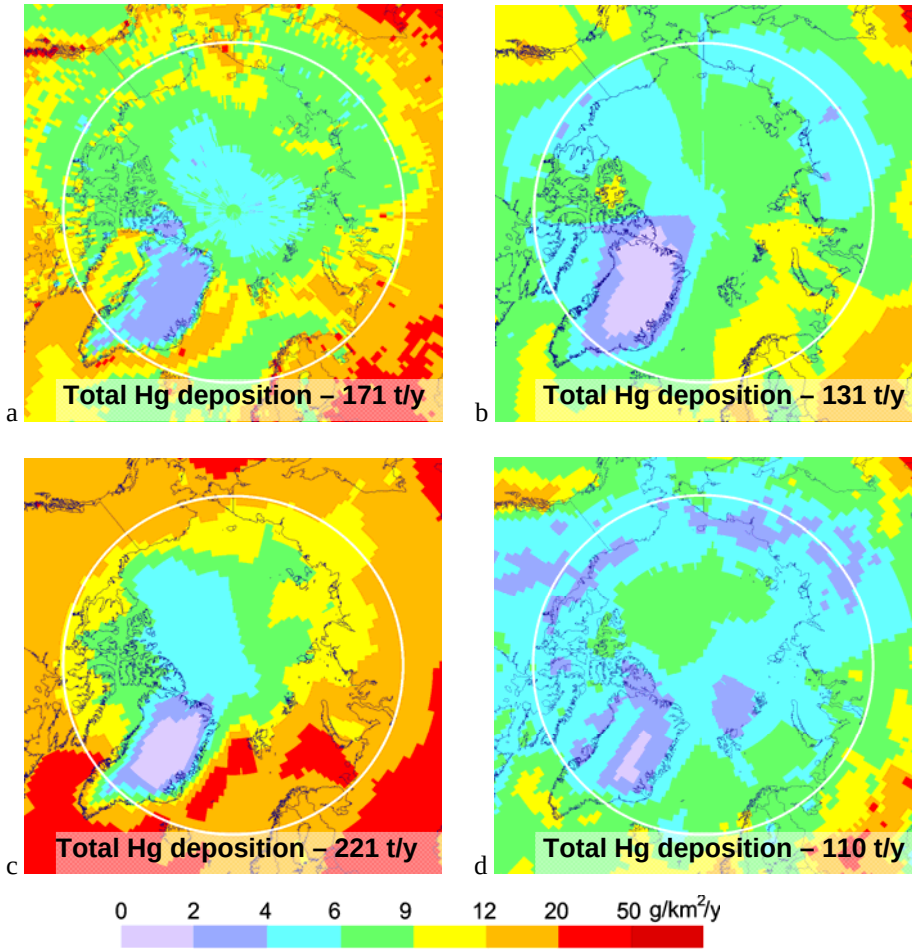

Fig. 5.6. *Spatial distribution of total mercury deposition to the Arctic simulated by GRAHM (a), GLEMOS (b), GEOS-Chem (c), DEHM (d). Circle on the figures depicts the Arctic circle (66.5°N). Total deposition estimates relate to deposition within the Arctic circle*

5.4. Marine Conventions (HELCOM)

MSC-E along with CCC and MSC-W continued the cooperation with the Baltic Marine Environment Protection Commission (HELCOM). In accordance with the Memorandum of Understanding between the HELCOM and the United Nations Economic Commission for Europe the EMEP Centres have prepared an annual joint report on the evaluation of airborne pollution load to the Baltic Sea [*Bartnicki et al*., 2009]. MSC-E contributed to this report with the evaluation of atmospheric input of heavy metals (lead, cadmium, and mercury) to the Baltic Sea. The atmospheric transport and deposition were assessed on the base of the EMEP officially submitted emission data. Besides, this report provided detailed information on emissions of heavy metals in HELCOM countries, contributions of individual countries to the deposition over the Baltic Sea, and the comparison of modelling results against measurement data collected in the HECLOM region in 2007. The report was welcomed and endorsed by the Contracting Parties at the HELCOM MONAS 12 meeting in October 2009 and was recommended to be published on the EMEP and HELCOM websites.

Along with the contribution to the joint annual report, MSC-E prepared environmental indicator fact sheets with the updated information on variations of atmospheric emissions of heavy metals and levels of their deposition to the Baltic Sea for the period from 1990 to 2007. These indicator fact sheets are available in the Internet at the web site of the Helsinki Commission [www.helcom.fi].

According to the officially reported data, emissions in HELCOM countries declined by 48%, 51%, and 85% for cadmium, mercury, and lead, respectively, in the period from 1990 to 2007 (Fig. 5.7). The reduction of heavy metal emissions in this area is mostly caused by the extensive use of unleaded gasoline and application of cleaner production technologies in countries. Besides, it is partly connected with the economic re-structuring taken place in Poland, Estonia, Latvia, Lithuania, and Russia since early 1990s. The highest decrease of cadmium emissions can be seen in Lithuania (89%) and Estonia (85%). In case of lead emission, the most significant decrease took place in Denmark and Sweden where the emissions in 2007 were more than 20 times lower than in 1990. Essential reduction of annual lead emission of HELCOM countries from 2003 to 2004 was mostly caused by the change of emission in Russia. Mercury emission most significantly decreased in Latvia (92%) and Germany (80%).

Following the reduction of atmospheric emissions, deposition of heavy metals decreased for the period 1990 – 2007 as shown in Fig. 5.8. Deposition of lead is characterized by the most essential decline (69%). The decrease of cadmium deposition made up 46%, and mercury – 23%. The most essential decrease in HM deposition over individual sub-basins of the Baltic Sea is noted for lead deposition to the Gulf of Bothnia (74%). In case of cadmium deposition the most substantial decrease takes place in the Gulf of Finland (63%). Largest decrease in mercury deposition is obtained for the Belt Sea and the Kattegat (41%).

The highest level of HM deposition fluxes over the Baltic Sea in 2007 is noted for its southern and western parts, in particular, the Belt Sea, the Kattegat, and the Baltic Proper. Among the HELCOM countries the most significant contributions to deposition over the Baltic Sea belong to Poland, Germany, and Russia.

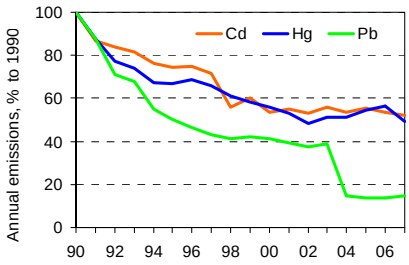

Fig. 5.7. *Trend of anthropogenic emissions of cadmium, mercury, and lead from HELCOM countries in 1990-2007 according to official emissions data*

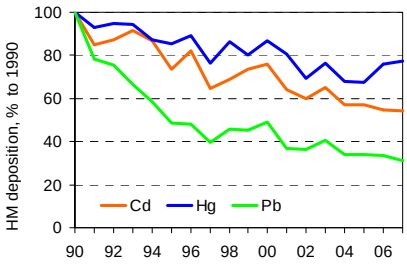

Fig. 5.8. *Temporal variations of cadmium, mercury, and lead deposition to the Baltic Sea in 1990-2007*

5.5. Cooperation with national experts

In 2010 MSC-E continued close cooperation with national experts.

In order to support national scale modelling MSC-E co-operated with experts from ENEA - Ricerca sul Sistema Elettrico S.p.A. (ERSE S.p.A.), Italy. In particular, the Centre supported the national experts with input information required for the national scale simulations of mercury pollution levels over Italy (including 3D concentrations of mercury species for setting up initial and boundary conditions, natural emissions data) and participated in the analysis of the modelling results. The experts from ENEA developed and applied a national scale model for simulations of mercury concentrations and deposition over the territory of Italy. The modelling results were analysed and compared with the regional scale simulations produced with the MSCE-HM model. Detailed information on this activity is presented in Annex B.

Special attention this year was paid to strengthening cooperation with EECCA countries. In particular, Memorandum of Understanding between MSC-E and Institute for National Resources Use and Ecology of the National Academy of Science of Belarus was signed. The main aim of the Memorandum is a complex of joint works within scientific research activities in the framework of transboundary air pollution by heavy metals, creation of scientific basis of the compliance with international agreements concerning the protection of atmospheric air.

Kazakhstan has provided MSC-E with measurement data collected at national monitoring network [www.eco.gov.kz]. Since the information on measured concentrations and deposition of heavy metals in the Central Asia region is not available in the CCC database, national data have been used for the validation of modelling results for this country. The comparison results for Kazakhstan stations are depicted in Fig. 5.9 and 5.10.

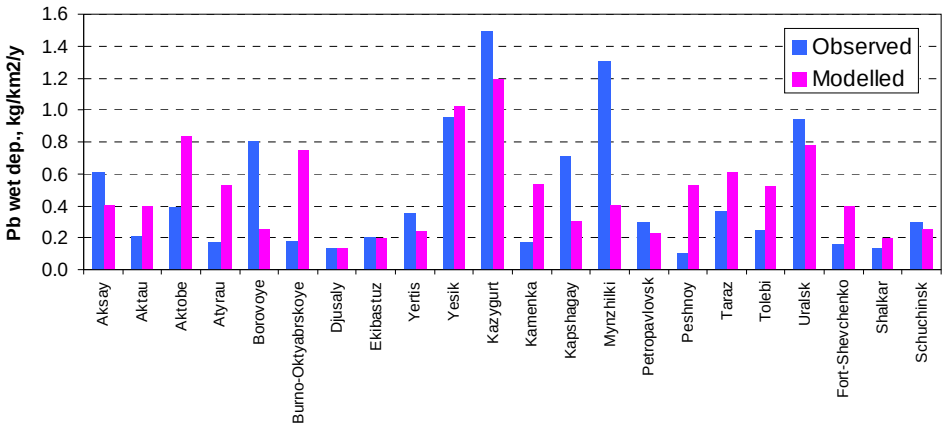

Fig. 5.9. *Modelled and measured annual wet deposition flux of lead at individual stations in Kazakhstan in 2008, kg/km^2/y*

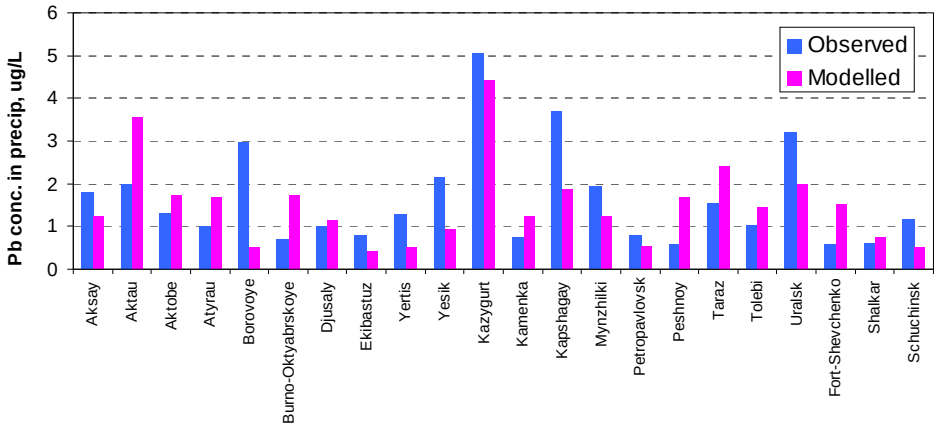

Fig. 5.10. *Modelled and measured annual mean concentrations of lead in precipitation at individual stations in Kazakhstan in 2008, μg/L*

As seen from the figures (5.9, 5.10), the difference between modelled and measured concentrations and wet deposition fluxes stays within a factor of 3 for most of stations. For 10 stations this difference is within ±50%. Keeping in mind essential uncertainties of the emission data used for Kazakhstan (see Chapter 4), the assessment of pollution levels over this country may be considered satisfactory. Besides, no information is available about uncertainties of these measurements. Development of national emission inventories of heavy metals and monitoring network will favour further improvement of the assessment of the pollution levels for this country.

6. FUTURE ACTIVITIES

In order to further improve the quality of the pollution level assessment of lead, cadmium and mercury over the EMEP region, the following activities of MSC-E and CCC are proposed for 2010:

Annual activities:

Review, store and make available monitoring data for the modelling centres and Parties.

Publish and report the validated 2009 data; contribute to preparation, review and assessments of observations data presented in the series of EMEP reports.

Arrange laboratory intercomparisons for heavy metals.

Address global scale integration of quality assessment/quality control (QA/QC) activities of regional monitoring programmes.

Maintain close interaction with relevant organizations and bodies in relation to integration of observations.

Preparation of meteorological data for operational modelling based on the European Centre for Medium-Range Weather Forecasts (ECMWF) analysis and continue work on update/development of the meteorological drivers.

Prepare anthropogenic heavy metal emission data as input for operational modelling on the basis of gridded emission dataset provided by CEIP.

Calculate heavy metal (lead, cadmium and mercury) air concentrations and ecosystem-dependent deposition fluxes over the extended EMEP domain for 2009.

Compute country-to-country deposition matrices for heavy metals for 2009.

Estimate heavy metal deposition to regional seas (the Baltic, Black, Caspian, Mediterranean and North Seas).

Analyse the agreement between measured and modelled pollution levels using standardized matrix and criteria for the evaluation of model performance.

Calculate mercury dispersion on a hemispheric/global scale for evaluation of contributions of intercontinental transport to regional pollution levels.

Prepare individual country status reports in English and Russian for the EECCA countries and make results of model calculations available on the web for use by Parties.

Contribution to the work of the subsidiary bodies to the Convention and EMEP Task Forces:

- WGE: Continue collaboration with ICP Vegetation on evaluation of heavy metal pollution levels in Europe using modelling results and measurements in mosses;

- TFMM, TFHTAP: Continue cooperation in the field of heavy metal modelling on both regional and global scales (contribute to the work on intercontinental transport of mercury on the global scale).

Cooperate with international bodies: AMAP, UNEP, EU, HELCOM, OSPAR and national experts.

Disseminate results (e.g. via status reports, technical notes, the website, publication in peer-reviewed journals).

Research and development activities:

Contribute to the development of standard methods and QA/QC procedures in relation to the new parameters included in the monitoring requirements of the 2010–2019 strategy; update the EMEP manual for sampling and chemical analysis in accordance to these outputs.

Continue work on the EMEP Case Study aimed at the improvement of the quality of heavy metal pollution assessment, including:

- Adaptation of MSC-E- heavy metal model for simulations at national and local scales including the model code modification and preparation of meteorological data with finer resolution;

- Model assessment of pollution levels with finer resolution based on detailed country-specific data;

Develop global scale modelling involving:

- Further develop and test the global modelling framework GLEMOS in application to simulation of heavy metals including improvement of the modular architecture, elaboration of the multi-media approach and refinement of the pollutant specific processes.

- Continue cooperation with MSC-W in the field of development of the EMEP global modelling framework

Continue work on refinement of the Hg chemical scheme for both regional and global modelling including evaluation of the role of different oxidation mechanisms in the atmosphere.

Continue analysis of the effect of altering meteorological parameters associated with the climate change on heavy metal pollution levels in Europe.

Participate in elaboration of the criteria and metrics for evaluation of modelling results in cooperation with TFMM.

CONCLUSIONS

The main activities of the EMEP Centres (CCC and MSC-E) in the field of heavy metal pollution assessment in 2010 included a variety of tasks related to the development and application of monitoring and modelling methods for the evaluation of heavy metal pollution levels on different scales: global, regional and national/local scale pollution in individual EMEP countries. The Centres closely cooperated with the subsidiary bodies to the Convention, EMEP Task Forces, international organizations and programmes as well as with national experts. The main conclusions of the activities of MSC-E and CCC are formulated below.

Global modelling framework

1. To facilitate the development of the common EMEP global modelling framework MSC-E elaborated a pilot version of the modular architecture based on the newly developed GLEMOS modelling system. The framework was adapted and applied for simulation of two groups of contaminants with diverse properties and characters of the environmental cycling – heavy metals and persistent organic pollutants.

2. New developments of GLEMOS for heavy metals include updates of the mercury chemical scheme. In particular, chemical reactions of elemental mercury with reactive halogens (Br, BrO) were included into the chemical scheme in order to take into account fast mercury oxidation during the Atmospheric Mercury Depletion Events (AMDEs) in the Polar Regions. Besides, another important process accompanying the increased mercury deposition during AMDEs - the prompt re-emission of newly deposited mercury – was also implemented into the model. Pilot modelling results demonstrated considerable improvement of the model performance with regard to observational data.

3. The global scale levels of mercury concentration and deposition simulated by GLEMOS were analyzed and evaluated against measurements. It was obtained that the model successfully reproduced measured Hg^0 air concentration. The model trends to somewhat overestimate measured wet deposition but in 80% of cases the deviation between model and observations did not exceed a factor of 2. The source attribution estimates showed that contribution of intercontinental transport from external anthropogenic and natural sources to mercury deposition in Europe varied from 40% in Central Europe to about 80% in Scandinavia and in the eastern part of the European territory of Russia.

EMEP contribution to TF HTAP

1. Within the framework of cooperation with the TF HTAP MSC-E coordinated the HTAP activities in the inter-comparison of global scale chemical transport models for mercury, and led publication of the multi-model experiment results in the HTAP 2010 Assessment Report.

2. The results of the multi-model experiment showed that ambient concentrations of elemental gaseous mercury, species responsible for long-range atmospheric transport, were reliably simulated by contemporary models (within a factor of 1.2). Uncertainty of simulated mercury deposition was higher and largely associated with dry uptake of various Hg forms by the surface

because of the absence of systematic observations of dry deposition. The contribution of mercury intercontinental transport was significant, particularly in regions with few local emission sources. The contribution of foreign anthropogenic sources to annual deposition fluxes varied from 10% to 30%, on average anywhere on the globe. Besides, global natural and secondary emissions contributed from 35 to 70% of total deposition in most regions.

EMEP Case Study on heavy metal pollution assessment

1. The work on the EMEP Case Study on heavy metal pollution assessment was started. Six countries-volunteers (the Czech Republic, Croatia, Italy, the Netherlands, Slovakia, Spain) expressed their wish to take part in this project. Some countries (the Czech Republic, Croatia, the Netherlands) began to provide MSC-E with necessary country-specific data (emissions, monitoring etc.).

2. Special country-oriented Case Study programme, time table, input data and list of deliverables were agreed with the Czech Republic. National measurement data were submitted to MSC-E from the Czech Republic. Input data (meteorology, land cover, soil concentrations) with fine resolution (10×10 km^2) were prepared by MSC-E for the Czech Republic, Croatia and the Netherlands. Pilot modelling of deposition and concentrations was performed for the Czech Republic this year.

Assessment of heavy metal pollution levels

1. The measurement obligations set by the EMEP monitoring strategy for 2009 - 2019 led to improvements of spatial coverage of the EMEP region. Number of sites submitting measurement information in 2008 increased compared to previous year. However, there is still a lack of measurements in the south-eastern and eastern parts of Europe and in Central Asia.

2. Results of most of national laboratories participated in the intercalibration tests met the requirements of the current data quality objective. However, there were some countries which submitted measurement information without participation in these tests. Data from these countries were of unknown quality. Therefore they were strongly recommended to take part in the annual laboratory intercomparison.

3. Sensitivity of heavy metal pollution levels in countries to meteorological parameters (precipitation, temperature, wind velocity, friction velocity) associated with climate change was analysed for the Czech Republic, Italy, the United Kingdom and Finland using the approach based on multiple regression analysis. Precipitation amounts and wind velocity were among the most important meteorological parameters controlling deposition levels in countries. It is planned to continue the development of this approach.

4. Spatial distribution of concentrations and deposition was characterized by modelling results and monitoring data. The highest regional-scale heavy metal pollution levels were obtained for Poland, north of Italy, the Benelux, the Balkan region, and the European part of Russia. In the Central Asian region elevated concentrations occurred in the southern parts of Kazakhstan. Heavy metal deposition in Central Asia was not as high as deposition in Europe because of relatively low precipitation amount.

5. Deposition of lead and cadmium in Europe and Central Asia as a whole in 2008 was about 14% and 10% lower than that in 2007, respectively. Mercury deposition to the EMEP region

remained almost the same. Decrease of lead and cadmium deposition in the southern, central and western parts of Europe was caused by the decline of emission values and re-suspension. Increase of precipitation amounts caused the rise of deposition of lead and cadmium in the western part of the United Kingdom and the central part of Kazakhstan and of mercury in the north-western Italy, Russia and most of Scandinavia. Deposition of mercury in Denmark, Cyprus, France, Norway and Germany decreased, whereas in Slovakia and Romania increased because of the corresponding changes of the emissions.

6. Transboundary atmospheric transport is one of the most important factors conditioning heavy metal pollution levels in the EMEP region. Its contribution to deposition from anthropogenic sources in Europe and Central Asia exceeded 50% in 38, 35 and 27 countries for lead, cadmium and mercury, respectively. The fraction of national emissions of the European and the Central Asian countries transported outside their territories ranged from 60% to 90% for lead and cadmium. In case of mercury, this fraction commonly varied from 70% to almost 100%.

7. Quality of the air pollution assessment was characterized by means of integrated approach taking into account uncertainties of the model, emission data and measurements. The uncertainty of country totals of heavy metal emission typically ranged between 30 – 60%. Overall uncertainty of measured wet deposition estimated using results of field campaigns was around 20% for lead and cadmium, and 40% of mercury. However, these estimates did not include the effect of representativeness of stations location.

8. Modelling results agreed with measurement data with satisfactory accuracy, keeping in mind uncertainties of the emission and monitoring data. At most of stations calculated and observed levels of lead and cadmium agreed within ±50%. The discrepancy between the simulated and observed mercury concentrations did not exceed ±15% for air concentrations. For concentrations in precipitation and wet deposition fluxes the bias was within ±30% for most of stations.

Cooperation

1. MSC-E contributed to the project in support of the revision of the Heavy Metal Protocol initiated by the Dutch Ministry of Hosing, Spatial Planning and the Environment (VROM). Calculations of lead, cadmium and mercury deposition for 2010 and three scenarios for 2020 were carried out. The reduction of deposition between 2010 and scenarios for 2020 was 15 – 24% for lead and 15 – 27% for cadmium. For mercury the changes varied between 4% growth and 5% reduction. Relatively low changes of mercury deposition were explained by the significant influence of intercontinental transport. The changes for individual countries were highly variable because of the influence of transboundary transport.

2. Applicability and peculiarities of use of auxiliary measurements for the assessment of pollution levels and the model validation were investigated in cooperation with the ICP-Vegetation of WGE. Both wet and dry deposition should be considered when concentrations in mosses and deposition are compared. The agreement between the two types of data increased in regions with high density of measurements of concentrations in mosses.

3. MSC-E took part in preparation of the AMAP Assessment 2010 for mercury. In particular, the Centre participated in drafting and discussion of parts of the Assessment relating to the multi-model assessment of mercury atmospheric transport to the Arctic. Besides, MSC-E performed

collection and processing of the modelling results for the multi-model assessment of the Arctic pollution with mercury.

4. Contribution to the EMEP Centres joint report on the evaluation of airborne pollution loads to the Baltic Sea for Helsinki Commission was prepared by MSC-E. Information on lead, cadmium and mercury deposition was provided for 2007. Evaluation of long-term trends of deposition to the Baltic Sea indicated that atmospheric load to the sea declined by 69% (Pb), 46% (Cd) and 23% (Hg) for the period from 1990 to 2007.

5. MSC-E was actively involved in cooperation with national experts. MSC-E supported national-scale modelling of mercury over Italy. Evaluation of the modelling results for Kazakhstan was carried out in cooperation with national experts. Memorandum of Understanding between MSC-E and Belarus focused on the investigation of heavy metal transboundary transport was signed.

6. To support EECCA countries the country-oriented reports were prepared in Russian language.

REFERENCES

Aas W, Breivik K. [2010]. Heavy metals and POP measurements 2008, Norwegian Institute for Air Research. EMEP/CCC-Report 3/2010.

Aas W. [2006]. Data quality 2004, quality assurance and field comparisons. EMEP/CCC Report 4/2006.

Aas W., Alleman L.Y., Bieber E., Gladtke D., Houdret J.L., Karlsson V., Monies C. [2009]. Comparison of methods for measuring atmospheric deposition of arsenic, cadmium, nickel and lead. J. Environ. Monit., vol. 11, pp. 1276 - 1283 doi: 10.1039/B822330K.

AMAP [2011] (in prep). AMAP Assessment 2010: Mercury in the Arctic. Arctic Monitoring and Assessment Programme (AMAP).

AMAP/UNEP [2008] Technical Background Report to the Global Atmospheric Mercury Assessment. Arctic Monitoring and Assessment Programme / UNEP Chemicals Branch (http://www.chem.unep.ch/mercury/Atmospheric_Emissions/Technical_background_report.pdf).

Ariya P., Dastoor A., Amyot M., Schroeder W., Barrie L., Anlauf K., Raofie F., Ryzhkov A., Davignon D., Lalonde J., and Steffen A. [2004] The Arctic: A sink for mercury, *Tellus B*, vol. 56, No. 5, pp. 397–403.

Baker P.G.L., Brunke E.-G., Slemr F., Crouch A.M. [2002] Atmospheric mercury measurements at Cape Point, South Africa, *Atmospheric Environment,* vol. 36 (14), pp. 2459-2465.

Bartnicki J., A. Gusev, W. Aas, S. Valiyaveetil [2009] Atmospheric Supply of Nitrogen, Lead, Cadmium, Mercury and Dioxins/Furans to the Baltic Sea in 2007. MSC-W Technical Report 2/2009.

CITEPA [2010] Inventaire des emissions de polluants atmospheriques en France au titre de la convention sur la pollution atmospherique transfrontaliere a longue distance et de la directive Europeenne relative aux plafonds d'emissions nationaux (NEC). CEE–NU/NFR & NEC Mars 2010. p.221.

Constant P., L. Poissant, R. Villemur, E. Yumvihoze, Lean D. [2007] Fate of inorganic mercury and methyl mercury within the snow cover in the low arctic tundra on the shore of Hudson Bay (Que´bec, Canada), *Journal of Geophysical Research*, vol. 112, pp. D08309.

Dastoor A.P., D.Davignon, N. Theys, M.V., M.V.Roozendael, A.Steffen, and P.A.Ariya [2008] Modelling Dynamic Exchange of Gaseous Elemental Mercury at Polar Sunrise, *Environmental Science and Technology*, vol. 42,No. 14, pp.5183-5188.

Denier van der Gon D. H.A.C., van het Bolscher M., Visschedijk A.J.H. and Zandveld P.Y.J. [2005]. Study to the effectiveness of the UNECE Heavy Metals Protocol and costs of possible additional measures. Phase I: Estimation of emission reduction resulting from the implementation of the HM Protocol. TNO-report B&O-A R 2005/193.

Dommergue A., Ferrari C.P., Poissant L., Gauchard P.A., Boutron C.F. [2003] Diurnal cycles of gaseous mercury within the snowpack at Kuujjuarapik/ Whapmagoostui, Quebec, Canada. *Environmental Science and Technology*, vol. 37, pp. 3289-3297.

Ebinghaus R., Kock H. H., Temme C., Einax J. W., Lowe A. G., Richter A., Burrows J. P., and Schroeder W. H. [2002] Antarctic springtime depletion of atmospheric mercury, *Environ. Sci. Technol*., vol. 36, pp.1238–1244.

EU [2004] Directive 2004/107/EC of the European Parliament and of the council of 15 Dec. 2004 relating to arsenic, cadmium, mercury, nickel and polycyclic aromatic hydrocarbons in ambient air. Off. *J. Eur. Comm*., L23, 26/01/2005, pp. 3-16.

EU [2008] Directive 2008/50/EC of the European Parliament and of the Council of 21 May 2008 on ambient air quality and cleaner air for Europe. *Off. J.Eur. Com.*, L 141, 11/06/2008, 1-44.

Ferrari C.P., Padova C., Faïn X, Gauchard P.-A., Dommergue A., Aspmo K., Berg T., Cairns W., Barbante C., Cescon P., Kaleschke L., Richter A., Wittrock F., Boutron C. [2008] Atmospheric mercury depletion event study in Ny-Alesund (Svalbard) in spring 2005. Deposition and transformation of Hg in surface snow during springtime. *Science of the Total Environment*, vol. 397,1pp. 67-177.

Fu X. W., Feng X., Dong Z. Q., Yin R. S., Wang J. X., Yang Z. R. and Zhang H. [2010] Atmospheric gaseous elemental mercury (GEM) concentrations and mercury depositions at a high-altitude mountain peak in south China. *Atmos. Chem. Phys*., vol. 10, pp.2425–2437.

Goodsite M. E., Plane J. M. C. and Skov H. [2004] A Theoretical Study of the Oxidation of Hg^0 to $HgBr_2$ in the Troposphere, *Environ. Sci. Technol*., vol. 38, pp. 1772–1776.

Gusev A., Mantseva E., Shatalov V., and B.Strukov [2005] Regional multicompartment model MSCE-POP. MSC-E Technical Report 5/2005.

Harmens H. and Norris D. and participants of the moss survey [2008]. Spatial and temporal trends in heavy metal accumulation in mosses in Europe (1990 - 2005). Report of ICP Vegetation, 51 pp.

Hettelingh J-P., Sliggers J. (eds). [2006]. Heavy metal emissions, depositions, critical loads and exceedances inEurope. Joint report of TNO, MSC-E, ALTERRA, WGE, VROM and Netherlands Environmental Assessment Agency, 93pp.

Hurrell, Y. Kushnir, G. Ottersen, and M. Visbeck, Eds. [2003]. The North Atlantic Oscillation: Climate Significance and Environmental Impact. J.W. Geophysical Monograph Series, 134, 279pp.

Ilyin I., Gusev A., Travnikov O., Shatalov V., Sokovykh V. [2010] Technical report: Modelling of heavy metals and persistent organic pollutants: New developments. EMEP/MSC-E Technical report 1/2010.

Ilyin I., Rozovskaya O., Sokovykh V., Travnikov O. and Aas W. [2009]. Heavy Metals: Transboundary Pollution of the Environment. EMEP Status Report 2/2009. 55 pp.

Jaffe D., E. Prestbo, P. Swartzendruber, P. Weiss-Penzias, S. Kato, A. Takami, S. Hatakeyama, and K. Yoshizumi [2005] Export of atmospheric mercury from Asia, *Atmospheric Environment,* vol. 38, pp. 3029-3038.

Jonson J. E. and O. Travnikov (Eds.). [2010] Development of the EMEP global modeling framework: Progress report. Joint MSC-W/MSC-E Report X/2010. (under preparation).

Johnson K.P., Blum J.D., Keeler G.J., Douglas T. [2008] Investigation of the deposition and emission of mercury in arctic snow during an atmospheric mercury depletion event. *Journal of Geophysical Research Atmospheres*, vol. 113(D17304).

Kim K.-H., M.-Y. Kim J. Kim and G. Lee [2002] The concentrations and fluxes of total gaseous mercury in a western coastal area of Korea during late March 2001, *Atmospheric Environment,* vol. 36; pp. 3413-3427.

Kirk J.L., St. Louis, V.L.; Sharp M.J. [2006] Rapid reduction and reemission of mercury deposited to snowpacks during atmospheric mercury depletion events at Churchill, Manitoba, Canada. *Environmental Science and Technology*, vol. 40, pp. 7590–7596.

Lalonde J.D., Poulain A.J., Amyot M. [2002] The role of mercury redox reactions in snow on snow–to–air mercury transfer. *Environmental Science and Technology*, vol. 36, pp. 174–178.

Laurier F.J.G., Mason R.P., Whalin L. and Kato S. [2003] Reactive gaseous mercury formation in the North Pacific Ocean's marine boundary layer: A potential role of halogen chemistry. *J. Geophys. Res*. Vol. 108, No. (D17), p. 4529.

Lindberg S. E.; Brooks S.; Lin C.-J.; Scott K. J.; Landis M.S., Stevens R. K., Goodsite M., Richter A. [2002] Dynamic oxidation of gaseous mercury in the Arctic troposphere at Polar sunrise. *Environmental Science and Technology*, vol. 36, pp. 1245–1256.

Murphy D.M., Hudson P.K., Thomson D.S., Sheridan P.J. and Wilson J.C. [2006] Observations of mercury-containing aerosols, *Environ. Sci. Technol*., vol. 40, pp. 3163–3167.

Murrells T.P., Passant N.R., Thistlethwaite G., Wagner A., Li Y., Bush T., Norris J., Whiting R., Walker C., Stewart R.A., Tsagatakis I., Conolly C., Brophy N.C.J. and S. Okamura [2010] UK Informative Inventory Report (1970 to 2008). UK Emissions Inventory Team, AEA Group, p.50.

Nielsen O.-K., Winther M., Mikkelsen M.H., Hoffmann L., Nielsen M., Gyldenkaerne S., Fauser P., Plejdrup M.S., Albrektsen R. and K.Hjelgaard [2010] Annual Danish Informative Inventory Report to UNECE. Emission inventories from the base year of the protocols to year 2008. NERI Technical Report no.774, p.34.

Peterson and Baringer [2009]. State of the climate in 2008. Special Supplement to the Bulletin of the American Meteorological Society. Vol. 90, No. 8

Pacyna J.M., Scholtz M.T, and Li Y.-F (Arthur). [1995]. Global budget of trace metal sources. *Environ. Rev.*, vol.3(2), pp.145–159.

Poulain A.J., Lalonde J.D., Amyot M., Shead J.A., Raofie F., Ariya P.A. [2004] Redox transformations of mercury in an Arctic snowpack at springtime, *Atmospheric Environment*, vol. 38, pp. 6763–6774.

Raofie F. and Ariya P. A. [2003] Kinetics and products study of the reaction of BrO radicals with gaseous mercury, Journal de Physique IV, vol. 107, pp. 1119–1121.

Seigneur C., and K. Lohman [2008] Effect of bromine chemistry on the atmospheric mercury cycle, Journal of Geophysical Research - Atmospheres, 113(D23).

SEPA [2010] Informative Inventory Report 2010. Sweden. Annexes. Swedish Environmental Protection Agency, p.74.

Skov H., Christensen J.H., Heidam N.Z., Jensen B., Wahlin P., and Geernaert G. [2004] Fate of elemental mercury in the Artcic during atmospheric depletion episodes and the load of atmospheric mercury to the Arctic, *Environ. Sci. Technol*., vol. 38, pp. 2373–2382.

Sprovieri F., I. M. Hedgecock, and N. Pirrone [2010] An investigation of the origins of reactive gaseous mercury in the Mediterranean marine boundary layer. *Atmos. Chem. Phys*., vol. 10, pp. 3985–3997.

Sprovieri F., Pirrone N., Hedgecock I. M., Landis M. S. and Stevens R. K. [2002] Intensive atmospheric mercury measurements at Terra Nova Bay in Antarctica during November and December 2000, *J. Geophys. Res*., vol. 107, pp. 4722.

St. Louis V.L., Sharp M.J., Steffen A.; May A.; Barker J., Kirk J.L., Kelly D.J.A., Arnott S.E., Keatley B., Smol J.P. [2005] Some sources and sinks of monomethyl and inorganic mercury on Ellesmere Island in the Canadian High Arctic. *Environmental Science and Technology*, vol. 39, pp. 2686–2701.

Steffen A., Douglas T., Amyot M., Ariya P., Aspmo K., Berg T., Bottenheim J., Brooks S., Cobbett F., Dastoor A., Dommergue A., Ebinghaus R., Ferrari C., Gardfeldt K., Goodsite M.E., Lean D., Poulain A.J., Scherz C., Skov H., Sommar J., and Temme C. [2008] A synthesis of atmospheric mercury depletion event chemistry in the atmosphere and snow, *Atmos. Chem. Phys.*, vol. 8, pp. 1445-1482.

SYKE [2010] Air Pollutant Emissions in Finland 1980-2008. Informative Inventory Report. Finnish Environment Institute. Consumption and Production Centre, Environmental Performance Division Air Emissions Team, p.55.

Talbot R., Mao H., Scheuer E., Dibb J., and Avery M. [2007] Total depletion of Hg_ in the upper troposphere-lower stratosphere, *Geophys. Res. Lett.,* vol. 34, p. L23804.

Tarrasón L. and A. Gusev Ed. [2008] Towards the development of a common EMEP global modelling framework EMEP/MSC-W Technical Report 1/2008

Temme C., Einax J.W., Ebinghaus R., Schroeder W.H. [2003] Measurements of Atmospheric Mercury Species at a Coastal Site in the Antarctic and over the South Atlantic Ocean during Polar Summer. Environmental Science & Technology, vol. 37, pp. 22-31.

Theys N., De Smedt I., Van Roozendael M., Fayt C., Chabrillat S., Chipperfield M., Post P., Van Der A.R. [2004] Total and tropospheric BrO derived from GOME and SCIAMACHY as part of the TEMIS project. Proceedings of the Envisat & ERS Symposium.

Travnikov O. and I.Ilyin [2005] Regional Model MSCE-HM of Heavy Metal Transboundary Air Pollution in Europe. EMEP/MSC-E Technical Report 6/2005, 59 pp.

Travnikov O., J.E. Jonson, A.S Andersen, M. Gauss, A. Gusev, O. Rozovskaya, D. Simpson, V. Sokovykh, S. Valiyaveetil and P. Wind [2009] Development of the EMEP global modelling framework: Progress report. Joint MSC-E/MSC-W Report. EMEP/MSC-E Technical Report 7/2009.

Travnikov, O. and I. Ilyin [2009], The EMEP/MSC-E Mercury modeling system, Chapter 20 in Mercury fate and transport in the global atmosphere: Emissions, measurements and models, N. Pirrone and R. Mason (eds), Springer, DOI:10.1007/978-0-387-93958-2_20, 637 pp.

UNECE [2009] Draft revised monitoring strategy. ECE/EB.AIR/GE.1/2009/15.

Valente R.J., Shea C., Lynn Humes K., Tanner R.L. [2007] Atmospheric mercury in the Great Smoky Mountains compared to regional and global levels, *Atmospheric Environment*, vol. 41 (9), pp. 1861-1873.

ANNEX A

COUNTRY-TO-COUNTRY DEPOSITION MATRICES FOR 2008

Table A.1. *Codes of countries, regions and seas*

Country/Region/Sea	Code	Country/Region/Sea	Code
Albania	AL	Monaco	MC
Armenia	AM	Montenegro	ME
Austria	AT	Netherlands	NL
Azerbaijan	AZ	Norway	NO
Belarus	BY	Poland	PL
Belgium	BE	Portugal	PT
Bosnia and Herzegovina	BA	Republic of Moldova	MD
Bulgaria	BG	Romania	RO
Croatia	HR	Russian Federation (European part)	RU
Cyprus	CY	Russian Federation (Asian part)	RUA
Czech Republic	CZ	Serbia	RS
Denmark	DK	Slovakia	SK
Estonia	EE	Slovenia	SI
Finland	FI	Spain	ES
France	FR	Sweden	SE
Georgia	GE	Switzerland	CH
Germany	DE	The Former Yugoslav Republic of Macedonia	MK
Greece	GR	Tajikistan	TJ
Hungary	HU	Turkey	TR
Iceland	IS	Turkmenistan	TM
Ireland	IE	Ukraine	UA
Italy	IT	United Kingdom	GB
Kazakhstan	KZ	Uzbekistan	UZ
Kyrgyzstan	KY	Baltic Sea	BAS
Latvia	LV	Black Sea	BLS
Lithuania	LT	Caspian Sea	CAS
Luxembourg	LU	North Sea	NOS
Malta	MT	Mediterranean Sea	MDT

***Table A.2**. Matrix of lead country-to-country deposition from anthropogenic sources in 2008, kg/y*

Receptors ↓ Emitters →

	AL	AM	AT	AZ	BA	BE	BG	BY	CH	CY	CZ	DE	DK	
AL	**2494**	0.9	14.4	0.9	224.8	17.5	2324	21.2	25.6	1.1	33.2	42.1	1.1	**AL**
AM	2.9	**1684**	0.9	482.5	6.5	1.3	62.8	8.2	1.6	5.7	2.4	3.7	0.2	**AM**
AT	45.3	0.9	**4642**	0.9	715.8	476.0	901.1	143.1	1034	0.2	1018	3018	20.2	**AT**
AZ	6.1	458.7	2.1	**3026**	14.5	3.9	138.3	27.6	3.6	10.6	5.9	10.2	0.8	**AZ**
BA	273.7	1.4	156.9	1.4	**13757**	71.6	1112	49.3	81.2	0.4	346.0	285.7	8.0	**BA**
BE	0.9	0.0	19.8	0.1	5.3	**10448**	11.1	20.8	114.0	0.0	42.1	1021	5.8	**BE**
BG	291.8	12.1	47.3	13.4	471.4	57.9	**105248**	181.2	40.9	4.6	185.5	165.6	6.8	**BG**
BY	68.9	15.9	173.0	20.4	517.3	382.4	3394	**21871**	148.8	2.7	950.9	1102	132.1	**BY**
CH	6.4	0.1	78.7	0.1	60.6	239.0	57.0	11.5	**6474**	0.0	41.7	714.1	2.8	**CH**
CY	2.9	1.4	0.4	0.9	4.2	0.4	40.2	1.1	0.6	**113.8**	0.8	1.1	0.0	**CY**
CZ	32.3	0.9	1003	0.8	354.0	504.5	1109	199.5	446.2	0.1	**6653**	3214	48.4	**CZ**
DE	24.8	0.6	1307	0.8	211.0	10952	334.8	326.6	4850	0.1	2316	**47974**	314.3	**DE**
DK	1.8	0.1	20.2	0.2	14.7	682.2	35.1	36.4	38.0	0.0	92.7	844.9	**779.1**	**DK**
EE	4.5	0.4	25.0	0.7	38.7	197.8	202.5	317.6	39.4	0.1	124.1	441.2	63.4	**EE**
ES	36.1	1.3	46.3	1.5	193.7	397.4	319.7	25.0	248.9	0.1	62.6	347.5	10.4	**ES**
FI	14.5	2.7	62.4	5.7	85.1	514.4	646.4	613.1	84.5	0.5	268.9	962.7	169.2	**FI**
FR	48.8	1.2	203.6	1.4	356.1	4809	389.4	96.3	3104	0.1	288.1	3723	35.3	**FR**
GB	3.3	0.3	49.7	0.4	20.1	2255	33.2	39.4	154.6	0.0	127.3	1672	93.2	**GB**
GE	9.4	629.6	3.4	733.5	22.9	5.8	277.0	45.3	5.0	12.4	9.5	15.2	1.2	**GE**
GR	482.7	12.9	32.9	11.2	338.2	43.1	13860	98.3	47.6	19.3	100.3	112.9	4.2	**GR**
HR	161.0	1.0	239.4	1.0	3078	69.8	918.9	50.8	100.4	0.3	295.8	276.1	5.9	**HR**
HU	136.7	1.5	439.0	1.7	2031	149.9	4260	128.7	148.4	0.8	743.8	572.2	12.2	**HU**
IE	0.3	0.0	6.3	0.1	2.6	203.5	5.1	3.2	24.3	0.0	13.3	166.7	10.1	**IE**
IS	0.4	0.1	3.1	0.1	2.6	68.0	6.2	6.4	11.3	0.0	7.9	85.7	12.0	**IS**
IT	426.7	3.0	615.5	3.4	2307	317.9	2494	117.5	1517	0.7	440.4	1116	14.3	**IT**
KY	4.9	59.2	2.4	86.5	13.7	4.2	106.3	16.6	4.5	5.0	5.6	11.1	0.7	**KY**
KZ	69.0	561.8	58.2	1044	278.2	113.6	2448	845.2	77.6	26.6	167.0	285.4	30.1	**KZ**
LT	13.7	1.2	85.3	1.8	140.4	278.4	512.0	1460	91.8	0.2	445.5	800.0	115.1	**LT**
LU	0.1	0.0	3.3	0.0	0.9	221.8	2.3	2.9	18.7	0.0	6.5	137.3	0.4	**LU**
LV	9.8	0.7	57.2	1.0	96.2	285.5	401.8	856.9	78.8	0.1	291.7	739.3	112.6	**LV**
MC	0.0	0.0	0.0	0.0	0.1	0.0	0.1	0.0	0.1	0.0	0.0	0.1	0.0	**MC**
MD	21.3	4.9	10.3	6.5	67.7	17.4	1313	120.1	10.0	0.7	44.3	52.1	3.3	**MD**
ME	431.4	0.4	12.7	0.4	588.7	11.8	637.5	10.1	15.6	0.4	29.9	33.0	0.9	**ME**
MK	503.6	1.3	11.1	1.2	140.8	12.7	5950	21.1	12.8	2.6	35.2	35.8	1.2	**MK**
MT	0.2	0.0	0.0	0.0	0.5	0.0	1.7	0.0	0.1	0.0	0.1	0.1	0.0	**MT**
NL	1.2	0.1	25.7	0.1	7.0	5175	10.3	24.2	79.2	0.0	75.1	1698	14.2	**NL**
NO	3.8	1.3	49.1	1.7	27.1	581.6	75.9	192.8	86.7	0.2	190.3	992.1	315.6	**NO**
PL	118.3	4.2	882.6	6.1	1113	1798	3587	2677	692.6	0.6	9574	7687	438.8	**PL**
PT	1.1	0.0	1.9	0.1	5.8	20.1	12.9	1.1	10.7	0.0	2.8	20.1	1.8	**PT**
RO	317.5	14.6	241.4	17.8	1881	224.3	20527	562.7	172.8	6.6	768.7	709.0	30.5	**RO**
RS	484.8	2.5	120.6	2.9	2666	77.1	10304	82.2	69.1	2.5	379.6	297.1	9.8	**RS**
RU	400.5	1114	635.4	2509	2044	1745	18712	19859	742.5	65.0	2498	4433	570.3	**RU**
RUA	73.8	341.5	92.4	546.4	374.2	200.1	2813	1282	130.1	17.9	294.4	499.8	63.6	**RUA**
SE	16.9	2.8	116.9	4.1	101.0	1535	413.7	485.5	166.2	0.4	453.0	2536	1260	**SE**
SI	35.3	0.3	277.1	0.3	604.6	42.4	281.9	25.7	69.3	0.1	122.3	171.7	2.1	**SI**
SK	66.4	1.1	352.8	1.2	830.0	142.0	2348	145.6	133.2	0.2	2695	579.3	18.7	**SK**
TJ	1.8	24.4	0.8	36.4	4.7	1.3	38.4	5.1	1.5	2.2	1.8	3.5	0.2	**TJ**
TM	2.6	51.8	1.1	151.7	6.4	2.1	63.3	16.1	1.9	3.4	3.1	5.6	0.5	**TM**
TR	259.4	1079	67.4	331.6	489.8	82.9	8836	374.4	83.5	249.4	161.8	223.1	10.6	**TR**
UA	286.6	162.7	321.9	241.3	1531	488.6	14366	4962	272.7	19.2	1575	1562	122.7	**UA**
UZ	3.4	58.9	1.6	113.5	9.1	3.3	81.3	22.2	2.7	3.8	4.7	8.5	0.8	**UZ**
BAS	37.7	3.0	193.3	4.5	208.2	2385	1255	813.0	290.6	0.4	966.4	5419	1392	**BAS**
BLS	149.9	238.1	81.6	194.1	488.7	89.5	9935	659.4	75.3	20.2	213.9	274.6	16.4	**BLS**
CAS	7.8	313.2	4.5	1661	22.6	9.0	248.7	96.9	6.5	8.7	14.0	23.3	2.4	**CAS**
MDT	2405	90.9	558.5	64.2	4931	533.5	20711	339.9	1180	533.7	721.4	1310	34.5	**MDT**
NOS	19.1	1.9	228.2	2.6	126.2	8546	257.9	256.4	571.6	0.2	790.2	7381	974.3	**NOS**
	AL	**AM**	**AT**	**AZ**	**BA**	**BE**	**BG**	**BY**	**CH**	**CY**	**CZ**	**DE**	**DK**	

***Table A.2**. Matrix of lead country-to-country deposition from anthropogenic sources in 2008, kg/y (continued)*

Receptors ↓ Emitters →

	EE	ES	FI	FR	GB	GE	GR	HR	HU	IE	IS	IT	KY	KZ	
AL	3.4	196.6	1.4	113.0	13.3	1.0	6541	7.2	76.2	2.9	0.0	2097	0.2	25.2	**AL**
AM	1.2	16.8	0.5	3.7	1.1	211.9	168.4	0.3	3.5	0.2	0.0	31.3	0.8	415.2	**AM**
AT	17.4	543.6	6.1	702.6	196.5	1.0	603.1	88.4	820.7	29.1	0.0	6604	0.1	39.1	**AT**
AZ	4.5	28.9	1.8	8.2	3.0	351.5	328.4	0.5	7.6	0.6	0.0	65.7	10.1	2278	**AZ**
BA	5.6	426.4	2.7	241.5	46.0	1.4	1750	163.9	942.3	8.1	0.0	3582	0.2	27.8	**BA**
BE	8.9	462.2	2.3	2286	595.7	0.0	18.9	0.5	7.4	69.1	0.0	127.0	0.0	3.5	**BE**
BG	26.0	203.3	11.2	109.7	36.9	17.0	14214	15.4	432.7	6.8	0.0	1189	2.8	392.5	**BG**
BY	498.5	281.4	154.5	309.1	265.1	23.4	2033	28.6	687.6	38.7	0.1	1157	1.4	1052	**BY**
CH	1.9	657.4	0.8	1171	148.0	0.1	121.5	8.1	36.0	25.5	0.0	6377	0.0	3.6	**CH**
CY	0.2	3.8	0.1	1.7	0.4	0.6	245.9	0.1	1.5	0.1	0.0	19.2	0.0	5.1	**CY**
CZ	39.1	286.0	13.4	497.1	237.4	1.0	497.9	36.0	1079	33.4	0.0	1552	0.3	39.6	**CZ**
DE	176.8	2343	55.1	7886	3308	0.5	373.4	19.0	431.0	438.7	0.3	3426	0.2	85.6	**DE**
DK	30.3	110.0	14.8	349.3	592.6	0.1	19.7	0.8	25.0	79.7	0.1	75.2	0.1	18.1	**DK**
EE	**3607**	106.2	302.8	147.3	116.1	0.5	86.7	2.3	47.0	16.2	0.0	130.0	0.2	67.5	**EE**
ES	7.7	**89550**	3.1	2678	395.4	1.2	641.9	14.8	88.9	129.1	0.1	2577	0.2	27.2	**ES**
FI	2921	160.3	**8392**	320.0	355.2	3.2	327.6	5.2	106.9	56.1	0.3	319.5	0.7	398.0	**FI**
FR	25.9	25885	10.4	**34536**	2716	1.0	741.8	33.8	212.6	591.5	0.4	9342	0.2	41.2	**FR**
GB	71.0	1262	28.6	1812	**15027**	0.2	52.6	1.9	32.9	1934	0.7	366.9	0.0	26.1	**GB**
GE	5.6	57.5	1.9	12.2	4.9	**2093**	579.1	0.9	13.3	0.9	0.0	99.6	2.6	914.8	**GE**
GR	14.3	331.1	6.3	156.0	34.9	15.5	**89599**	11.7	195.4	6.8	0.0	1919	1.2	238.2	**GR**
HR	6.0	479.9	2.4	275.0	41.0	1.0	1525	**510.8**	1088	7.4	0.0	4971	0.1	27.9	**HR**
HU	16.4	338.9	6.8	245.3	79.7	1.6	1988	176.7	**9431**	13.0	0.0	2962	0.4	65.7	**HU**
IE	7.1	322.3	3.6	204.0	574.4	0.0	4.0	0.3	3.1	**2837**	0.3	61.6	0.0	3.4	**IE**
IS	5.2	46.8	3.6	54.7	122.0	0.1	5.9	0.2	2.5	42.0	**36.4**	43.8	0.0	3.3	**IS**
IT	13.8	3631	6.0	2296	183.9	3.1	5919	212.8	887.3	37.7	0.1	**98055**	0.4	81.6	**IT**
KY	5.4	47.4	2.0	10.7	3.0	30.9	232.3	0.6	7.1	0.6	0.0	66.7	**7447**	22963	**KY**
KZ	229.7	353.1	92.1	150.5	84.8	426.1	3258	13.0	180.2	14.3	0.1	1112	3718	**226615**	**KZ**
LT	165.0	148.9	70.8	209.8	207.8	1.1	181.4	8.8	194.0	29.3	0.0	361.4	0.4	139.6	**LT**
LU	0.7	48.1	0.2	336.1	27.2	0.0	3.2	0.1	1.4	3.9	0.0	20.8	0.0	0.4	**LU**
LV	529.1	162.6	136.4	217.4	188.7	0.9	144.4	5.6	122.5	26.4	0.0	274.3	0.3	104.8	**LV**
MC	0.0	0.3	0.0	0.4	0.0	0.0	0.2	0.0	0.0	0.0	0.0	4.3	0.0	0.0	**MC**
MD	13.6	37.4	5.4	22.1	11.2	9.0	849.9	2.3	59.2	1.9	0.0	168.3	0.7	170.6	**MD**
ME	1.4	127.2	0.7	67.3	8.5	0.4	1228	7.5	78.3	1.8	0.0	1259	0.1	8.0	**ME**
MK	3.5	81.7	1.5	41.1	8.5	1.3	9531	4.4	82.1	1.6	0.0	553.4	0.3	42.9	**MK**
MT	0.0	1.7	0.0	0.8	0.1	0.0	7.2	0.0	0.1	0.0	0.0	6.0	0.0	0.1	**MT**
NL	17.8	346.1	5.5	1211	917.5	0.1	17.1	0.6	14.4	102.1	0.1	107.6	0.0	6.2	**NL**
NO	181.9	263.8	186.9	399.0	1278	1.1	57.9	2.0	54.6	192.4	1.5	218.7	1.5	124.2	**NO**
PL	270.0	876.0	114.7	1368	1120	4.6	1548	83.3	2267	161.3	0.2	3133	2.5	370.1	**PL**
PT	1.9	4338	0.6	97.5	33.8	0.0	18.2	0.5	2.9	16.1	0.0	98.6	0.0	1.2	**PT**
RO	68.4	466.1	30.5	308.5	128.8	18.8	7757	70.6	2124	22.9	0.0	3209	6.1	705.7	**RO**
RS	10.7	258.0	5.1	162.7	48.4	2.7	4469	62.9	1464	8.2	0.0	2091	0.6	80.6	**RS**
RU	17890	2027	4499	1578	1310	1859	16144	101.1	2002	202.6	1.4	6345	240.8	105191	**RU**
RUA	662.0	513.6	359.8	237.6	181.9	270.9	2697	17.2	290.1	34.8	0.7	1381	1069	126217	**RUA**
SE	627.7	331.6	1416	858.4	1224	2.5	234.6	6.6	187.4	176.8	0.6	432.3	3.6	342.5	**SE**
SI	3.9	177.7	1.4	134.1	20.5	0.3	305.0	137.1	280.0	3.4	0.0	3395	0.0	13.1	**SI**
SK	19.5	205.6	8.6	188.3	79.9	1.2	858.9	67.0	3018	12.3	0.0	1496	0.5	56.8	**SK**
TJ	1.5	15.8	0.5	3.6	1.0	12.0	100.2	0.2	2.3	0.2	0.0	24.0	668.6	4265	**TJ**
TM	5.1	15.2	2.0	4.2	1.7	36.6	148.8	0.3	3.8	0.3	0.0	29.3	103.7	4616	**TM**
TR	58.4	771.4	22.1	231.8	68.9	457.2	24596	18.4	299.7	12.8	0.0	2056	6.4	1894	**TR**
UA	423.3	681.9	152.9	518.0	333.0	243.6	10461	71.7	2060	52.0	0.2	3409	14.6	7718	**UA**
UZ	7.0	20.7	2.6	5.9	2.6	35.7	181.8	0.4	5.2	0.5	0.0	39.1	847.6	15876	**UZ**
BAS	3626	656.0	2664	1408	1542	2.7	631.7	12.2	319.1	210.1	0.3	756.3	2.0	368.5	**BAS**
BLS	86.2	238.0	32.7	135.4	69.3	627.9	8801	19.0	348.0	11.9	0.1	1326	18.6	4046	**BLS**
CAS	21.2	30.4	8.0	12.8	7.6	251.6	422.6	0.9	13.7	1.3	0.0	97.5	135.3	17697	**CAS**
MDT	47.8	24107	23.2	6974	530.3	71.1	114594	289.4	1446	129.6	0.2	55708	5.6	750.7	**MDT**
NOS	259.5	2920	133.7	6535	16321	1.5	243.1	8.7	252.6	1709	2.5	1249	1.8	182.1	**NOS**
	EE	**ES**	**FI**	**FR**	**GB**	**GE**	**GR**	**HR**	**HU**	**IE**	**IS**	**IT**	**KY**	**KZ**	

***Table A.2**. Matrix of lead country-to-country deposition from anthropogenic sources in 2008, kg/y (continued)*

Receptors ↓ Emitters →

	LT	LU	LV	MC	MD	ME	MK	MT	NL	NO	PL	PT	
AL	1.3	0.6	1.1	0.1	5.7	33.8	2295	5.2	10.3	0.5	311.7	11.2	**AL**
AM	0.5	0.0	0.4	0.0	0.8	0.2	13.9	0.2	0.9	0.1	35.3	2.2	**AM**
AT	16.7	24.8	12.1	0.6	2.5	8.5	182.4	1.2	292.4	4.2	6606	38.0	**AT**
AZ	1.7	0.1	1.4	0.0	1.8	0.5	29.2	0.4	2.9	0.4	96.2	3.3	**AZ**
BA	4.7	2.6	3.7	0.4	4.5	90.2	400.6	4.3	53.2	1.8	2750	25.3	**BA**
BE	4.2	109.7	4.4	0.0	0.1	0.1	2.7	0.2	1220	1.9	518.4	35.1	**BE**
BG	11.2	1.7	10.0	0.1	83.4	22.3	3533	3.4	42.3	3.1	2203	16.4	**BG**
BY	743.3	10.3	341.3	0.1	148.6	10.6	410.6	1.7	299.3	32.0	20362	24.6	**BY**
CH	1.6	17.2	1.4	0.9	0.3	0.8	16.8	0.5	90.8	1.0	367.4	43.9	**CH**
CY	0.1	0.0	0.1	0.0	0.2	0.2	12.9	0.1	0.3	0.0	9.3	0.2	**CY**
CZ	37.3	20.6	28.5	0.2	4.0	5.7	181.0	0.5	384.3	8.8	25811	20.6	**CZ**
DE	92.4	516.8	119.0	0.7	3.6	3.6	80.1	1.1	9158	43.1	20850	155.1	**DE**
DK	10.8	7.7	19.2	0.0	0.6	0.3	6.6	0.0	668.0	15.7	1518	7.0	**DK**
EE	140.4	4.7	366.4	0.0	5.7	0.8	26.9	0.1	154.6	22.2	2725	8.1	**EE**
ES	3.5	10.4	3.9	0.6	1.7	3.8	83.8	4.9	168.2	3.3	696.4	5686	**ES**
FI	154.6	9.9	296.8	0.0	15.1	2.1	87.9	0.3	405.5	166.0	5137	11.5	**FI**
FR	19.7	331.3	18.7	11.2	2.7	6.4	121.8	7.4	1348	11.1	3087	1126	**FR**
GB	18.4	30.9	33.6	0.1	0.4	0.4	8.9	0.5	1374	29.7	1805	173.9	**GB**
GE	2.6	0.2	2.1	0.0	5.0	0.8	49.7	0.6	4.5	0.5	160.5	7.6	**GE**
GR	6.3	1.4	5.3	0.1	38.3	15.9	3601	11.1	28.6	1.6	1187	22.2	**GR**
HR	4.1	2.6	3.2	0.5	3.5	22.8	271.4	4.1	47.3	1.4	2295	27.2	**HR**
HU	12.4	6.0	8.9	0.3	10.7	28.3	765.7	2.2	101.2	2.9	5977	25.9	**HU**
IE	1.4	3.5	2.9	0.0	0.1	0.0	0.8	0.0	118.9	3.6	163.2	67.2	**IE**
IS	1.7	1.4	2.7	0.0	0.1	0.0	1.3	0.0	50.0	8.7	130.1	6.4	**IS**
IT	10.5	16.2	10.4	8.8	8.9	46.6	912.4	37.7	165.5	4.0	3443	221.3	**IT**
KY	1.2	0.1	1.2	0.0	1.2	0.4	22.5	0.4	2.8	0.5	82.3	5.3	**KY**
KZ	55.1	2.9	56.7	0.1	44.3	7.5	374.2	2.9	86.5	18.9	2786	38.4	**KZ**
LT	**1760**	6.8	448.0	0.0	13.9	2.5	75.0	0.2	231.9	20.3	10723	10.0	**LT**
LU	0.4	**130.2**	0.4	0.0	0.0	0.0	0.5	0.0	38.2	0.1	68.2	3.2	**LU**
LV	665.7	6.8	**1687**	0.0	11.9	1.8	55.2	0.2	231.9	25.0	6449	11.6	**LV**
MC	0.0	0.0	0.0	**0.0**	0.0	0.0	0.0	0.0	0.0	0.0	0.2	0.0	**MC**
MD	6.8	0.5	5.0	0.0	**580.5**	2.3	126.7	0.5	13.8	1.2	838.0	3.2	**MD**
ME	0.7	0.4	0.7	0.1	1.8	**253.4**	422.3	2.4	7.6	0.3	244.6	6.6	**ME**
MK	1.3	0.4	1.2	0.0	7.5	9.8	**11980**	1.6	8.7	0.4	354.2	5.5	**MK**
MT	0.0	0.0	0.0	0.0	0.0	0.0	0.5	**4.9**	0.0	0.0	0.5	0.1	**MT**
NL	7.5	20.8	11.4	0.0	0.1	0.1	3.1	0.1	**6770**	4.1	927.8	28.0	**NL**
NO	43.9	11.7	61.8	0.0	2.5	0.6	14.9	0.1	483.6	**1834**	3479	28.9	**NO**
PL	377.6	51.5	277.0	0.3	30.9	20.6	605.5	2.0	1580	55.6	**225790**	61.3	**PL**
PT	0.2	0.6	0.4	0.0	0.1	0.1	2.8	0.2	9.6	0.5	31.2	**14880**	**PT**
RO	36.5	7.6	29.8	0.3	380.1	47.4	1979	4.7	159.7	9.3	9417	34.8	**RO**
RS	6.7	2.9	5.6	0.2	19.1	138.2	3419	2.7	57.2	2.6	3300	16.6	**RS**
RU	1395	40.9	1631	0.7	505.6	49.7	2332	11.8	1396	352.3	44591	175.2	**RU**
RUA	104.8	4.9	113.9	0.2	61.6	9.5	389.4	3.0	156.0	70.9	4724	53.5	**RUA**
SE	145.9	24.1	272.0	0.0	10.8	2.4	80.5	0.3	1343	680.5	8340	23.4	**SE**
SI	1.9	1.7	1.5	0.3	0.9	5.5	74.0	1.1	26.3	0.5	893.6	11.6	**SI**
SK	14.9	5.4	11.1	0.1	7.6	13.1	374.7	1.0	105.5	4.2	15944	15.8	**SK**
TJ	0.4	0.0	0.4	0.0	0.4	0.2	8.4	0.2	0.9	0.1	25.7	1.7	**TJ**
TM	0.9	0.1	1.0	0.0	1.0	0.2	13.2	0.2	1.6	0.4	51.5	1.9	**TM**
TR	21.9	2.6	18.0	0.2	79.9	19.0	1539	12.3	58.6	5.2	2208	83.9	**TR**
UA	239.2	14.7	168.1	0.3	846.3	36.6	1649	7.1	387.2	33.7	30348	60.7	**UA**
UZ	1.3	0.1	1.4	0.0	1.2	0.3	16.7	0.2	2.4	0.6	79.0	2.4	**UZ**
BAS	420.8	48.3	1330	0.1	20.5	5.5	223.0	0.5	2090	169.3	21222	46.3	**BAS**
BLS	38.8	2.8	30.3	0.1	230.8	15.7	954.0	4.0	68.1	6.4	3225	21.8	**BLS**
CAS	5.2	0.2	5.3	0.0	4.8	0.7	41.4	0.4	7.2	1.5	243.5	3.1	**CAS**
MDT	25.9	22.4	24.1	6.6	83.6	161.8	5821	327.0	294.5	12.6	6618	1234	**MDT**
NOS	90.7	97.5	146.0	0.2	5.2	2.5	56.3	1.4	7506	465.5	11724	271.9	**NOS**
	LT	**LU**	**LV**	**MC**	**MD**	**ME**	**MK**	**MT**	**NL**	**NO**	**PL**	**PT**	

***Table A.2**. Matrix of lead country-to-country deposition from anthropogenic sources in 2008, kg/y (continued)*

Receptors ↓ Emitters →

	RO	RS	RU	RUA	SE	SI	SK	TJ	TM	TR	UA	UZ	Total, t/y	
AL	220.6	1606	351.9	1.2	0.9	21.1	117.0	0.5	0.9	332.9	166.2	2.1	**19.8**	**AL**
AM	17.2	17.2	820.7	8.9	0.2	1.2	6.9	2.0	77.2	1334	72.7	55.2	**5.8**	**AM**
AT	244.2	1039	1000	3.7	7.0	2740	2357	0.4	0.8	178.1	192.1	1.6	**36.6**	**AT**
AZ	37.8	37.2	4876	39.9	0.8	2.6	15.4	27.8	419.0	1673	285.2	346.8	**15.3**	**AZ**
BA	505.7	3279	571.6	2.3	3.6	170.8	1108	0.4	0.9	255.0	215.0	1.8	**32.8**	**BA**
BE	4.4	8.4	128.0	0.6	1.6	4.9	21.3	0.0	0.1	2.1	9.5	0.1	**17.3**	**BE**
BG	4566	4408	4510	16.0	6.7	49.6	740.6	10.3	14.0	3823	2242	41.8	**150.5**	**BG**
BY	2262	1282	22669	94.7	96.2	157.8	2100	4.8	29.6	1476	7641	48.4	**96.9**	**BY**
CH	19.1	53.5	88.3	0.5	0.9	70.3	68.1	0.0	0.1	12.7	19.9	0.1	**17.1**	**CH**
CY	6.7	10.8	46.1	0.3	0.0	0.6	2.4	0.1	0.7	409.4	12.1	0.8	**1.0**	**CY**
CZ	285.1	874.2	1229	4.2	16.4	349.9	3031	1.3	1.0	139.7	242.6	4.2	**50.5**	**CZ**
DE	177.8	358.1	2756	11.8	62.8	227.9	1118	0.7	1.6	55.4	257.0	3.5	**122.8**	**DE**
DK	23.4	30.7	321.4	1.5	46.2	8.2	86.6	0.8	0.6	10.3	40.7	2.7	**6.6**	**DK**
EE	114.9	87.1	6351	10.3	91.3	16.0	147.7	0.5	2.2	51.2	290.3	4.5	**14.5**	**EE**
ES	75.0	171.2	248.9	2.2	3.7	85.1	156.4	0.5	1.2	68.4	73.2	2.2	**105.4**	**ES**
FI	299.1	209.6	23072	48.4	847.5	40.7	325.1	1.8	12.9	204.0	855.5	22.4	**43.1**	**FI**
FR	143.1	337.8	644.2	5.2	12.0	260.8	410.2	0.4	1.5	74.2	145.5	2.3	**95.3**	**FR**
GB	19.0	28.6	700.0	4.8	31.3	19.3	87.6	0.1	0.8	10.5	37.3	1.0	**29.3**	**GB**
GE	86.8	65.8	5707	23.0	1.0	4.3	26.9	6.3	127.9	3807	507.0	113.9	**18.9**	**GE**
GR	1132	1684	2525	12.2	3.6	43.9	345.6	4.0	9.7	5989	1080	20.0	**125.8**	**GR**
HR	375.3	1953	516.6	1.9	2.7	486.7	1158	0.4	0.8	232.2	190.1	1.6	**21.7**	**HR**
HU	2026	5542	1157	5.6	5.7	504.1	8729	1.6	2.5	370.4	579.4	6.9	**49.9**	**HU**
IE	2.6	3.2	78.6	0.7	3.9	3.2	8.7	0.0	0.1	1.7	5.7	0.1	**4.9**	**IE**
IS	3.6	3.6	66.8	1.3	5.3	2.2	6.3	0.1	0.2	3.8	10.9	0.5	**0.9**	**IS**
IT	578.4	2101	1351	6.5	7.3	1668	1369	1.0	3.0	624.5	387.8	5.2	**133.7**	**IT**
KY	27.3	31.3	2020	163.6	0.8	2.8	14.2	8689	795.8	710.3	126.7	22062	**66.0**	**KY**
KZ	903.6	687.9	119912	11368	38.1	71.0	401.6	7233	4658	6740	6292	34056	**429.8**	**KZ**
LT	343.3	296.2	5250	14.5	77.3	61.6	625.8	1.4	5.9	101.1	579.7	11.3	**25.6**	**LT**
LU	0.8	1.6	14.0	0.1	0.1	0.8	3.9	0.0	0.0	0.3	1.5	0.0	**1.1**	**LU**
LV	263.7	207.0	4795	14.3	104.3	38.3	389.7	1.1	3.4	86.0	552.1	7.9	**19.8**	**LV**
MC	0.0	0.1	0.1	0.0	0.0	0.1	0.1	0.0	0.0	0.0	0.0	0.0	**0.0**	**MC**
MD	1556	227.6	2606	8.6	3.0	9.8	146.9	2.7	4.7	765.0	1934	12.1	**12.4**	**MD**
ME	119.5	1503	146.7	0.5	0.6	15.8	104.1	0.2	0.3	125.6	57.5	0.7	**7.6**	**ME**
MK	292.5	1897	439.3	2.7	0.9	13.1	124.2	0.9	1.1	565.0	196.2	3.3	**33.0**	**MK**
MT	0.2	0.6	0.5	0.0	0.0	0.1	0.2	0.0	0.0	1.4	0.2	0.0	**0.0**	**MT**
NL	6.3	11.6	269.5	0.9	3.9	6.4	40.5	0.0	0.1	2.5	14.4	0.2	**17.9**	**NL**
NO	59.3	60.5	4304	24.7	331.9	23.1	182.0	8.4	5.4	55.9	186.5	26.3	**15.1**	**NO**
PL	1800	2451	10234	41.9	157.8	616.3	8624	11.1	12.3	437.7	2757	43.8	**295.6**	**PL**
PT	2.9	5.3	20.4	0.1	0.6	2.8	5.4	0.0	0.0	3.0	3.2	0.1	**19.7**	**PT**
RO	**31602**	7798	8295	34.1	20.7	244.3	3820	25.6	24.7	3569	5726	94.9	**114.9**	**RO**
RS	2072	**26584**	1109	6.2	4.9	120.6	1435	1.8	2.6	536.6	549.5	7.1	**62.6**	**RS**
RU	8463	5157	**1607960**	10687	999.1	596.0	5324	689.3	2530	25183	60934	5052	**2001.6**	**RU**
RUA	1273	867.6	232203	**136187**	120.1	97.8	713.7	2060	1624	5035	5694	8462	**520.6**	**RUA**
SE	253.2	241.3	8480	34.3	**3682**	59.4	537.6	20.9	14.5	137.5	666.4	67.2	**36.6**	**SE**
SI	101.3	452.6	198.6	0.9	1.0	**2847**	482.7	0.1	0.3	50.9	60.5	0.6	**11.3**	**SI**
SK	1041	2079	1149	4.7	9.1	372.0	**16188**	2.2	1.9	184.4	489.9	7.7	**51.4**	**SK**
TJ	8.7	10.7	637.1	40.3	0.2	1.0	4.5	**13030**	717.3	299.9	38.8	9819	**29.9**	**TJ**
TM	19.2	17.1	19440	89.2	0.7	1.3	7.7	1011	**4630**	511.3	139.4	6560	**20.8**	**TM**
TR	2002	1749	2249	72.5	10.4	82.4	540.2	17.5	189.3	**121462**	4782	195.5	**201.8**	**TR**
UA	10397	4140	76463	392.5	86.0	316.8	5857	42.5	249.5	10121	**75995**	434.4	**285.0**	**UA**
UZ	24.2	22.9	3196	187.3	1.0	1.9	11.0	6337	1979	586.1	190.9	**28955**	**59.0**	**UZ**
BAS	592.4	549.7	18643	41.8	1369	100.3	1055	9.4	15.4	235.7	1006	43.3	**68.3**	**BAS**
BLS	4149	1703	43202	122.2	15.2	88.2	706.0	59.7	127.2	22724	11242	296.4	**128.6**	**BLS**
CAS	81.3	58.5	18270	283.4	2.9	5.0	31.1	508.5	2505	1853	1139	3015	**51.9**	**CAS**
MDT	2915	6708	8392	33.7	20.5	1141	2299	16.8	45.3	35328	3027	79.4	**314.3**	**MDT**
NOS	210.1	217.8	3137	19.8	258.7	87.0	726.5	9.3	7.8	92.8	393.5	31.4	**74.0**	**NOS**
	RO	**RS**	**RU**	**RUA**	**SE**	**SI**	**SK**	**TJ**	**TM**	**TR**	**UA**	**UZ**	**Total, t/y**	

Table A.3*. Matrix of cadmium country-to-country deposition from anthropogenic sources in 2008, kg/y*

Receptors ↓ Emitters →

	AL	AM	AT	AZ	BA	BE	BG	BY	CH	CY	CZ	DE	DK	
AL	**43.28**	0.02	1.23	0.17	7.67	0.51	26.07	0.84	1.19	0.03	3.14	0.91	0.06	**AL**
AM	0.04	**42.26**	0.06	66.24	0.19	0.03	0.75	0.31	0.07	0.17	0.18	0.07	0.01	**AM**
AT	0.71	0.02	**362.8**	0.17	22.41	14.33	9.97	5.73	50.93	0.00	98.44	76.41	1.02	**AT**
AZ	0.09	11.35	0.15	**573.6**	0.44	0.10	1.71	1.09	0.16	0.32	0.47	0.20	0.03	**AZ**
BA	4.42	0.03	13.94	0.26	**515.0**	2.05	12.93	2.03	3.79	0.01	33.29	6.22	0.40	**BA**
BE	0.01	0.001	1.29	0.01	0.15	**367.9**	0.13	0.76	5.44	0.00	4.55	25.43	0.32	**BE**
BG	4.58	0.27	3.99	2.50	16.11	1.62	**1388**	7.65	1.93	0.13	16.11	3.59	0.34	**BG**
BY	1.01	0.33	12.87	3.56	16.36	10.83	38.78	**979.9**	6.57	0.08	78.54	24.81	6.77	**BY**
CH	0.10	0.002	8.10	0.02	1.69	7.83	0.62	0.45	**324.9**	0.00	4.00	14.27	0.14	**CH**
CY	0.05	0.03	0.03	0.12	0.15	0.01	0.51	0.05	0.03	**3.09**	0.07	0.03	0.00	**CY**
CZ	0.53	0.02	77.70	0.15	11.51	15.18	13.15	8.36	20.92	0.003	**809.3**	70.70	2.54	**CZ**
DE	0.37	0.02	92.05	0.16	6.38	358.6	3.62	13.19	239.5	0.002	308.7	**1102**	17.87	**DE**
DK	0.03	0.003	1.41	0.03	0.46	18.71	0.39	1.50	1.69	0.00	8.69	23.83	**42.89**	**DK**
EE	0.06	0.01	1.78	0.12	1.15	5.68	2.10	12.41	1.74	0.002	11.71	10.01	3.08	**EE**
ES	0.53	0.03	3.68	0.26	5.76	11.75	3.44	0.91	11.59	0.002	5.55	7.42	0.51	**ES**
FI	0.21	0.06	4.47	1.00	2.47	14.52	6.69	23.33	3.79	0.02	24.87	22.09	8.13	**FI**
FR	0.76	0.03	15.57	0.25	10.56	169.8	4.33	3.72	156.2	0.004	29.79	85.06	1.82	**FR**
GB	0.05	0.01	3.38	0.07	0.59	66.45	0.38	1.58	7.32	0.00	14.51	40.67	4.96	**GB**
GE	0.14	16.13	0.26	154.8	0.71	0.15	3.46	1.79	0.22	0.38	0.77	0.31	0.05	**GE**
GR	7.99	0.28	2.56	1.88	11.10	1.16	196.9	4.02	2.15	0.57	8.09	2.27	0.19	**GR**
HR	2.51	0.02	21.87	0.19	86.50	2.07	11.03	2.12	4.74	0.01	28.41	6.31	0.29	**HR**
HU	2.16	0.03	42.80	0.31	67.06	4.35	49.63	5.46	6.96	0.02	72.30	13.14	0.66	**HU**
IE	0.004	0.001	0.43	0.01	0.08	6.27	0.06	0.13	1.16	0.00	1.53	3.99	0.53	**IE**
IS	0.01	0.002	0.20	0.02	0.07	1.98	0.06	0.25	0.49	0.00	0.85	1.99	0.59	**IS**
IT	6.85	0.07	55.01	0.60	70.44	9.53	27.60	4.53	73.40	0.02	39.58	24.20	0.67	**IT**
KY	0.07	1.28	0.16	13.59	0.39	0.11	1.22	0.62	0.19	0.15	0.42	0.21	0.03	**KY**
KZ	1.02	12.65	4.10	190.7	8.41	3.09	29.19	35.17	3.33	0.79	13.50	5.96	1.37	**KZ**
LT	0.20	0.03	6.57	0.31	4.30	8.02	5.38	64.65	4.21	0.01	40.82	18.70	5.63	**LT**
LU	0.002	0.00	0.22	0.00	0.03	9.50	0.03	0.11	0.90	0.00	0.68	2.88	0.02	**LU**
LV	0.14	0.02	4.22	0.18	2.93	8.27	4.25	34.76	3.56	0.004	27.03	17.08	5.55	**LV**
MC	0.00	0.00	0.003	0.00	0.002	0.001	0.001	0.00	0.01	0.00	0.002	0.001	0.00	**MC**
MD	0.32	0.11	0.77	1.25	2.14	0.48	15.77	5.33	0.44	0.02	3.74	1.11	0.17	**MD**
ME	6.92	0.01	1.11	0.08	18.99	0.34	6.96	0.40	0.73	0.01	2.87	0.72	0.05	**ME**
MK	8.69	0.03	0.96	0.21	4.90	0.37	61.93	0.86	0.60	0.08	3.32	0.78	0.06	**MK**
MT	0.004	0.00	0.004	0.00	0.02	0.001	0.02	0.001	0.005	0.00	0.01	0.003	0.00	**MT**
NL	0.02	0.002	1.65	0.02	0.21	135.9	0.12	0.89	3.71	0.00	8.71	45.21	0.80	**NL**
NO	0.05	0.03	3.28	0.29	0.78	16.41	0.79	7.69	3.82	0.005	17.92	23.55	15.97	**NO**
PL	1.87	0.09	68.86	1.14	35.71	52.38	40.67	125.6	31.75	0.02	830.0	185.7	24.34	**PL**
PT	0.02	0.001	0.15	0.01	0.18	0.61	0.14	0.04	0.51	0.00	0.28	0.46	0.09	**PT**
RO	4.99	0.33	18.98	3.31	64.83	6.34	243.5	24.26	7.94	0.18	69.42	15.45	1.55	**RO**
RS	8.34	0.06	11.04	0.57	96.31	2.31	118.0	3.44	3.32	0.08	36.99	6.87	0.54	**RS**
RU	5.86	25.72	45.29	500.4	61.76	47.71	219.3	868.9	32.11	1.94	208.3	95.80	26.46	**RU**
RUA	1.08	7.67	6.56	95.88	11.11	5.37	33.01	50.60	5.56	0.53	23.80	10.48	2.86	**RUA**
SE	0.25	0.06	7.94	0.69	3.11	43.63	4.39	19.47	7.37	0.01	42.83	63.21	62.61	**SE**
SI	0.55	0.01	28.63	0.07	18.55	1.25	3.09	1.05	3.30	0.002	11.31	4.13	0.11	**SI**
SK	1.04	0.02	33.60	0.22	26.89	4.28	26.86	6.43	6.41	0.01	229.9	13.76	1.02	**SK**
TJ	0.03	0.53	0.05	5.66	0.13	0.03	0.43	0.19	0.06	0.07	0.13	0.06	0.01	**TJ**
TM	0.04	1.27	0.09	31.44	0.21	0.07	0.83	0.73	0.09	0.11	0.29	0.13	0.03	**TM**
TR	4.02	25.61	5.05	45.72	15.62	2.33	112.3	15.91	3.76	7.90	13.30	4.66	0.51	**TR**
UA	4.29	3.70	24.19	46.77	49.97	13.72	169.1	222.7	12.04	0.57	130.3	33.78	6.28	**UA**
UZ	0.05	1.30	0.12	19.65	0.28	0.10	1.00	0.96	0.12	0.12	0.40	0.19	0.04	**UZ**
BAS	0.57	0.06	13.49	0.77	6.48	67.83	13.39	33.18	12.75	0.01	92.71	130.9	72.78	**BAS**
BLS	2.26	5.36	6.01	35.01	15.63	2.41	120.9	27.30	3.32	0.61	17.31	5.66	0.79	**BLS**
CAS	0.12	7.02	0.31	371.2	0.67	0.23	2.98	3.83	0.27	0.26	1.09	0.47	0.10	**CAS**
MDT	37.07	1.95	45.26	9.75	152.8	15.56	251.7	13.31	54.50	17.70	62.60	27.51	1.60	**MDT**
NOS	0.27	0.04	15.50	0.43	3.67	229.7	2.74	10.02	25.68	0.005	80.15	196.1	51.32	**NOS**
	AL	**AM**	**AT**	**AZ**	**BA**	**BE**	**BG**	**BY**	**CH**	**CY**	**CZ**	**DE**	**DK**	

***Table A.3**. Matrix of cadmium country-to-country deposition from anthropogenic sources in 2008, kg/y (continued)*

Receptors ↓ Emitters →

	EE	ES	FI	FR	GB	GE	GR	HR	HU	IE	IS	IT	
AL	0.05	9.17	0.07	5.53	0.54	0.03	49.16	2.37	3.50	0.09	0.002	78.26	**AL**
AM	0.02	0.75	0.02	0.15	0.04	7.34	1.02	0.07	0.14	0.01	0.00	0.99	**AM**
AT	0.28	24.48	0.33	24.39	8.07	0.03	3.80	26.05	34.73	0.95	0.01	151.3	**AT**
AZ	0.07	1.33	0.09	0.34	0.11	14.16	2.05	0.15	0.32	0.02	0.001	2.08	**AZ**
BA	0.09	19.20	0.15	11.07	1.83	0.04	11.44	55.96	39.47	0.26	0.01	109.5	**BA**
BE	0.14	21.37	0.12	71.04	28.73	0.00	0.12	0.12	0.33	2.43	0.02	3.52	**BE**
BG	0.44	9.30	0.62	4.54	1.44	0.51	74.42	4.84	20.42	0.22	0.01	38.39	**BG**
BY	9.23	12.60	8.76	10.10	10.81	0.62	12.02	8.03	32.68	1.31	0.04	30.57	**BY**
CH	0.03	29.48	0.04	41.91	6.36	0.00	0.79	2.15	1.48	0.85	0.01	160.1	**CH**
CY	0.00	0.18	0.00	0.08	0.02	0.02	1.70	0.05	0.06	0.00	0.00	0.72	**CY**
CZ	0.66	12.94	0.75	16.13	9.98	0.03	3.27	10.72	43.92	1.14	0.01	37.98	**CZ**
DE	3.13	106.3	3.18	247.5	141.5	0.02	2.44	5.19	16.91	15.05	0.13	88.27	**DE**
DK	0.53	5.08	0.87	10.89	24.00	0.00	0.13	0.21	1.02	2.70	0.04	1.80	**DK**
EE	**69.87**	4.67	16.59	4.76	4.70	0.01	0.51	0.61	2.02	0.54	0.01	3.25	**EE**
ES	0.12	**4484**	0.16	110.7	16.25	0.04	3.92	4.11	3.62	4.48	0.06	113.7	**ES**
FI	51.40	7.26	**557**	10.02	14.27	0.09	1.90	1.36	4.51	1.84	0.12	7.60	**FI**
FR	0.42	1229	0.56	**1514**	124.4	0.03	4.78	9.22	8.86	20.51	0.18	297.9	**FR**
GB	1.19	62.84	1.62	60.62	**644.9**	0.01	0.35	0.52	1.39	68.25	0.31	9.82	**GB**
GE	0.09	2.59	0.10	0.50	0.19	**70.14**	3.66	0.26	0.58	0.03	0.00	3.31	**GE**
GR	0.23	15.35	0.33	7.10	1.34	0.43	**646.1**	3.48	8.25	0.22	0.01	69.39	**GR**
HR	0.10	21.44	0.13	12.67	1.66	0.03	9.59	**161.5**	48.11	0.24	0.00	144.4	**HR**
HU	0.28	15.32	0.39	9.62	3.27	0.05	13.26	56.86	**452.6**	0.43	0.01	76.57	**HU**
IE	0.12	16.73	0.21	7.59	24.39	0.00	0.03	0.08	0.13	**101**	0.11	1.57	**IE**
IS	0.08	2.18	0.21	1.83	5.02	0.00	0.04	0.06	0.10	1.40	**14.54**	1.01	**IS**
IT	0.21	166.3	0.31	108.2	7.35	0.09	38.48	60.65	37.23	1.23	0.02	**2679**	**IT**
KY	0.08	2.05	0.09	0.42	0.11	0.94	1.38	0.15	0.28	0.02	0.00	2.08	**KY**
KZ	3.79	15.82	4.90	5.59	3.33	13.65	20.19	3.49	7.71	0.46	0.05	30.24	**KZ**
LT	2.97	6.68	4.21	6.80	8.25	0.03	1.14	2.52	8.62	0.96	0.02	9.33	**LT**
LU	0.01	2.20	0.01	9.61	1.29	0.00	0.02	0.02	0.06	0.14	0.00	0.59	**LU**
LV	9.70	7.28	7.88	7.13	7.65	0.02	0.90	1.57	5.38	0.88	0.02	7.17	**LV**
MC	0.00	0.01	0.00	0.02	0.00	0.00	0.001	0.002	0.002	0.00	0.00	0.11	**MC**
MD	0.24	1.69	0.31	0.80	0.45	0.27	5.11	0.65	2.90	0.06	0.00	4.94	**MD**
ME	0.02	5.74	0.04	3.24	0.34	0.01	8.10	2.51	3.39	0.06	0.00	44.09	**ME**
MK	0.05	3.80	0.08	1.85	0.35	0.04	77.20	1.42	3.81	0.05	0.00	19.29	**MK**
MT	0.00	0.08	0.00	0.04	0.003	0.00	0.05	0.01	0.005	0.00	0.00	0.28	**MT**
NL	0.30	16.15	0.29	37.63	40.61	0.00	0.12	0.15	0.58	3.54	0.02	2.83	**NL**
NO	3.01	12.61	11.10	12.56	51.31	0.03	0.37	0.49	2.03	6.49	0.58	4.96	**NO**
PL	4.96	39.58	7.13	43.72	45.87	0.14	10.26	24.17	106.3	5.49	0.09	80.37	**PL**
PT	0.03	239.5	0.03	4.30	1.40	0.00	0.11	0.14	0.13	0.58	0.01	3.68	**PT**
RO	1.18	21.42	1.74	11.65	5.17	0.58	47.73	21.34	110.1	0.74	0.02	88.97	**RO**
RS	0.18	12.16	0.30	7.06	2.05	0.09	34.63	21.04	61.28	0.28	0.01	64.06	**RS**
RU	324.3	89.74	241.3	53.14	50.94	58.52	97.75	27.25	88.42	6.43	0.55	167.3	**RU**
RUA	10.57	22.95	18.88	8.51	7.04	8.69	16.70	4.56	12.45	1.10	0.30	36.60	**RUA**
SE	10.83	15.34	92.35	26.74	49.87	0.07	1.48	1.72	7.56	5.99	0.24	10.09	**SE**
SI	0.06	8.06	0.07	5.85	0.83	0.01	1.95	40.00	12.74	0.11	0.00	89.89	**SI**
SK	0.33	9.40	0.50	6.99	3.41	0.04	5.63	20.23	144.9	0.42	0.01	39.69	**SK**
TJ	0.02	0.68	0.02	0.14	0.04	0.36	0.59	0.05	0.09	0.01	0.00	0.75	**TJ**
TM	0.09	0.77	0.11	0.19	0.07	1.30	0.98	0.08	0.18	0.01	0.00	1.00	**TM**
TR	0.96	35.14	1.16	10.07	2.71	10.53	155.2	5.29	12.62	0.42	0.02	69.98	**TR**
UA	7.38	30.76	8.61	17.96	13.24	7.04	63.23	20.92	111.2	1.69	0.07	93.90	**UA**
UZ	0.12	0.98	0.14	0.24	0.11	1.16	1.13	0.10	0.23	0.02	0.00	1.23	**UZ**
BAS	65.57	29.08	159.7	43.06	61.20	0.07	3.89	3.23	13.81	6.95	0.11	18.47	**BAS**
BLS	1.43	10.65	1.69	5.12	2.62	16.05	53.42	5.42	14.98	0.37	0.02	37.59	**BLS**
CAS	0.33	1.39	0.40	0.49	0.28	8.57	2.60	0.25	0.58	0.04	0.01	2.84	**CAS**
MDT	0.76	1172	1.19	350.4	21.10	1.95	708.6	85.27	59.42	4.24	0.09	2275	**MDT**
NOS	4.22	140.4	7.35	207.1	682.3	0.04	1.63	2.26	10.12	57.95	0.98	30.88	**NOS**
	EE	**ES**	**FI**	**FR**	**GB**	**GE**	**GR**	**HR**	**HU**	**IE**	**IS**	**IT**	

***Table A.3**. Matrix of cadmium country-to-country deposition from anthropogenic sources in 2008, kg/y (continued)*

Receptors ↓ Emitters →

	KY	KZ	LT	LU	LV	MC	MD	ME	MK	MT	NL	NO	PL	
AL	0.01	0.50	0.06	0.02	0.03	0.01	0.27	1.86	446.6	3.92	0.36	0.04	19.98	**AL**
AM	0.07	10.04	0.02	0.00	0.01	0.00	0.04	0.02	2.50	0.13	0.03	0.01	2.35	**AM**
AT	0.01	0.75	0.75	0.61	0.31	0.07	0.11	0.89	29.60	0.82	10.31	0.44	378.0	**AT**
AZ	0.85	58.03	0.07	0.00	0.04	0.00	0.09	0.04	5.37	0.26	0.10	0.04	6.94	**AZ**
BA	0.01	0.59	0.22	0.06	0.10	0.05	0.21	10.69	74.38	3.25	1.88	0.18	161.3	**BA**
BE	0.00	0.07	0.25	3.15	0.12	0.00	0.00	0.01	0.48	0.11	48.83	0.21	33.72	**BE**
BG	0.17	7.88	0.53	0.04	0.28	0.01	4.17	1.81	427.9	2.47	1.46	0.30	150.0	**BG**
BY	0.13	21.69	25.85	0.24	10.52	0.01	6.86	1.02	63.93	1.16	10.75	3.20	1909	**BY**
CH	0.001	0.07	0.08	0.42	0.03	0.11	0.01	0.07	2.90	0.35	3.32	0.10	21.39	**CH**
CY	0.002	0.11	0.00	0.00	0.00	0.00	0.01	0.02	2.57	0.06	0.01	0.00	0.65	**CY**
CZ	0.02	0.70	1.85	0.50	0.79	0.02	0.18	0.61	30.52	0.39	14.43	0.93	1303	**CZ**
DE	0.01	1.68	7.01	13.83	3.39	0.08	0.15	0.32	13.48	0.79	357.6	4.59	1334	**DE**
DK	0.01	0.33	0.95	0.19	0.51	0.00	0.02	0.03	1.12	0.03	25.04	1.69	111.1	**DK**
EE	0.02	1.29	13.69	0.11	11.49	0.00	0.24	0.07	4.02	0.06	5.53	2.24	234.6	**EE**
ES	0.01	0.48	0.19	0.25	0.09	0.07	0.07	0.30	14.11	3.61	6.01	0.33	41.88	**ES**
FI	0.07	8.17	12.95	0.24	8.30	0.00	0.63	0.19	13.47	0.18	14.43	13.59	410.6	**FI**
FR	0.01	0.76	1.07	8.58	0.49	1.48	0.11	0.54	20.88	5.47	52.18	1.14	199.1	**FR**
GB	0.00	0.56	1.68	0.81	0.89	0.01	0.02	0.03	1.61	0.34	53.20	3.07	134.8	**GB**
GE	0.23	23.17	0.11	0.00	0.06	0.00	0.25	0.06	9.00	0.47	0.15	0.04	11.84	**GE**
GR	0.08	4.86	0.27	0.03	0.14	0.02	1.85	1.21	607.8	8.27	0.93	0.14	73.50	**GR**
HR	0.01	0.54	0.20	0.06	0.09	0.06	0.16	2.16	48.34	3.10	1.70	0.14	137.1	**HR**
HU	0.03	1.27	0.57	0.14	0.25	0.03	0.48	3.09	127.5	1.61	3.65	0.30	398.6	**HU**
IE	0.00	0.07	0.14	0.09	0.08	0.00	0.00	0.00	0.14	0.01	4.58	0.35	11.42	**IE**
IS	0.002	0.06	0.14	0.03	0.07	0.001	0.01	0.00	0.20	0.02	1.83	0.80	9.75	**IS**
IT	0.03	1.53	0.55	0.38	0.25	1.14	0.40	3.82	165.4	29.80	5.65	0.38	194.7	**IT**
KY	**710.0**	311.3	0.05	0.003	0.03	0.00	0.05	0.03	3.80	0.29	0.09	0.04	5.30	**KY**
KZ	416.3	**5758**	2.84	0.07	1.53	0.02	2.13	0.64	63.48	2.01	2.94	1.69	205.4	**KZ**
LT	0.04	2.90	**75.35**	0.17	13.31	0.005	0.60	0.24	11.29	0.15	8.39	2.05	1035	**LT**
LU	0.00	0.01	0.02	**3.51**	0.01	0.001	0.00	0.00	0.10	0.02	1.53	0.01	4.40	**LU**
LV	0.03	2.13	101.2	0.17	**55.87**	0.004	0.51	0.17	8.38	0.11	8.41	2.58	573.0	**LV**
MC	0.00	0.00	0.00	0.00	0.00	**0.01**	0.00	0.00	0.003	0.001	0.00	0.00	0.01	**MC**
MD	0.05	3.51	0.30	0.01	0.14	0.002	**29.98**	0.20	20.17	0.37	0.48	0.12	68.25	**MD**
ME	0.005	0.16	0.03	0.01	0.02	0.01	0.08	**19.85**	80.67	1.75	0.27	0.03	15.26	**ME**
MK	0.02	0.80	0.06	0.01	0.03	0.005	0.35	0.70	**2842**	1.19	0.31	0.04	22.89	**MK**
MT	0.00	0.001	0.00	0.00	0.00	0.00	0.00	0.001	0.10	**4.02**	0.001	0.00	0.03	**MT**
NL	0.00	0.13	0.61	0.55	0.31	0.003	0.01	0.01	0.57	0.08	**269.4**	0.44	60.01	**NL**
NO	0.06	2.22	3.15	0.28	1.59	0.004	0.11	0.05	2.34	0.06	17.65	**204.1**	258.1	**NO**
PL	0.16	7.15	20.02	1.25	8.14	0.04	1.42	2.05	100.1	1.45	58.11	5.91	**17795**	**PL**
PT	0.00	0.02	0.02	0.01	0.01	0.004	0.00	0.01	0.46	0.11	0.36	0.05	2.10	**PT**
RO	0.37	13.79	1.76	0.18	0.84	0.03	17.92	4.86	319.1	3.45	5.65	0.94	675.3	**RO**
RS	0.04	1.64	0.32	0.07	0.16	0.02	0.92	17.17	547.0	2.03	2.13	0.28	204.2	**RS**
RU	22.49	2253	74.71	0.95	47.51	0.08	23.89	4.37	374.2	8.13	48.02	29.70	3537	**RU**
RUA	119.5	3810	5.37	0.11	2.99	0.02	2.78	0.82	63.92	2.09	5.23	5.25	347.2	**RUA**
SE	0.17	6.13	12.84	0.58	7.26	0.01	0.46	0.23	12.75	0.19	49.42	63.34	681.8	**SE**
SI	0.004	0.25	0.09	0.04	0.04	0.03	0.04	0.55	12.05	0.78	0.93	0.06	52.77	**SI**
SK	0.03	1.04	0.73	0.13	0.32	0.02	0.34	1.37	59.49	0.74	4.00	0.46	1022	**SK**
TJ	18.52	38.82	0.02	0.001	0.01	0.00	0.02	0.01	1.42	0.11	0.03	0.01	1.57	**TJ**
TM	8.30	87.44	0.05	0.00	0.03	0.00	0.05	0.02	2.53	0.12	0.06	0.03	4.26	**TM**
TR	0.48	40.43	0.98	0.06	0.49	0.03	4.14	1.54	273.2	9.04	2.00	0.48	155.4	**TR**
UA	1.40	165.2	10.56	0.34	4.79	0.04	44.00	3.39	265.8	5.04	13.66	3.26	2607	**UA**
UZ	48.20	195.4	0.07	0.002	0.04	0.001	0.06	0.02	3.00	0.14	0.09	0.05	5.99	**UZ**
BAS	0.12	7.08	47.68	1.15	36.38	0.01	0.85	0.53	35.57	0.35	75.70	16.81	1871	**BAS**
BLS	1.22	80.73	1.65	0.06	0.81	0.02	12.01	1.32	157.7	2.86	2.27	0.55	233.8	**BLS**
CAS	9.60	437.7	0.24	0.01	0.14	0.001	0.24	0.06	7.09	0.29	0.24	0.11	17.23	**CAS**
MDT	0.37	14.96	1.19	0.52	0.59	0.85	3.99	11.96	978.5	258.9	10.08	1.15	376.6	**MDT**
NOS	0.07	3.02	7.28	2.42	3.75	0.03	0.20	0.21	9.68	0.94	282.4	50.01	809.4	**NOS**
	KY	**KZ**	**LT**	**LU**	**LV**	**MC**	**MD**	**ME**	**MK**	**MT**	**NL**	**NO**	**PL**	

Table A.3*. Matrix of cadmium country-to-country deposition from anthropogenic sources in 2008, kg/y (continued)*

Receptors ↓ Emitters →

	PT	RO	RS	RU	RUA	SE	SI	SK	TJ	TM	TR	UA	UZ	Total	
AL	0.81	11.87	132.7	11.38	0.10	0.04	0.67	15.61	0.00	0.00	10.72	6.40	0.02	**900.1**	**AL**
AM	0.17	0.84	1.26	23.70	0.80	0.01	0.03	0.72	0.02	0.26	55.43	2.35	1.02	**224.8**	**AM**
AT	2.28	15.35	99.44	34.52	0.33	0.35	98.89	366.6	0.00	0.00	6.12	8.44	0.03	**1978**	**AT**
AZ	0.26	1.83	2.80	126.8	3.76	0.04	0.07	1.70	0.31	1.52	77.70	9.26	6.49	**898.3**	**AZ**
BA	1.77	36.89	317.9	19.96	0.22	0.18	5.48	165.5	0.00	0.00	8.52	9.46	0.02	**1666**	**BA**
BE	2.07	0.27	0.69	4.63	0.06	0.08	0.15	4.37	0.00	0.00	0.08	0.44	0.00	**634.4**	**BE**
BG	1.18	193.6	370.5	149.9	1.44	0.35	1.62	85.06	0.09	0.04	126.7	87.60	0.46	**3222**	**BG**
BY	1.73	111.9	99.20	781.0	9.77	5.23	4.77	230.8	0.05	0.10	54.50	353.6	0.73	**5460**	**BY**
CH	2.75	1.23	4.63	2.96	0.04	0.04	2.10	9.77	0.00	0.00	0.39	0.80	0.00	**659.4**	**CH**
CY	0.02	0.35	0.83	1.53	0.03	0.00	0.02	0.30	0.00	0.00	21.09	0.47	0.01	**34.8**	**CY**
CZ	1.26	17.97	74.44	44.21	0.38	0.83	11.56	1295	0.01	0.00	4.90	10.85	0.06	**3992**	**CZ**
DE	8.93	11.40	28.49	109.8	1.20	3.15	7.15	210.7	0.01	0.01	2.07	11.81	0.05	**4912**	**DE**
DK	0.39	1.58	2.36	12.68	0.17	2.19	0.25	16.76	0.01	0.00	0.41	1.70	0.03	**327.7**	**DK**
EE	0.49	5.90	6.30	368.0	1.11	5.07	0.48	23.07	0.00	0.01	1.82	11.24	0.08	**675.6**	**EE**
ES	401.7	4.37	13.77	8.19	0.20	0.17	2.61	20.41	0.01	0.00	2.57	2.62	0.02	**5316**	**ES**
FI	0.72	14.31	14.78	1239	6.92	45.41	1.20	53.43	0.02	0.04	7.78	31.08	0.38	**2064**	**FI**
FR	68.15	9.48	28.96	23.02	0.51	0.58	8.05	60.38	0.00	0.00	2.75	5.78	0.03	**4192**	**FR**
GB	11.47	1.28	2.30	28.15	0.49	1.58	0.61	15.47	0.00	0.00	0.43	1.46	0.02	**1249**	**GB**
GE	0.62	3.89	5.10	130.2	2.24	0.05	0.13	2.93	0.08	0.48	194.3	16.91	2.30	**789.4**	**GE**
GR	1.63	47.91	115.5	79.66	1.11	0.18	1.32	38.07	0.04	0.03	210.2	41.62	0.22	**2231**	**GR**
HR	1.89	28.47	213.7	17.72	0.17	0.14	15.01	161.1	0.00	0.00	8.00	8.53	0.02	**1217**	**HR**
HU	1.72	158.1	498.4	39.97	0.49	0.30	15.93	701.5	0.02	0.01	13.01	28.35	0.11	**2897**	**HU**
IE	5.68	0.17	0.27	3.25	0.08	0.20	0.10	1.59	0.00	0.00	0.07	0.21	0.00	**194.1**	**IE**
IS	0.45	0.20	0.27	2.77	0.16	0.25	0.06	0.94	0.00	0.00	0.16	0.39	0.01	**51.6**	**IS**
IT	15.79	37.49	183.1	44.92	0.57	0.34	50.08	179.3	0.01	0.01	20.78	15.51	0.06	**4368**	**IT**
KY	0.39	1.22	2.21	62.56	13.09	0.04	0.07	1.46	103.6	2.04	34.23	3.97	365.5	**1647**	**KY**
KZ	2.89	42.04	52.81	5245	1165	1.88	1.99	43.28	85.15	14.47	325.4	211.4	532.3	**13511**	**KZ**
LT	0.64	21.06	22.37	261.5	1.51	4.17	1.95	96.95	0.01	0.02	3.88	27.63	0.19	**1943**	**LT**
LU	0.18	0.05	0.14	0.49	0.00	0.01	0.02	0.90	0.00	0.00	0.01	0.07	0.00	**39.9**	**LU**
LV	0.70	15.03	15.44	198.0	1.50	5.84	1.18	58.60	0.01	0.01	3.26	23.71	0.14	**1286**	**LV**
MC	0.001	0.002	0.01	0.00	0.00	0.00	0.003	0.01	0.00	0.00	0.00	0.001	0.00	**0.2**	**MC**
MD	0.22	37.68	17.15	88.93	0.82	0.16	0.30	14.52	0.03	0.02	27.37	91.50	0.17	**461.8**	**MD**
ME	0.47	7.19	112.7	4.74	0.04	0.03	0.50	14.20	0.00	0.00	4.19	2.29	0.01	**371.9**	**ME**
MK	0.40	14.45	109.6	13.98	0.22	0.05	0.42	16.66	0.01	0.00	18.15	7.56	0.04	**3243**	**MK**
MT	0.01	0.01	0.05	0.02	0.00	0.00	0.003	0.02	0.00	0.00	0.05	0.01	0.00	**4.8**	**MT**
NL	1.47	0.41	0.92	10.25	0.09	0.20	0.19	7.61	0.00	0.00	0.10	0.64	0.00	**654.0**	**NL**
NO	1.88	3.52	4.18	507.8	3.16	17.48	0.66	31.89	0.06	0.01	2.60	7.06	0.32	**876.5**	**NO**
PL	3.71	137.7	198.5	369.7	4.25	8.70	19.65	1466	0.10	0.04	15.89	138.4	0.66	**22391**	**PL**
PT	**1268**	0.17	0.41	0.80	0.01	0.03	0.09	0.74	0.00	0.00	0.11	0.12	0.00	**1526**	**PT**
RO	2.42	**1988**	619.6	282.7	3.17	1.10	7.60	386.3	0.23	0.07	128.4	256.3	1.25	**5523**	**RO**
RS	1.19	121.7	**2490**	37.88	0.55	0.27	3.95	201.6	0.02	0.01	19.63	23.32	0.09	**4173**	**RS**
RU	12.04	381.9	384.6	**66149**	1257	50.17	17.16	610.3	7.68	8.44	1154	2183	78.55	**82063**	**RU**
RUA	3.86	60.38	64.33	10083	**19719**	5.68	2.74	78.31	23.95	4.97	247.5	191.8	133.9	**34924**	**RUA**
SE	1.43	15.82	17.47	407.1	4.10	**208.7**	1.69	85.38	0.16	0.04	5.93	26.34	0.87	**1998**	**SE**
SI	0.82	7.58	48.00	6.97	0.08	0.05	**94.25**	67.81	0.00	0.00	1.84	2.80	0.01	**530.2**	**SI**
SK	0.97	83.97	173.8	40.25	0.42	0.49	12.09	**2429**	0.02	0.01	6.40	24.11	0.11	**4452**	**SK**
TJ	0.13	0.37	0.73	18.35	3.06	0.01	0.03	0.46	**115.5**	1.40	14.38	1.18	133.7	**360.1**	**TJ**
TM	0.16	0.97	1.40	648.5	9.58	0.04	0.04	0.94	8.07	**15.79**	26.66	5.10	117.4	**405.9**	**TM**
TR	6.71	88.78	132.9	83.27	6.69	0.53	2.44	59.24	0.18	0.59	**6310**	177.7	3.20	**8285**	**TR**
UA	3.94	509.8	329.6	2611	36.50	4.59	9.63	511.7	0.48	0.86	408.6	**3173**	6.97	**12682**	**UA**
UZ	0.19	1.17	1.75	126.2	18.46	0.05	0.05	1.24	70.80	6.30	28.89	6.72	**572.5**	**1095**	**UZ**
BAS	2.69	36.41	39.34	838.0	4.37	74.56	2.94	176.4	0.08	0.05	8.65	40.62	0.63	**3930**	**BAS**
BLS	1.61	146.2	135.6	1372	10.00	0.76	2.63	73.57	0.52	0.40	907.2	432.3	3.64	**3382**	**BLS**
CAS	0.24	3.47	4.31	561.2	25.33	0.14	0.14	3.32	4.83	7.98	89.16	35.54	48.41	**1558**	**CAS**
MDT	102.6	141.9	511.9	266.1	3.00	0.95	34.92	290.6	0.16	0.13	1455	112.3	0.93	**9931**	**MDT**
NOS	16.78	13.29	16.11	114.9	1.81	12.00	2.55	124.9	0.06	0.02	3.69	14.30	0.35	**3266**	**NOS**
	PT	**RO**	**RS**	**RU**	**RUA**	**SE**	**SI**	**SK**	**TJ**	**TM**	**TR**	**UA**	**UZ**	**Total**	

***Table A.4**. Matrix of mercury country-to-country deposition from anthropogenic sources in 2008, kg/y*

Receptors ↓ Emitters →

	AL	AM	AT	AZ	BA	BE	BG	BY	CH	CY	CZ	DE	
AL	**27.27**	0.01	0.33	0.02	2.68	0.27	2.56	0.08	0.34	0.01	1.00	0.37	**AL**
AM	0.02	**43.78**	0.04	13.79	0.12	0.06	0.15	0.05	0.05	0.12	0.14	0.08	**AM**
AT	0.28	0.01	**170.9**	0.03	9.49	8.08	0.79	0.62	19.59	0.003	66.22	25.50	**AT**
AZ	0.04	9.57	0.11	**151.0**	0.28	0.18	0.34	0.14	0.12	0.23	0.37	0.23	**AZ**
BA	1.75	0.02	4.06	0.04	**322.4**	1.12	1.00	0.22	1.22	0.01	12.47	2.41	**BA**
BE	0.01	0.001	0.43	0.004	0.08	**391.6**	0.03	0.10	2.00	0.00	2.39	20.76	**BE**
BG	1.47	0.10	1.25	0.22	6.41	0.92	**274.2**	0.70	0.69	0.09	4.91	1.51	**BG**
BY	0.36	0.17	3.77	0.51	6.52	4.93	4.02	**166.0**	2.15	0.05	25.89	9.66	**BY**
CH	0.04	0.003	2.21	0.01	0.67	4.95	0.11	0.07	**162.3**	0.000	2.36	5.95	**CH**
CY	0.01	0.02	0.01	0.02	0.04	0.01	0.06	0.01	0.01	**9.91**	0.03	0.02	**CY**
CZ	0.18	0.01	29.98	0.02	4.49	7.81	0.76	0.96	7.40	0.002	**735.1**	37.12	**CZ**
DE	0.12	0.01	33.67	0.05	2.47	193.8	0.35	1.55	98.19	0.003	214.9	**819.8**	**DE**
DK	0.01	0.003	0.46	0.01	0.21	8.88	0.03	0.19	0.67	0.001	4.16	10.51	**DK**
EE	0.02	0.01	0.51	0.02	0.44	2.42	0.18	1.50	0.54	0.002	4.29	3.59	**EE**
ES	0.12	0.01	0.73	0.03	1.33	4.97	0.33	0.11	2.82	0.002	1.97	2.56	**ES**
FI	0.09	0.05	1.28	0.19	1.07	7.07	0.73	2.48	1.28	0.01	8.83	8.59	**FI**
FR	0.24	0.02	4.37	0.06	3.46	128.7	0.56	0.49	65.73	0.004	14.40	50.84	**FR**
GB	0.02	0.01	0.99	0.02	0.30	36.58	0.07	0.22	2.60	0.001	6.33	17.54	**GB**
GE	0.06	11.53	0.15	26.83	0.41	0.20	0.69	0.21	0.14	0.28	0.49	0.28	**GE**
GR	3.22	0.09	0.74	0.18	3.74	0.72	42.26	0.36	0.70	0.27	2.50	0.98	**GR**
HR	0.91	0.01	6.71	0.03	38.75	1.17	0.78	0.21	1.32	0.01	11.42	2.38	**HR**
HU	0.63	0.02	14.48	0.05	26.82	2.39	3.04	0.64	2.10	0.01	29.64	5.25	**HU**
IE	0.002	0.001	0.13	0.004	0.04	3.07	0.01	0.02	0.40	0.00	0.72	1.60	**IE**
IS	0.004	0.003	0.09	0.01	0.06	0.99	0.03	0.04	0.18	0.001	0.50	0.80	**IS**
IT	2.61	0.04	14.91	0.10	24.78	4.95	2.60	0.49	24.81	0.01	16.88	8.16	**IT**
KY	0.05	0.92	0.16	2.47	0.38	0.26	0.32	0.13	0.19	0.14	0.50	0.33	**KY**
KZ	0.48	7.81	2.43	32.04	4.95	3.98	5.04	4.26	2.48	0.67	8.71	5.46	**KZ**
LT	0.06	0.02	1.69	0.06	1.55	3.26	0.37	11.39	1.30	0.004	13.97	6.67	**LT**
LU	0.001	0.00	0.06	0.00	0.01	5.49	0.00	0.01	0.32	0.00	0.30	2.05	**LU**
LV	0.05	0.01	1.11	0.03	1.13	3.47	0.32	4.80	1.07	0.003	9.44	6.16	**LV**
MC	0.00	0.00	0.00	0.00	0.001	0.00	0.00	0.00	0.002	0.00	0.001	0.00	**MC**
MD	0.10	0.06	0.26	0.15	0.85	0.29	2.32	0.65	0.17	0.01	1.39	0.53	**MD**
ME	3.25	0.01	0.31	0.01	8.45	0.19	0.60	0.04	0.23	0.01	0.99	0.30	**ME**
MK	4.07	0.01	0.28	0.02	1.79	0.21	6.99	0.08	0.21	0.04	1.05	0.33	**MK**
MT	0.001	0.00	0.001	0.00	0.004	0.001	0.002	0.00	0.001	0.00	0.002	0.001	**MT**
NL	0.01	0.001	0.43	0.01	0.07	100.7	0.01	0.09	1.27	0.00	3.87	36.21	**NL**
NO	0.02	0.03	1.04	0.09	0.42	8.77	0.13	1.02	1.37	0.01	7.80	9.70	**NO**
PL	0.58	0.06	19.39	0.19	12.88	21.35	2.61	21.51	9.94	0.01	309.0	98.42	**PL**
PT	0.004	0.001	0.04	0.00	0.05	0.32	0.02	0.01	0.13	0.00	0.14	0.21	**PT**
RO	1.52	0.16	6.49	0.42	26.16	3.37	29.82	2.65	2.61	0.11	24.82	6.45	**RO**
RS	3.28	0.03	3.26	0.06	43.47	1.15	8.56	0.33	1.07	0.04	12.31	2.57	**RS**
RU	2.30	15.20	15.74	75.55	26.86	30.35	28.60	111.9	13.26	1.44	80.96	45.82	**RU**
RUA	0.78	5.18	4.90	16.63	8.87	11.11	7.10	7.43	5.04	0.50	19.46	14.21	**RUA**
SE	0.10	0.06	2.39	0.16	1.50	19.75	0.42	2.41	2.47	0.01	17.40	24.45	**SE**
SI	0.18	0.004	10.68	0.01	6.80	0.72	0.24	0.10	0.90	0.001	5.22	1.43	**SI**
SK	0.29	0.01	10.35	0.04	9.69	2.03	1.49	0.76	1.97	0.004	62.86	5.73	**SK**
TJ	0.02	0.38	0.06	1.03	0.13	0.09	0.12	0.04	0.07	0.06	0.17	0.11	**TJ**
TM	0.03	1.24	0.12	8.27	0.26	0.23	0.27	0.18	0.13	0.11	0.42	0.30	**TM**
TR	1.31	20.16	1.97	7.97	6.13	2.09	26.45	1.68	1.67	7.48	5.84	2.87	**TR**
UA	1.39	1.98	7.21	6.11	19.68	7.16	22.60	28.87	4.17	0.41	43.49	14.64	**UA**
UZ	0.03	0.90	0.14	3.81	0.29	0.27	0.29	0.22	0.16	0.10	0.51	0.36	**UZ**
BAS	0.21	0.06	4.15	0.17	2.69	29.81	1.01	4.82	4.46	0.01	39.35	55.28	**BAS**
BLS	0.67	2.68	1.72	4.16	5.33	1.47	27.31	2.72	1.12	0.42	6.16	2.51	**BLS**
CAS	0.06	4.40	0.21	91.21	0.45	0.36	0.60	0.46	0.22	0.19	0.76	0.49	**CAS**
MDT	15.73	0.77	11.55	1.10	50.11	7.17	38.61	1.35	13.14	21.75	22.29	9.10	**MDT**
NOS	0.11	0.04	4.69	0.13	1.61	136.5	0.38	1.20	9.60	0.01	34.80	81.50	**NOS**
	AL	**AM**	**AT**	**AZ**	**BA**	**BE**	**BG**	**BY**	**CH**	**CY**	**CZ**	**DE**	

Table A.4*. Matrix of mercury country-to-country deposition from anthropogenic sources in 2008, kg/y (continued)*

Receptors ↓ Emitters →

	DK	EE	ES	FI	FR	GB	GE	GR	HR	HU	IE	IS	
AL	0.04	0.02	1.15	0.02	1.15	0.42	0.01	55.07	0.65	1.87	0.05	0.002	**AL**
AM	0.02	0.01	0.21	0.01	0.10	0.10	3.83	1.44	0.03	0.16	0.01	0.001	**AM**
AT	0.95	0.10	4.95	0.06	12.12	7.13	0.01	4.55	7.92	27.95	0.52	0.01	**AT**
AZ	0.06	0.04	0.45	0.04	0.25	0.30	7.90	3.02	0.08	0.37	0.03	0.004	**AZ**
BA	0.31	0.03	3.09	0.03	3.19	1.55	0.01	11.21	21.12	29.20	0.15	0.004	**BA**
BE	0.30	0.04	3.41	0.02	46.56	26.20	0.00	0.24	0.04	0.28	1.27	0.003	**BE**
BG	0.25	0.14	1.72	0.09	1.58	1.26	0.13	83.82	1.39	11.80	0.13	0.01	**BG**
BY	5.79	3.72	2.66	0.97	4.44	8.39	0.19	14.65	2.22	17.83	0.72	0.02	**BY**
CH	0.13	0.02	6.14	0.02	23.76	6.03	0.00	1.38	0.67	1.11	0.49	0.004	**CH**
CY	0.002	0.002	0.04	0.001	0.03	0.02	0.01	2.00	0.01	0.04	0.002	0.00	**CY**
CZ	2.21	0.19	2.55	0.09	8.01	7.80	0.01	2.88	2.81	32.76	0.59	0.01	**CZ**
DE	19.75	0.95	17.94	0.36	138.7	114.0	0.01	3.35	1.46	10.30	7.64	0.03	**DE**
DK	**75.08**	0.22	0.93	0.10	4.91	18.68	0.00	0.13	0.06	0.66	1.35	0.005	**DK**
EE	2.56	**34.83**	0.84	1.62	1.86	3.39	0.01	0.49	0.17	1.12	0.26	0.01	**EE**
ES	0.32	0.06	**1071**	0.07	26.16	11.88	0.01	3.33	0.70	1.54	1.99	0.02	**ES**
FI	6.80	21.02	1.89	**102.3**	4.73	11.82	0.05	2.72	0.38	2.50	1.04	0.04	**FI**
FR	1.51	0.17	204.1	0.17	**985.8**	115.5	0.02	6.92	2.45	5.33	10.79	0.05	**FR**
GB	3.78	0.35	10.54	0.19	32.75	**1113**	0.01	0.65	0.17	0.97	42.07	0.03	**GB**
GE	0.07	0.05	0.64	0.04	0.31	0.35	**49.59**	5.78	0.12	0.58	0.04	0.004	**GE**
GR	0.14	0.07	2.24	0.06	1.89	1.22	0.10	**1861**	0.99	4.56	0.13	0.01	**GR**
HR	0.23	0.04	3.00	0.03	3.45	1.44	0.01	8.75	**78.09**	40.29	0.14	0.004	**HR**
HU	0.56	0.11	2.44	0.07	3.54	2.80	0.02	10.89	20.48	**575.3**	0.25	0.01	**HU**
IE	0.38	0.04	2.68	0.03	3.93	24.59	0.00	0.06	0.03	0.11	**90.22**	0.01	**IE**
IS	0.44	0.04	0.53	0.06	0.83	3.71	0.00	0.13	0.03	0.13	0.66	**0.06**	**IS**
IT	0.54	0.10	24.14	0.10	33.63	6.55	0.04	43.29	19.23	22.20	0.65	0.02	**IT**
KY	0.07	0.06	0.86	0.06	0.42	0.41	0.53	2.92	0.11	0.47	0.04	0.01	**KY**
KZ	1.80	2.01	7.29	1.34	5.16	6.88	6.46	31.54	1.61	7.88	0.69	0.09	**KZ**
LT	4.86	1.31	1.31	0.41	2.82	5.73	0.01	1.02	0.62	4.52	0.47	0.01	**LT**
LU	0.02	0.00	0.35	0.00	4.85	1.15	0.00	0.03	0.01	0.04	0.07	0.00	**LU**
LV	4.63	4.06	1.41	0.76	2.91	5.47	0.01	0.81	0.41	2.82	0.43	0.01	**LV**
MC	0.00	0.00	0.002	0.00	0.01	0.00	0.00	0.001	0.001	0.001	0.00	0.00	**MC**
MD	0.16	0.09	0.34	0.05	0.35	0.47	0.08	6.28	0.19	1.79	0.05	0.002	**MD**
ME	0.04	0.01	0.84	0.01	0.78	0.28	0.01	8.30	0.77	2.10	0.03	0.001	**ME**
MK	0.05	0.02	0.62	0.01	0.53	0.30	0.01	84.55	0.42	2.27	0.03	0.002	**MK**
MT	0.00	0.00	0.008	0.00	0.006	0.002	0.00	0.06	0.001	0.003	0.00	0.00	**MT**
NL	0.80	0.08	2.44	0.03	18.87	34.73	0.00	0.16	0.04	0.25	1.83	0.003	**NL**
NO	14.47	1.15	2.70	2.09	6.23	39.37	0.03	0.74	0.17	1.42	3.52	0.05	**NO**
PL	21.54	1.71	7.30	0.76	17.89	32.93	0.06	9.67	6.26	64.55	2.65	0.03	**PL**
PT	0.06	0.01	32.85	0.01	1.04	0.99	0.00	0.11	0.03	0.08	0.23	0.004	**PT**
RO	1.20	0.44	4.14	0.27	4.64	4.65	0.19	50.77	6.91	79.81	0.44	0.02	**RO**
RS	0.36	0.06	2.16	0.05	2.31	1.60	0.03	27.49	8.15	47.61	0.15	0.005	**RS**
RU	23.91	154.3	25.81	33.47	29.63	52.14	24.79	131.5	8.52	54.61	4.61	0.34	**RU**
RUA	4.95	5.99	14.69	6.08	11.61	20.14	4.52	35.46	2.88	14.96	2.07	0.38	**RUA**
SE	65.35	3.75	3.31	25.09	12.34	38.77	0.05	2.15	0.52	4.55	3.09	0.05	**SE**
SI	0.09	0.02	1.25	0.01	1.85	0.76	0.00	1.87	15.80	9.73	0.07	0.002	**SI**
SK	0.79	0.11	1.50	0.07	2.68	2.57	0.01	4.57	6.08	146.5	0.22	0.005	**SK**
TJ	0.02	0.02	0.31	0.02	0.15	0.14	0.21	1.24	0.04	0.16	0.02	0.002	**TJ**
TM	0.08	0.08	0.49	0.07	0.29	0.38	1.00	2.17	0.08	0.38	0.04	0.01	**TM**
TR	0.55	0.40	6.61	0.28	3.81	3.55	5.37	237.4	1.60	8.15	0.37	0.03	**TR**
UA	5.43	2.73	6.73	1.11	8.10	11.61	2.59	78.34	5.86	60.21	1.04	0.05	**UA**
UZ	0.10	0.11	0.58	0.08	0.35	0.46	0.66	2.23	0.09	0.44	0.05	0.01	**UZ**
BAS	100.6	32.97	5.50	26.31	18.78	48.27	0.05	3.93	0.88	7.86	3.67	0.03	**BAS**
BLS	0.70	0.51	2.30	0.27	2.08	2.54	7.49	75.80	1.30	8.00	0.25	0.02	**BLS**
CAS	0.16	0.17	0.66	0.12	0.46	0.66	3.96	4.15	0.13	0.65	0.07	0.01	**CAS**
MDT	1.15	0.31	213.7	0.29	95.84	14.88	0.56	1402	29.00	31.19	1.87	0.05	**MDT**
NOS	51.70	1.36	24.92	0.87	114.6	620.2	0.04	2.52	0.66	5.58	31.59	0.08	**NOS**
	DK	**EE**	**ES**	**FI**	**FR**	**GB**	**GE**	**GR**	**HR**	**HU**	**IE**	**IS**	

***Table A.4**. Matrix of mercury country-to-country deposition from anthropogenic sources in 2008, kg/y (continued)*

Receptors ↓ Emitters →

	IT	KY	KZ	LT	LU	LV	MC	MD	ME	MK	MT	NL	NO	
AL	16.72	0.003	0.22	0.01	0.03	0.004	0.04	0.13	1.16	34.78	0.95	0.08	0.02	**AL**
AM	0.45	0.02	4.88	0.01	0.01	0.002	0.00	0.03	0.01	0.19	0.03	0.02	0.01	**AM**
AT	81.27	0.01	0.72	0.16	1.54	0.03	0.25	0.08	0.49	1.63	0.24	2.80	0.14	**AT**
AZ	1.07	0.20	31.45	0.03	0.02	0.01	0.01	0.08	0.03	0.41	0.07	0.05	0.03	**AZ**
BA	35.42	0.005	0.36	0.05	0.15	0.01	0.12	0.10	6.99	3.87	0.73	0.41	0.06	**BA**
BE	1.40	0.001	0.10	0.05	11.23	0.01	0.01	0.01	0.01	0.05	0.03	46.34	0.06	**BE**
BG	10.68	0.03	3.21	0.12	0.10	0.03	0.05	2.47	0.90	29.45	0.48	0.32	0.09	**BG**
BY	12.02	0.03	12.92	7.90	0.52	1.65	0.05	3.29	0.53	3.35	0.34	2.34	0.94	**BY**
CH	87.04	0.001	0.13	0.02	1.09	0.004	0.35	0.01	0.04	0.20	0.11	1.09	0.04	**CH**
CY	0.15	0.001	0.06	0.001	0.001	0.00	0.001	0.01	0.005	0.10	0.01	0.003	0.001	**CY**
CZ	15.66	0.01	0.55	0.34	1.24	0.07	0.07	0.09	0.31	1.48	0.11	3.61	0.24	**CZ**
DE	34.69	0.01	1.48	1.39	37.55	0.29	0.22	0.09	0.15	0.69	0.19	116.8	1.28	**DE**
DK	0.76	0.003	0.29	0.23	0.38	0.05	0.00	0.01	0.01	0.05	0.01	6.14	0.63	**DK**
EE	1.31	0.01	0.82	3.56	0.21	2.01	0.01	0.10	0.04	0.20	0.02	1.13	0.61	**EE**
ES	19.77	0.01	0.49	0.05	0.47	0.01	0.16	0.05	0.10	0.58	0.57	1.21	0.12	**ES**
FI	3.68	0.04	6.28	2.98	0.49	1.05	0.02	0.31	0.11	0.90	0.08	3.16	4.11	**FI**
FR	115.5	0.01	1.06	0.22	33.49	0.05	7.54	0.10	0.23	1.18	1.18	17.12	0.40	**FR**
GB	4.29	0.01	0.62	0.31	1.73	0.07	0.03	0.02	0.02	0.15	0.10	15.27	0.77	**GB**
GE	1.46	0.06	10.54	0.04	0.02	0.01	0.01	0.20	0.04	0.69	0.12	0.06	0.03	**GE**
GR	17.21	0.02	1.89	0.06	0.08	0.02	0.05	0.90	0.55	61.97	1.68	0.23	0.05	**GR**
HR	52.49	0.004	0.40	0.04	0.15	0.01	0.15	0.07	1.08	2.18	0.64	0.41	0.05	**HR**
HU	28.39	0.01	0.89	0.12	0.35	0.03	0.09	0.27	1.61	5.61	0.38	0.93	0.10	**HU**
IE	0.74	0.001	0.10	0.03	0.22	0.01	0.01	0.01	0.003	0.02	0.00	1.06	0.09	**IE**
IS	0.59	0.01	0.21	0.03	0.07	0.01	0.00	0.01	0.005	0.03	0.01	0.39	0.21	**IS**
IT	**1760**	0.01	1.36	0.13	0.82	0.03	4.20	0.22	1.71	8.42	9.02	1.43	0.15	**IT**
KY	1.58	**180.4**	163.1	0.03	0.03	0.01	0.01	0.06	0.04	0.43	0.10	0.07	0.05	**KY**
KZ	18.87	133.5	**5947**	0.95	0.38	0.27	0.11	1.63	0.45	5.15	0.65	1.29	1.04	**KZ**
LT	3.57	0.01	1.75	**29.04**	0.33	1.84	0.02	0.24	0.11	0.47	0.05	1.67	0.57	**LT**
LU	0.20	0.00	0.01	0.00	**18.77**	0.001	0.002	0.00	0.001	0.01	0.003	0.78	0.004	**LU**
LV	2.71	0.01	1.39	32.86	0.34	**11.78**	0.01	0.21	0.08	0.39	0.04	1.71	0.71	**LV**
MC	0.06	0.00	0.00	0.00	0.00	0.00	**0.03**	0.00	0.00	0.00	0.00	0.00	0.00	**MC**
MD	1.56	0.01	1.76	0.09	0.03	0.02	0.01	**41.57**	0.09	1.13	0.08	0.12	0.04	**MD**
ME	10.54	0.002	0.09	0.01	0.02	0.002	0.03	0.04	**16.42**	4.59	0.44	0.06	0.01	**ME**
MK	5.16	0.004	0.37	0.02	0.03	0.004	0.02	0.16	0.38	**266.5**	0.31	0.07	0.02	**MK**
MT	0.09	0.00	0.00	0.00	0.00	0.00	0.00	0.00	0.00	0.005	**3.13**	0.00	0.00	**MT**
NL	1.02	0.001	0.13	0.10	1.26	0.02	0.01	0.004	0.01	0.03	0.02	**111.9**	0.11	**NL**
NO	2.61	0.04	2.51	0.75	0.63	0.17	0.02	0.07	0.03	0.19	0.03	4.31	**80.17**	**NO**
PL	30.75	0.04	4.76	4.92	2.42	0.78	0.14	0.70	0.94	4.63	0.39	12.21	1.67	**PL**
PT	0.69	0.001	0.05	0.01	0.03	0.002	0.01	0.003	0.004	0.03	0.02	0.09	0.02	**PT**
RO	31.38	0.07	6.71	0.44	0.42	0.10	0.11	11.58	2.52	17.35	0.77	1.35	0.30	**RO**
RS	20.62	0.01	0.76	0.07	0.16	0.02	0.07	0.45	12.61	43.37	0.49	0.44	0.08	**RS**
RU	75.73	4.30	1629	19.03	2.76	6.97	0.37	13.08	2.42	23.80	2.48	12.49	10.03	**RU**
RUA	33.52	23.48	2201	2.11	0.93	0.61	0.19	2.42	0.81	7.45	1.04	3.27	3.71	**RUA**
SE	4.66	0.07	5.41	2.91	1.18	0.69	0.02	0.25	0.13	0.79	0.08	10.53	22.59	**SE**
SI	47.25	0.002	0.22	0.02	0.10	0.004	0.08	0.02	0.25	0.51	0.20	0.24	0.02	**SI**
SK	14.96	0.01	0.73	0.15	0.30	0.03	0.05	0.19	0.64	2.49	0.17	0.89	0.13	**SK**
TJ	0.58	4.81	19.67	0.01	0.01	0.003	0.00	0.02	0.01	0.16	0.04	0.02	0.02	**TJ**
TM	1.03	3.49	91.69	0.04	0.02	0.01	0.01	0.08	0.03	0.33	0.05	0.07	0.05	**TM**
TR	19.93	0.18	20.71	0.29	0.23	0.07	0.10	2.75	0.76	15.97	1.86	0.67	0.25	**TR**
UA	34.25	0.28	93.14	2.77	0.80	0.62	0.15	37.01	1.69	14.41	1.20	3.23	1.06	**UA**
UZ	1.19	23.91	189.5	0.05	0.03	0.01	0.01	0.09	0.03	0.35	0.06	0.08	0.06	**UZ**
BAS	7.63	0.06	5.86	13.48	2.26	4.76	0.04	0.42	0.26	1.91	0.12	17.35	5.71	**BAS**
BLS	11.59	0.26	38.48	0.42	0.16	0.10	0.06	9.48	0.58	8.91	0.60	0.59	0.21	**BLS**
CAS	1.78	2.23	422.9	0.09	0.03	0.03	0.01	0.20	0.05	0.62	0.10	0.12	0.09	**CAS**
MDT	744.6	0.12	6.98	0.30	0.99	0.07	2.88	2.09	5.07	49.57	96.06	2.14	0.39	**MDT**
NOS	13.32	0.05	3.08	1.37	5.44	0.30	0.09	0.13	0.11	0.66	0.27	94.59	16.40	**NOS**
	IT	**KY**	**KZ**	**LT**	**LU**	**LV**	**MC**	**MD**	**ME**	**MK**	**MT**	**NL**	**NO**	

Table A.4*. Matrix of mercury country-to-country deposition from anthropogenic sources in 2008, kg/y (continued)*

Receptors ↓ Emitters →

	PL	PT	RO	RS	RU	RUA	SE	SI	SK	TJ	TM	TR	UA	UZ	Total	
AL	2.64	0.11	8.91	32.31	0.76	0.06	0.01	0.41	1.82	0.001	0.001	4.23	1.24	0.01	**202.19**	**AL**
AM	0.60	0.04	1.06	0.35	2.24	0.25	0.01	0.04	0.21	0.004	0.08	28.55	0.88	0.21	**104.65**	**AM**
AT	58.08	0.44	11.51	22.03	3.18	0.25	0.09	76.73	45.73	0.001	0.002	2.27	2.23	0.02	**679.82**	**AT**
AZ	1.67	0.07	2.43	0.80	11.86	1.02	0.03	0.10	0.50	0.04	0.57	32.59	3.26	1.37	**266.00**	**AZ**
BA	22.64	0.24	22.70	73.14	1.62	0.14	0.05	3.67	18.76	0.001	0.001	2.98	2.08	0.01	**613.10**	**BA**
BE	4.73	0.30	0.33	0.21	0.48	0.05	0.03	0.10	0.52	0.00	0.00	0.07	0.16	0.002	**561.95**	**BE**
BG	20.92	0.19	245.8	65.54	9.77	0.45	0.09	1.08	14.13	0.01	0.01	64.83	20.77	0.10	**890.04**	**BG**
BY	279.1	0.34	83.26	18.91	78.66	2.29	1.16	2.89	36.74	0.01	0.03	19.82	90.40	0.18	**965.60**	**BY**
CH	3.91	0.50	1.27	1.10	0.46	0.07	0.02	1.57	1.34	0.00	0.00	0.29	0.35	0.004	**319.52**	**CH**
CY	0.11	0.004	0.27	0.11	0.15	0.01	0.001	0.01	0.04	0.00	0.001	12.95	0.13	0.005	**26.44**	**CY**
CZ	251.7	0.25	12.68	14.26	3.68	0.23	0.18	6.37	63.55	0.002	0.002	1.54	2.41	0.02	**1264.4**	**CZ**
DE	173.5	1.51	7.22	5.52	9.35	0.73	0.78	4.35	16.17	0.003	0.004	1.08	2.80	0.04	**2095.7**	**DE**
DK	15.92	0.08	1.05	0.42	1.30	0.10	0.76	0.15	1.48	0.001	0.001	0.18	0.46	0.01	**157.48**	**DK**
EE	27.23	0.10	3.88	1.14	46.47	0.31	1.14	0.27	2.19	0.001	0.002	0.61	2.54	0.02	**124.39**	**EE**
ES	4.91	66.90	2.78	2.07	1.05	0.33	0.07	1.10	1.74	0.002	0.002	0.97	0.78	0.02	**1238.6**	**ES**
FI	44.78	0.24	10.12	2.91	88.44	2.80	10.95	0.71	4.68	0.01	0.02	3.25	7.77	0.16	**349.49**	**FI**
FR	27.31	9.25	7.14	5.68	2.89	0.69	0.21	4.96	6.71	0.004	0.004	1.79	1.96	0.04	**1848.5**	**FR**
GB	14.22	1.72	1.17	0.65	2.52	0.42	0.33	0.41	1.53	0.002	0.002	0.37	0.59	0.02	**1316.2**	**GB**
GE	2.42	0.11	4.98	1.32	15.11	0.63	0.03	0.15	0.78	0.01	0.13	84.58	5.33	0.43	**226.28**	**GE**
GR	9.57	0.23	41.73	19.55	5.10	0.35	0.05	0.83	5.22	0.01	0.01	106.1	8.44	0.06	**2211.7**	**GR**
HR	19.28	0.24	17.82	54.22	1.47	0.13	0.04	11.65	20.80	0.001	0.001	2.59	1.85	0.01	**387.10**	**HR**
HU	68.46	0.25	116.2	113.2	3.49	0.27	0.09	10.53	358.4	0.003	0.003	4.11	6.70	0.03	**1422.4**	**HU**
IE	1.29	0.67	0.22	0.09	0.34	0.08	0.04	0.07	0.19	0.00	0.00	0.07	0.11	0.004	**133.50**	**IE**
IS	1.57	0.09	0.37	0.14	0.49	0.25	0.08	0.06	0.19	0.002	0.001	0.18	0.24	0.02	**14.53**	**IS**
IT	27.35	1.97	23.29	31.17	4.26	0.55	0.12	53.28	20.78	0.004	0.01	7.31	3.72	0.04	**2212.9**	**IT**
KY	1.91	0.13	2.21	0.97	6.61	3.04	0.04	0.15	0.59	11.06	0.78	16.44	1.97	121.6	**525.70**	**KY**
KZ	40.23	1.10	47.27	14.07	480.1	397.6	0.97	2.22	10.82	9.06	5.65	134.3	70.08	177.2	**7668.4**	**KZ**
LT	128.9	0.13	12.44	3.82	38.36	0.44	0.86	1.01	9.55	0.003	0.01	1.35	6.05	0.05	**289.99**	**LT**
LU	0.56	0.03	0.05	0.03	0.05	0.005	0.002	0.01	0.08	0.00	0.00	0.01	0.02	0.00	**35.38**	**LU**
LV	69.16	0.15	9.41	2.79	21.89	0.45	1.25	0.63	5.78	0.002	0.004	0.99	5.28	0.04	**216.02**	**LV**
MC	0.001	0.00	0.001	0.001	0.00	0.00	0.00	0.002	0.001	0.00	0.00	0.00	0.00	0.00	**0.12**	**MC**
MD	11.49	0.04	64.72	3.09	6.36	0.24	0.04	0.21	3.23	0.003	0.005	11.86	28.25	0.04	**195.14**	**MD**
ME	2.20	0.07	5.28	26.68	0.37	0.03	0.01	0.33	1.65	0.001	0.00	1.70	0.50	0.004	**98.67**	**ME**
MK	3.14	0.06	11.80	25.71	0.92	0.08	0.01	0.29	2.15	0.001	0.001	7.14	1.48	0.01	**429.95**	**MK**
MT	0.004	0.001	0.01	0.01	0.00	0.00	0.00	0.001	0.002	0.00	0.00	0.01	0.001	0.00	**3.36**	**MT**
NL	5.65	0.23	0.25	0.17	0.77	0.07	0.05	0.10	0.44	0.00	0.00	0.07	0.14	0.003	**324.37**	**NL**
NO	33.58	0.39	2.84	0.92	13.92	1.78	4.48	0.45	2.80	0.01	0.01	1.52	2.25	0.15	**254.93**	**NO**
PL	**4098**	0.73	79.73	35.59	34.13	1.52	1.88	10.67	170.4	0.01	0.02	5.54	34.82	0.20	**5203.4**	**PL**
PT	0.37	**337.3**	0.16	0.09	0.13	0.05	0.01	0.04	0.10	0.00	0.00	0.06	0.06	0.003	**375.63**	**PT**
RO	109.3	0.43	**2752**	135.4	20.86	1.11	0.29	5.50	96.26	0.02	0.02	54.54	66.26	0.26	**3580.3**	**RO**
RS	29.94	0.19	106.8	**858.8**	2.64	0.22	0.07	2.75	27.17	0.003	0.002	6.88	4.77	0.03	**1285.9**	**RS**
RU	482.1	3.45	308.7	76.05	7930	387.1	12.85	12.24	92.03	0.85	2.66	443.9	642.6	17.67	**13205.5**	**RU**
RUA	85.57	2.33	75.55	23.42	872.2	**7195**	3.54	4.03	22.34	2.76	1.80	114.8	72.41	36.80	**10857.1**	**RUA**
SE	85.59	0.38	11.14	3.58	29.64	2.09	**68.65**	1.01	8.20	0.03	0.02	2.74	6.81	0.30	**493.52**	**SE**
SI	7.65	0.12	4.97	9.15	0.66	0.06	0.02	**101.9**	8.75	0.001	0.001	0.70	0.62	0.01	**241.27**	**SI**
SK	179.9	0.15	56.42	32.87	3.32	0.22	0.11	7.21	**594.3**	0.002	0.002	1.95	5.67	0.03	**1163.6**	**SK**
TJ	0.63	0.04	0.76	0.34	2.07	0.83	0.01	0.05	0.20	**15.38**	0.56	6.87	0.62	43.57	**102.01**	**TJ**
TM	1.88	0.07	2.23	0.74	59.80	4.53	0.05	0.11	0.52	1.31	**25.45**	14.25	3.33	75.60	**257.79**	**TM**
TR	25.29	0.96	85.68	23.08	12.92	2.28	0.23	1.84	9.98	0.04	0.19	**4328**	49.22	0.87	**5001.9**	**TR**
UA	431.4	0.80	423.2	63.80	248.3	8.31	1.13	6.31	132.1	0.06	0.25	168.1	**1651**	1.45	**3796.9**	**UA**
UZ	2.31	0.09	2.45	0.82	17.56	7.35	0.06	0.13	0.61	13.35	5.45	13.17	3.84	**420.1**	**715.82**	**UZ**
BAS	252.2	0.60	24.37	7.10	103.8	1.81	25.31	1.71	17.80	0.02	0.02	3.36	10.43	0.27	**841.90**	**BAS**
BLS	33.26	0.30	167.0	20.83	153.5	2.69	0.22	1.51	11.63	0.06	0.09	536.8	146.8	0.79	**1287.3**	**BLS**
CAS	3.76	0.11	4.59	1.28	58.86	8.39	0.08	0.19	0.93	0.50	4.73	32.79	12.78	11.39	**684.62**	**CAS**
MDT	48.08	10.07	99.37	75.03	19.19	1.71	0.30	21.38	31.00	0.04	0.04	824.7	24.54	0.36	**4054.1**	**MDT**
NOS	90.62	2.95	8.66	3.27	10.65	1.51	3.27	1.62	10.56	0.01	0.01	1.91	4.01	0.16	**1398.4**	**NOS**
	PL	**PT**	**RO**	**RS**	**RU**	**RUA**	**SE**	**SI**	**SK**	**TJ**	**TM**	**TR**	**UA**	**UZ**	**Total**	

Annex B

MODELLING RECONSTRUCTION OF MERCURY POLLUTION OVER ITALY

G. Pirovano, G.M. Riva, A. Toppetti (ENEA - Ricerca sul Sistema Elettrico S.p.A., Italy)
A. Leuci, A. Balzarini (University of Milano Bicocca, Italy)

B.1. Introduction

Mercury pollution represents a critical issue for health and environmental vulnerability, mostly relying on its chemical and physical properties. Mercury is an extremely toxic compound, undergoing to a complex chain of chemical and physical processes. Mercury, in elemental form, is a low solubility compound that can be subject to long range transport; it is produced by anthropogenic sources as well as by natural processes (mobilization). An accurate and thorough reconstruction of mercury fate in atmosphere requires adequate modelling tools able to simulate the whole sequence of phenomena: anthropogenic and natural emissions, dispersion, chemical transformation and deposition. EMEP MSC-E has been applying a state of art modelling chain from several years, providing a modelling reconstruction of mercury concentration over Europe. In our study we carried out a modelling application focused on Italy, that represents one of the first attempts to reconstruct mercury fate specifically over the Italian area. We performed our study by means of the CAMx chemical transport model [*ENVIRON*, 2008], a state of art model, implementing the so called *one atmosphere* approach. Indeed, CAMx allows to reproduce within the same modelling framework the fate of both mercury and all the main species involved in its transformation pathways in gas and aerosol phase. A specific module aimed at estimating the contribution of Hg natural sources have been implemented too. The modelling system has been evaluated against an observed data set of conventional pollutants and also compared to an analogous EMEP simulation, carried out at European scale.

B.2. Modelling configuration

Modelling simulations have been performed by means of CAMx chemical transport model [version 4.51, *ENVIRON*, 2008]. The model implements Bott algorithm [*Bott*, 1989] to solve horizontal advection, while vertical advection and diffusion are integrated by a fully implicit scheme. Model can be fed by both diffuse (at first level) and point emissions. Dry deposition is simulated by means of a resistance scheme, while wet deposition is expressed by a scavenging coefficient computed within and below clouds. Both deposition terms are specifically defined for gas and particles.

Chemical transformations of gas phase species are described by CB-05 mechanism [*Yarwood et al.*], including main atmospheric compounds, such as: NO_X, SO_X, NH_3, HNO_3, VOC , O_3 and other radicals and secondary species. ISORROPIA algorithm [*Nenes et al.*, 1998] is implemented to reproduce thermodynamical equilibrium of inorganic aerosol, whereas SOAP module [*Strader et al*., 1998] is used as a partition scheme for organic aerosol. Aerosol size distribution has been simulated by a static coarse/fine size bins approach. CAMx mercury scheme considers three different species: elemental gaseous mercury Hg(0); reactive gaseous mercury Hg (II); particulate mercury Hg(p). CAMx implements a set of equations describing main transformation pathways taking place in both gas and aqueous phase [*ENVIRON*, 2008]. Gas phase reactions concern the oxidation of Hg(0) to Hg(II) by main oxidants such as ozone, Chlorine, and radicals. Heterogeneous chemistry takes into account dissolution and dissociation processes of both elemental and reactive mercury as well as aqueous phase oxidation and reduction kinetics. Hg chemistry is fully coupled with CAMx gas and aerosol

chemistry, giving rise to a *one atmosphere* modelling approach. CAMx implementation is based on the assumption that the mercury species concentrations are much smaller than those of the species with which they react. Thus, the concentrations of the non-mercury species can be assumed to be constant during the mercury chemistry calculations and analytical solutions are available for both the gas-phase and aqueous-phase conversions. Deposition characteristics have been set up according to several parameters, such as Henry law constant, molecular diffusivity and surface reactivity. Differently from the official CAMx release, Hg(0) dry deposition velocity has been considered not zero and set up according to literature [*Wen*, 2006].

B.3. Simulations outline

The CAMx model has been applied over a computational domain in Lambert conformal projection extending over 86x98 cells and covering the whole of Italy. Horizontal resolution was 15 km. Vertical domain has been subdivided into 13 layers of growing thickness, starting from 30 m agl. Simulations have performed over the whole year 2005; CAMX provides hourly output fields of air concentration, wet and dry deposition fluxes of gas and aerosol species.

Meteorological fields have been produced by WRF [*Skamarock et al*., 2008]. WRF has been run over 2 nested domain covering Europe (45 km) and Italy (15 km). CAMx and WRF share the same modelling domain, thus preventing additional interpolation of meteorological fields. CAMx vertical levels have been defined by aggregating subsets of WRF levels (above PBL), whereas inside the PBL the same vertical structure has been adopted. Vertical diffusion coefficients have been derived by a diagnostic approach based on O'Brien (1970). Water Content were derived from rainfall rate and prognostic 3D field.

Boundary conditions have been derived from 2 large scale simulations: an EMEP model [*Travnikov and Ilyin*, 2005] run at 50 km resolution providing Hg species and a CHIMERE model [*Vautard et al.*, 2005] simulation at 5 degrees resolution for all the other long lived species. Horizontal and vertical interpolation of the large scale fields onto CAMx grid have been performed together with an appropriate chemical speciation.

The Italian national emission inventory [*ISPRA*, 2009] has been used to define area and point emissions for all anthropogenic sources within Italian boundaries (Fig. B.1). Outside Italy, emissions for all species except Hg have derived from EMEP webdab (Reportcode: W-07emis05-V9[1]). Point sources have been defined at SNAP-sector level following CHIMERE/EMEP approach [*EMEP*, 2003]. Finally, mercury emissions have been provided by EMEP/MSC-E.

Sea Salt natural emissions have been estimated by means of specific CAMx pre-processor, on both Gong and Smith and Harrison functions [*Gong et al.*, 2002; *Gong* 2003]. Biogenic VOC emissions have been reconstructed by MEGAN model [*Guenther et al*., 2006].

Finally, a specific procedure has been developed and implemented in order to estimate Hg natural emissions (Fig. B.1). Land emissions are based on EMEP approach [*Travnikov and Ilyin*, 2005] on the basis of soil data gently provided by EMEP/MSC-E. Sea emissions have been computed on the basis of literature data of global emissions [*Travnikov and Ryaboshapko*, 2002; *Travnikov*, 2005] and both

[1] Vestreng, V. et al., 2007: Inventory Report 2007. Emission data reported to LRTAP Convention and NEC Directive

global [*Behrenfeld and Falkowski*, 1997; http://marine.rutgers.edu/opp] and Italian database [*Colella and Santoleri*, 2006] of C productivity to perform spatial disaggregation.

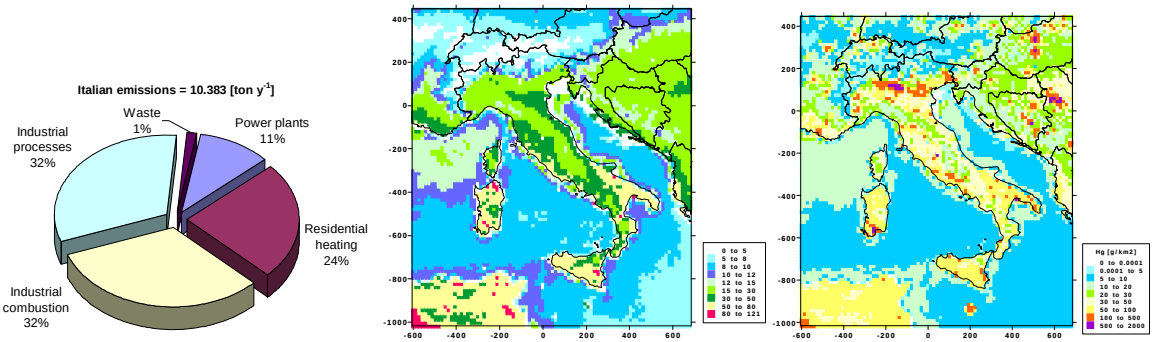

Fig. B.1. *Sector distribution of the Italian anthropogenic emissions (left); yearly natural emissions of Hg(0), g/km^2 (center) and yearly Hg total emissions (anthropogenic + natural), g/km^2*

CAMx results have been compared also to a comprehensive data set of air quality observations collected at 215 Italian stations. Model evaluation (not shown) was focused on conventional pollutants such as NO_X, SO_2, O_3 and PM10, proving model skill in reproducing background concentration of both primary and secondary pollutants. Moreover CAMx wet deposition fields have been compared to a set of observed samples of main inorganic ions collected at 7 sites placed in Northern Italy (not shown). Observed and computed deposition fluxes showed a rather good agreement, though at some stations some overestimations took place, due to a corresponding overestimation of the precipitation field.

B.4. Results and discussion

Mercury concentration and deposition fields

Fig. B.2 shows the yearly mean concentration of the three mercury species computed by CAMx for 2005. Elemental mercury concentrations range between 1.4 and 5.0 ng/m^3, with peaks taking place mainly in the Po valley and in correspondence of the highly industrialized areas, such as Taranto in Puglia region, Eastern Sicily and south of Sardinia. Concentrations over sea are rather homogenous, ranging between 1.4 and 1.6 ng/m^3.

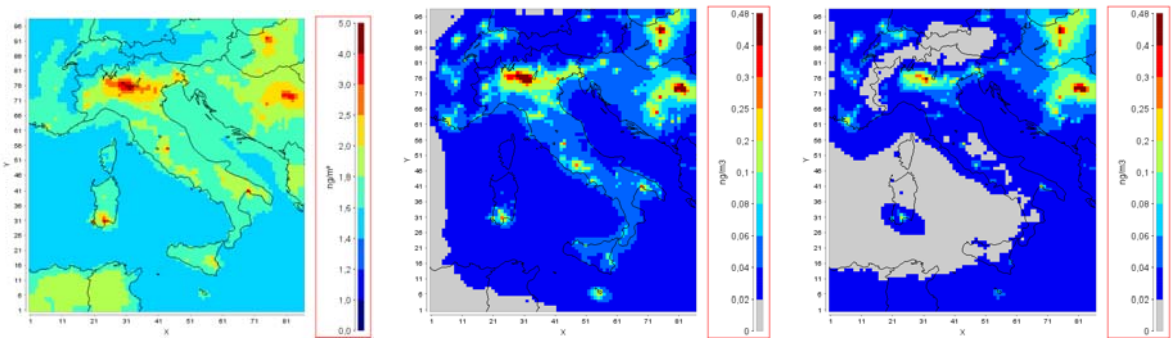

Fig. B.2 *– Yearly mean concentration of Hg(0) (left); Hg(II) (centre); Hg(p) (right) computed for 2005*

Spatial pattern of reactive gaseous mercury peaks follow closely the spatial distribution of the anthropogenic emissions. Highest concentrations take place in the Po valley and in the industrial areas already highlighted for Hg(0), showing values ranging between 0.2 and 0.5 ng/m^3. High Hg(II) concentrations are simulated also in industrial areas of Hungary and Bosnia. Over the sea as well as in rural areas, CAMx predicts values ranging between 0.02 and 0.06 ng/m^3 due to the transformation of Hg(0). Hg(p) shows a similar pattern to Hg(II) in terms of peaks, while concentrations in rural and remote areas are clearly lower, because Hg(p) is not directly build up by the oxidation of elemental Hg.

Elemental mercury is sparingly soluble, hence it is not significantly removed by wet deposition as shown in Fig. B.3. Differently, both divalent and particulate mercury are efficiently removed by rain scavenging. Hg(II) and Hg(p) show a similar deposition patterns, well related to the spatial distribution of precipitation rate (not shown). The highest deposition yields range between 12 and 20 μg/m^3/y, taking place along the coasts and the hilly areas of Apennines and Prealps. High deposition loads take place also in Eastern Po valley as well as along the Ex-Yugoslavia coast. It is worth noting that Hg(p) yields are generally higher than Hg(II), probably because CAMx overestimates scavenging efficiency for the former. Indeed, Hg(II) is highly soluble and is commonly expected to be better scavenged than Hg(p).

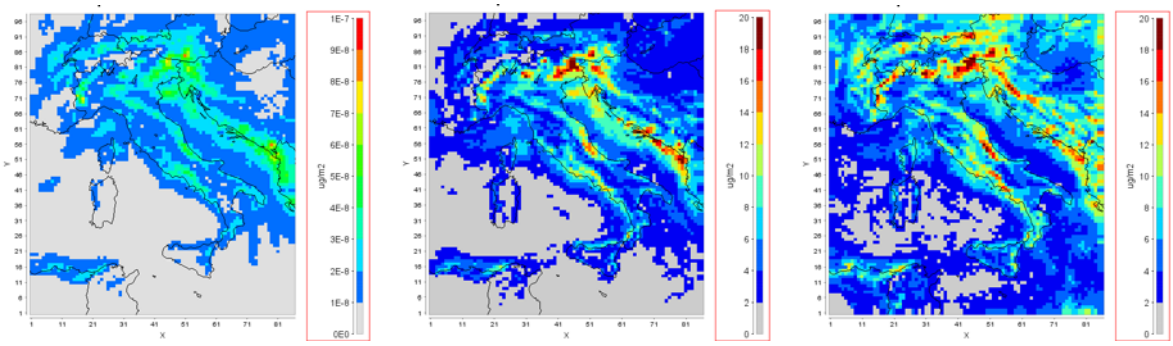

Fig. B.3. *Wet deposition of Hg(0) (left); Hg(II) (centre); Hg(p) (right) computed for 2005*

Comparison with EMEP model

CAMx results have been also compared to mercury concentration and deposition fields produced by EMEP model. Because of the unavailability of mercury observations in the framework of this study, the comparison to EMEP fields represented a very useful, though indirect, evaluation of CAMx performances.

The following maps depict the comparison between CAMx and EMEP yearly concentration and deposition fields. MSC-E concentrations of elemental Hg are somewhat higher than those computed by CAMx model over sea but lower over land (Fig. B.4). In regional-scale modelling of Hg, transport level of Hg(0) concentrations is mostly controlled by the concentrations set at boundaries of modelling domain and by deposition processes. CAMx derives boundary concentrations by EMEP, hence lower values are related to deposition. Indeed CAMx proved to overestimate dry deposition over sea [*Leuci*, 2010]. Differently, the concentrations computed by CAMx over land seem relatively correct, because measurements in background regions demonstrate levels around 1.5-1.7 ng/m^3. It is also worth noting that EMEP concentrations over the Alps are undoubtedly lower than CAMx. This is, probably, due to a different Hg(0) data processing between CAMx and EMEP/MSC-E. MSC-E results present a non-normalized surface concentration of Hg(0), otherwise CAMx presents the concentrations reduced to normal conditions. Thus, MSC-E and CAMx are not comparable in this region.

Fields of gaseous oxidized Hg are shown in Fig. B.5. Much higher concentrations of Hg(II) calculated by CAMx compared to EMEP can be caused by higher oxidation rates of Hg(0), and also by interpretation of oxidation products. In EMEP gas-phase, oxidation leads mostly to formation of particulate Hg. Probably, it was a reason of higher concentrations of Hg(p) over Mediterranean calculated by EMEP (Fig. B.6). Differently, EMEP Hg(p) concentrations over the Alps are lower than CAMx, due to the influence of the elevation in the computation of mass concentration as previously highlighted.

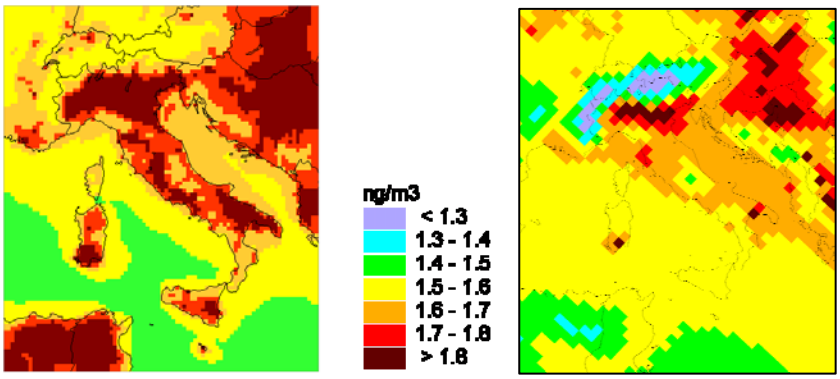

Fig. B.4. *Elemental Hg in air in 2005. Left: CAMx, right: MSCE-HM*

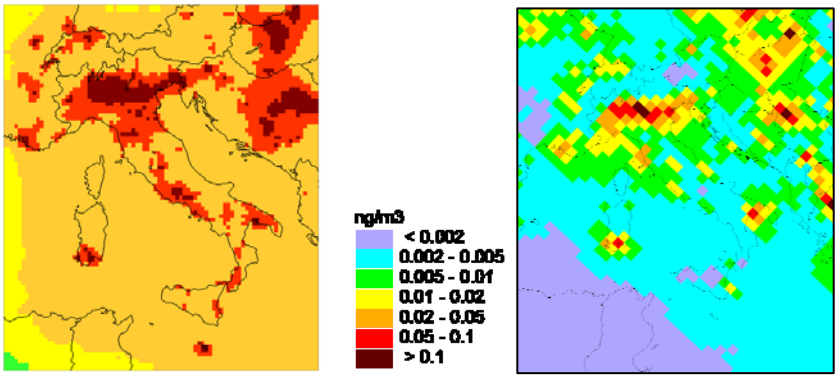

Fig. B.5. *Gaseous oxidized Hg in air in 2005. Left: CAMx, right: MSCE-HM*

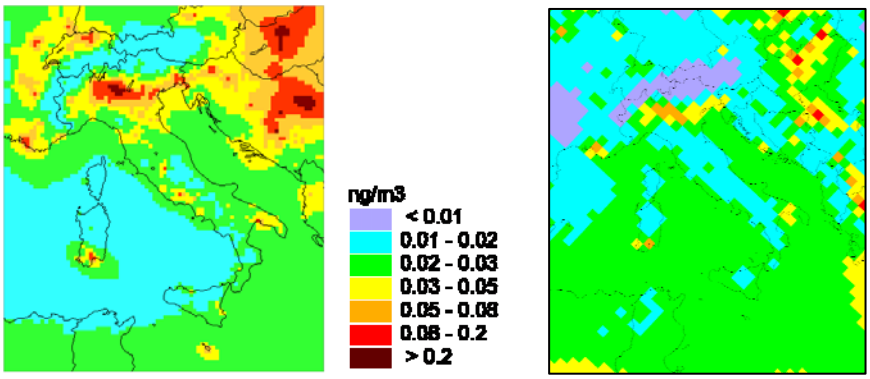

Fig. B.6. *Particulate Hg in air in 2005. Left: CAMx, right: MSCE-HM*

Among forms of mercury, oxidized gaseous Hg is scavenged by precipitation most readily followed by Hg(p). Concentrations of Hg(II) calculated by CAMx are much higher than those of EMEP. Concentrations of Hg(p) calculated by the both models are comparable. This leads to higher wet deposition in CAMx model. Besides, precipitation amounts used in simulation is also important factor

controlling amount of wet deposition and as already noted, CAMx input precipitation is partially overestimated. It is worth mentioning that EMEP (and many other models) tends to overestimate wet deposition fluxes compared to measurements. Therefore, CAMx model is expected to produce even higher overestimation.

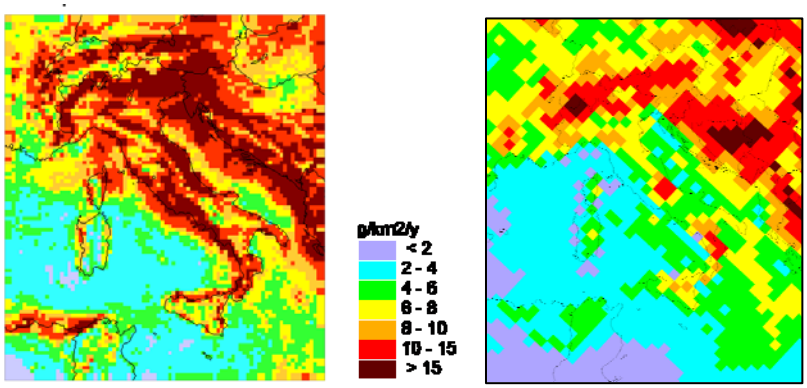

Fig. B.7. *Wet deposition of Hg in 2005. Left: CAMx, right: MSCE-HM*

B.5. Conclusions

A comprehensive modelling system based on the CAMx model, implementing the so called *one atmosphere approach*, has been implemented to reconstruct mercury pollution over Italy. The modelling system provided hourly concentration and deposition fields of three mercury species at 15 km resolution. CAMx proved to reconstruct reliable background concentrations of main pollutants. Comparison to EMEP model shows an overall agreement between the models, also highlighting some discrepancies mainly concerning Hg(II) concentration and wet deposition fields as well as dry deposition fluxes of Hg(0) and Hg(p) over forested areas.

Acknowledgements

This work has been financed by the Research Fund for the Italian Electrical System under the Contract Agreement between ERSE and the Ministry of Economic Development - General Directorate for Energy and Mining Resources stipulated on July 29, 2009 in compliance with the Decree of March 19, 2009. Authors are really grateful to O. Travnikov and I. Ilyin for their valuable help in the discussion of CAMx results. Authors are also grateful to INERIS to have kindly provided CHIMERE fields at European scale.

REFERENCES

Behrenfeld and Falkowski [1997] A consumer's guide to phytoplankton primary productivity models, *Limnology and Oceanography*.

Colella S., Santoleri R. [2006] Variabilità interannuale della produzione primaria nel Mar Mediterraneo: 8 anni di osservazioni SeaWiFS", CNR Roma 2006.

EMEP [2003] Transboundary Acidification, Eutrophication and Ground Level Ozone in Europe PART I - Unified EMEP Model Description - EMEP Status Report 2003, ISSN 0806-4520

EMEP MSC-E [2007] Heavy Metals: transboundary pollution of the environment. *Status Report* 2/2007.

ENVIRON [2008] CAMx (Comprehensive Air Quality Model with extensions) User's Guide Version 4.51, *Internal Report*, Environ Int. Corp.

Gong S. L., L. A. Barrie and M. Lazare [2002] "Canadian Aerosol Module (CAM): A size-segregated simulation of atmospheric aerosol processes for climate and air quality models 2. Global sea-salt aerosol and its budgets." *Journal of Geophysical Research* 107: 4779-4793.

Gong S. L. [2003] A parameterization of sea-salt aerosol source function for sub- and super-micron particles." *Global Biogeochemical Cycles* 17: 1097-1104.

Guenther A., T. Karl, P. Harley, C. Wiedinmyer, P. Palmer, and C. Geron [2006] Estimates of global terrestrial isoprene emissions using MEGAN (Model of Emissions of Gases and Aerosols from Nature), *Atmos. Chem Phys*., 6, 3181-3210.Nenes, A., Pandis, S.N., Pilinis, C., 1998. ISORROPIA: a new thermodynamic equilibrium model for multiphase multicomponent inorganic aerosols. *Aquatic Geochemistry* 4, 123–152.

ISPRA [2009] La disaggregazione a livello provinciale dell'inventario nazionale delle emissioni. Rapporto 92/2009

Leuci A. [2010] Ricostruzione modellistica dell'inquinamento atmosferico da mercurio sul territorio italiano. Degree thesis, University of Milano Bicocca, 2010 (in Italian).

O'Brien J. J. [1970] A note on the vertical structure of the eddy exchange coefficient in the planetary boundary layer. *J. Atmos. Sci.,* 27**,** 1213–1215.

Skamarock W.C., Joseph B. Klemp, Jimy Dudhia, David O. Gill, Dale M. Barker, Michael G. Duda, Xiang-Yu Huang, Wei Wang , Jordan G. Powers [2008] A Description of the Advanced Research WRF Version 3, *NCAR Technical Note* NCAR/TN-475+STR, Boulder, Colorado.

Travnikov O., Ryaboshapko A. [2002] Modelling of Mercury Hemispheric Transport and Depositions, EMEP MSC-E Technical report 6/2002.

Travnikov O, Ilyin I. [2005] Regional model MSCE-HM of heavy metal transboundary air pollution in Europe. EMEP/MSC-E Technical Report 6/2005, Meteorological Synthesizing Centre - East, Moscow, Russia. (www.msceast.org/publications.html)

Travnikov O. [2005] Contribution of the intercontinental atmospheric transport to mercury pollution in the Northern Hemisphere. *Atmos. Environ*. 39, 7541-7548

Vautard R., Bessagnet B., Chin M., Menut L. [2005] On the contribution of natural aeolian sources to particulate matter concentrations in Europe: Testing hypotheses with a modelling approach. *Atmospheric Environment*, 39, 3291-3303.

Yarwood G., S. Rao, M. Yocke, and G.Z. Whitten [2005] Updates to the Carbon Bond chemical mechanism: CB05. *Final Report prepared for U.S. EPA*. Available at http://www.camx.com.

Wen Deyong [2006] Modelling of Atmospheric Mercury Emission, Transport, Transformation and Deposition in North America. Phd thesis, University of Waterloo, Ontario, Canada.